LASER DRIVEN ACCELERATION OF CHARGED PARTICLES IN VACUUM

By

Vikram Sagar

INSTITUTE FOR PLASMA RESEARCH, GUJARAT.

A thesis submitted to the
Board of Studies in Physical Sciences

In partial fulfillment of the requirements

For the Degree of

DOCTOR OF PHILOSOPHY

of

HOMI BHABHA NATIONAL INSTITUTE

July 2013

Homi Bhabha National Institute

Programme: Ph.D.

Board of Studies in PHYSICAL **Sciences**

1. Name of the Constituent Institution: INSTITUTE FOR PLASMA RESEARCH

2. Name of the Student:	VIKRAM SAGAR
3. Enrolment Number:	PHYS 06200704006
4. Date of Enrolment in HBNI:	03 SEPTEMBER 2007
5. Date of Submission of Thesis:	25 JULY 2013
6. Title of the Thesis:	LASER DRIVEN ACCELERATION OF CHARGED PARTICLES IN VACUUM

7. Composition of the Doctoral Committee:

Sr No	Composition	Designation in HBNI	Name
a.	**Chairman**	SENIOR PROF.	PROF. A. SEN
b.	**Convener** (Guide)	SENIOR PROF.	PROF. P. K. KAW
c.	**Co-Guide**, if any	—	—
d.	**Member**	ASSO. PROF.	PROF. A. DAS
e.	**Member**	ASST. PROF.	DR. S. SENGUPTA
f.	**The Technology Adviser**, if any	**Invitee**	—

8. Number of Doctoral Committee Meetings held with respective dates:

1. 10/11/2008 2. 27/01/2010 3. 18/01/2011
4. 06/02/2012 5. 11/09/2012 6. 12/04/2013 (synopsis)

9. Name and Organization of the Examiner 1: PROF. A. SURJALAL SHARMA UNIV. OF MARYLAND, USA.

Recommendations of the Examiner 1 (Thesis Evaluation) (i) accepted, (ii) accepted after revisions, or (iii) rejected:

10. Name and Organization of the Examiner 2: PROF. A. C. DAS PHYSICAL RESEARCH LABORATORY AHMEDABAD

Recommendations of the Examiner 2 (Thesis Evaluation) (i) accepted, (ii) accepted after revisions, or (iii) rejected:

Name & Signature of Dean-Academic, CI:

Smukherjee

[Dr. S. Mukherjee]

Recommendations of the Viva Voce Board

1. **Date of Viva Voce Examination:** 18 SEPTEMBER 2013

2. **Recommendations for the award of the Ph.D. degree: Recommended / ~~Not Recommended~~**
(If Recommended, give summary of main findings and overall quality of thesis)
(If Not Recommended, give reasons for not recommending and guidelines to be communicated by Convener of the Doctoral committee to the student for further work)

In this thesis, two prominent schemes, namely
- "laser driven auto-resonant acceleration" and
- "direct acceleration of particles by focussed laser fields"

have been systematically studied.

It has been demonstrated that these two schemes are very efficient in accelerating particles.

The work done in this thesis is of high standard with many interesting and important orginal contributions. Some of these results are already published in peer-reviewed journals.

The thesis is strongly recommended for the award of a PhD degree.

[signature]

In case Not Recommended, another date will be fixed by the Dean-Academic, CI, which shall not be earlier than a month after and not later than six months from the date of first viva.

Date:

Name and Signature of the Viva Voce Board (Doctoral Committee and External Examiner):

PROF. A. SEN — [signature]
PROF. P. K. KAW — [signature]
PROF. A. DAS — Amita Das
DR. S. SENGUPTA — [signature]
PROF. A. C. DAS — [signature]
(EXTERNAL EXAMINER)

Homi Bhabha National Institute

Recommendations of the Viva Voce Board

As members of the Viva Voce Board, we recommend that the dissertation prepared by **Vikram Sagar** entitled "Laser Driven Acceleration Of Charged Particles In Vacuum" may be accepted as fulfilling the dissertation requirement for the Degree of Doctor of Philosophy.

-- **Date :18/09/2013**
External Examiner : Prof. A C Das

-- **Date :18/09/2013**
Chairman : Prof. Abhjit Sen

Pkaw
-- **Date :18/09/2013**
Convener : Prof. P K Kaw

Amita Das
-- **Date :18/09/2013**
Member : Prof. Amita Das

-- **Date :18/09/2013**
Member : Dr. Sudip Sengupta

Final approval and acceptance of this dissertation is contingent upon the candidate's submission of the final copies of the dissertation to HBNI.

I hereby certify that I have read this dissertation prepared under my direction and recommend that it may be accepted as fulfilling the dissertation requirement.

Pkaw
-- **Date :18/09/2013**
Guide : Prof. P.K.Kaw
Institute For Plasma Research, Gujarat

Evaluation Report on the Thesis entitled: "Laser Driven Acceleration of Charged Particles in Vacuum" submitted by Vikram Sagar for the award of the degree of Doctor of Philosophy of Homi Bhabha National Institute.

I have gone through the thesis and my comments are given below.

The principal aim of the thesis is to carry out systematic studies on the problem of laser driven acceleration of charged particles in vacuum. It contains several chapters dealing with the investigation of various processes that are responsible for acceleration of particles by lasers in vacuum. It has , however, emphasized two prominent schemes namely 'Laser driven auto resonant acceleration' and 'direct acceleration of particle by focused laser fields'. In fact it has demonstrated that these two schemes are very efficient in accelerating particles as a result of interaction with lasers. The thesis also has presented many other interesting and important results. Some details are given below.

An extended review of earlier work done in this field of research has been outlined in chapter 1. It is quite exhaustive and has been a very useful prelude to the rest of the thesis. In chapter 2, both analytical and numerical studies on the particle dynamics in the field of a relativistically intense homogeneous continuous as well as pulsed laser have been carried out by solving exact relativistic equation of motion by using three constants of motion . It has been shown that in the continuous laser, the interaction of charged particles with relativistically intense laser does not result in the net transfer of energy from laser to particles. It appears to happen even for a finite duration pulsed laser because of light pressure effect.

The particle dynamics has been studied in chapter 3 by solving Gaussian shaped temporal envelope in the combined field of a finite duration laser and static axial magnetic field,This is what forms the basis for the "Laser driven auto resonant acceleration scheme" mentioned above, wherein, it is shown that the initial particle-laser resonance is self-sustained due to precise cancellation of two relativistic effects associated with particle dynamics. I find it very interesting to see how the 'phase locked' or 'trapped' particle in a quasi-electrostatic field of a laser causes continuous acceleration. Furthermore, the particle in the field of finite duration laser pulse interacts with the spectrum of frequencies and can be accelerated by resonating with characteristic laser frequency in the spectrum. It has further shown an inverse relation between the length of the laser pulse and the intensity of laser pulse for an effective gain of particle energy. It is quite interesting. This result appears to support,in general , the mechanism of generation of particle energy (or emissions) by short and long pulses during active experiments in presence of magnetic field in space plasmas.

In chapter 4, another scheme of accelerating particles has been described by considering the particle dynamics in a focused continuous and finite duration pulsed laser field. In this scheme the net transfer of energy from the laser to the particle is due to an asymmetry in the acceleration and deceleration phases of focused laser field. The numerical study has been extended to more realistic case of focused finite duration laser pulse with the aim of determining the optimum initial condition in terms of peak intensity, pulse length, focal length for maximizing energy gain by the particle.

The chapter 5, however, deals with adiabatic formulation of charged particle dynamics in an inhomogeneous electromagnetic field of laser. Because of slow variation in laser intensity the particle dynamics is expressed in terms of constants of motion and an adiabatic invariant. In this approximation the particle dynamics is separated in terms of fast varying motion and a phase averaged slow motion. The estimate of energy gain are obtained numerically by solving the relativistic equation of motion.

A new scheme has been discussed in chapter 6, in which the particle is subjected to a combined field of focused finite duration laser pulse and homogeneous static magnetic field. The combined effect of focusing and magnetic field improves the efficiency of scheme by increasing energy gain as well as the required peak laser intensity.

In my opinion, the work done in the thesis is of high standard with many interesting and important original contribution in the area of accelerating charged particles in laser field Some of the results are already published in peer reviewed journals. The presentation is good except that a few figures are rather small to read the statement written in the margin of the axis. I therefore strongly recommend that the thesis be accepted for the award of the degree of Doctor of Philosophy of Homi Bhabha National Institute.

Attar.

Homi Bhabha National Institute

Ph.D. Thesis Evaluation Report

1. **Name of the Constituent Institution:** Institute for Plasma Research
2. **Name of the Student:** Vikram Sagar
3. **Enrolment No. :** PHYS06200704006
4. **Title of the Thesis:** Laser Driven Acceleration of Charged Particle In Vacuum
5. **Board of Studies:** Physical Sciences

Recommendations

Tick one of the following:

1. The thesis in its present form is commended for the award of the Ph.D. Degree. [X]
2. The thesis is commended for the award of the Ph.D. degree. However, my suggestions for improving the thesis may be considered at the time of the viva voce examination and if the viva voce board deems it appropriate, the same may be incorporated in the thesis based on the discussions during the viva voce examination. The revised thesis need not be sent to me. [ ]
3. The thesis should be revised as per the suggestions enclosed. I would like to see the revised thesis incorporating my suggestions before I give further recommendations. [ ]
4. The thesis is not acceptable for the award of the Ph.D. degree. [ ]

(Signature): A. Surjalal Sharma.

Name of Examiner: A. SURJALAL SHARMA

Date: Sep. 16, 2013

Please give your detailed report in the attached sheet. You may use additional sheets, if required.

1. **Name of the Student:** Vikram Sagar

2. **Enrolment No.:** PHYS06200704006

3. **Title of the Thesis:** **Laser Driven Acceleration of Charged Particle In Vacuum**

4. **Board of Studies:** Physical Sciences

DETAILED REPORT

Write your comments, if any.

The thesis presents a systematic study of the relativistic dynamics of a charged particle (an electron in most cases) in the intense field of a laser and is of interest and relevance to laboratory experiments and to astrophysics. The studies encompass three physical mechanisms, viz. auto-resonance in the presence of an axial field, a focused laser beam, and a combination of these two. The analytical studies combine electrodynamics and Hamiltonian mechanics, and use approaches such as Hamilton-Jacobi equation and Lie transform. Although closed analytical expressions are obtained in most cases their complexity requires numerical computations, and this yields a major part of the results. The thesis provides a comprehensive body of research results deserving of a Ph. D. degree.

The results of the research have two related aspects, viz. the physical mechanisms of acceleration and the dependence on the relevant parameters. There is a shift in the balance between these two aspects across the chapters. For example, the studies of the auto-resonance process (Chap. 2 and 3) are rich in elucidating the physical mechanism and this changes to a stronger emphasis on quantifying the dependence on parameters in the studies of a focused laser beam (Chap. 4 and 5), and more so in the case that combines these two processes (Chapter 6). While such a shift should be expected as the processes become more complicated, the results in the cases which can be treated analytically can be used fruitfully in interpreting the simulations that use the equations directly or experiments where available. Such an approach to the use of the analytical results will enable a better understanding of the more complicated scenarios.

Name of Examiner: A. SURJALAL SHARMA

Signature and Date: A. Surjalal Sharma. Sep. 16, 2013

STATEMENT BY AUTHOR

This dissertation has been submitted in partial fulfillment of requirements for an advanced degree at Homi Bhabha National Institute (HBNI) and is deposited in the Library to be made available to borrowers under rules of the HBNI.

Brief quotations from this dissertation are allowable without special permission, provided that accurate acknowledgement of source is made. Requests for permission for extended quotation from or reproduction of this manuscript in whole or in part may be granted by the Competent Authority of HBNI when in his or her judgment the proposed use of the material is in the interests of scholarship. In all other instances, however, permission must be obtained from the author.

Vikram Sagar

Vikram Sagar

DECLARATION

I, hereby declare that the investigation presented in the thesis has been carried out by me. The work is original and the work has not been submitted earlier as a whole or in part for a degree/diploma at this or any other Institution or University.

Vikram Sagar

Vikram Sagar

CERTIFICATION FROM GUIDE

This is to certify that the corrections as suggested by the Referees in the thesis evaluation report have been incorporated in the copy of the thesis submitted to HBNI.

PKaw

Date: 18/09/2013 Guide: Prof. P.K.Kaw

. . . . . . to my beloved wife and family . . . . . .

“ Life is like riding a bicycle.

To keep your balance, you must keep moving”

-Albert Einstein

ACKNOWLEDGEMENTS

Foremost, I would like to express my sincere gratitude to my advisor Prof. P K Kaw and Dr. Sudip Sengupta. There continuous support and guidance had been inspiring. There enthusiasm and friendly nature had made this voyage a success. I really appreciate there tolerance for listening and answering to my every childlike questions during the entire duration of my work. I am also thankful to them for providing me enough independence during this work and involving me in some fruitful collaborations.

I am grateful to Prof. Abhjit Sen and Prof. Amita Das for being my doctoral committee members. Their comments during my reviews had been quite helpful in improving this work. I would like to thank Prof. J K Bhattacharjee for improving my understanding of the subject.

I would like to thank Prof. Shishir Deshpande, Prof. R Singh, Dr. P Chattopadhyay, Dr. M Warrier, Dr. R Ganesh, Dr. N Ramsubramaniam, Dr. Joydeep Ghosh, Dr. Devendra Sharma, Dr. S Mukherji, Prof. A Das, Prof. R Jha and Ritesh for their endurance while teaching us during the $1st$ year course.

Thanks to the library, computer and administrative staff of IPR for being always cooperative. I thank Mr. Saroj Das, Mr. Shravan Kumar, Ms. Smita Parmar, Mrs. Arundhati Das, Mrs. Pragya Pathak, Mrs. Sutapa Ranjan, Mr. Shailendra Trivedi, Mr. Arvind Singh, Mr. Hemant Joshi, Mr. Gaurav Garg, Mr. Govind Lokhande, Mr. M Sourabhan, Mr. M. H. Vartak, Mr. H. K. Sharma, Mr. H. C. Khanduri, Mr. Hitesh Mehta, Mr. Dinesh Nair, Mr. Silel Shah, and Ms. Shirin Bhesania for their helps on numerous occasions.

I enjoyed the friendly hostel life at IPR. Greetings and best wishes to my dear Pintu da, Ritu di, Neeraj Jain, Suraj Sinha, Manash Paul, Rajneesh Yadav, Anand Srivastava, Bhaskar Chaudhary, Anurag Mishra, Vikrant Saxena, Kishore Karatiparambil, Padduvatti N. Maya, Subhas, Sanjay Mishra, Swati Baruah, Jugal Chaudhury, Satyanand Kar, Sharad Yadav, Shekhar T. Goud, Sunita Negi, Kshitish Barada, Deepak Sangwan, Prabal Singh Verma, Ashwin Joy, Ujjwal Shinha, Sita Sunder, Gurudatt, Sanjib, Tayyab, Arabind, Lintish, Kushal, Sushil, Rameswar, Sanat, Pravesh, Partha, Sayak, Manjit, Soumen, Aditya, Iliyas, Vikram Jr, Rana, Veda, Sandeep, Zuber, Rupendra, Mangilal, Bibhu parasad, Varaprasad, Harish, Sameer, Neeraj, Deepa, Akanksha, Vidhi, Dushyant, Anup, Arghya, Bhumika, Debraj, Modhuchandran, Narayan, Amit, Rajnarayan, Ratan, Sonu, Surabhi, Umesh ...

I would like to have special mention of Ujjwal, Ashwin, Kushal and Kshitish with whom I had discussions on vivid topics. I will certainly miss my morning badminton session with Aditya, Gurudatt and Kshitish.

I would like to express my gratitude to our cook Jiva, who worked round the clock making us feel at home and always serving with smile.

I take this opportunity to thank my teachers during my MSc at Panjab University, especially, Prof. D.Mehta and Dr. C. N. Kumar for motivating me to pursue higher studies.

Many thanks to my university seniors Varun, Anjana, Pooja, Rudra, Gautam, Tulasi and Kiran who helped me along my initial days.

Thanks a lot again to Sanjay Mishra, Anup and Daisy for spending their valuable time in proof reading of the draft.

Also, I would like to mention there are several people who helped in many ways at different point of times in my studies and would like to thank all of them for their support.

I would also like to have a special mention of a very special person who has been a friend as well as a companion my wife Daisy. It is outcome of her unconditional love, care, affection and encouragement. At last, my heart felt gratitude to my family, parents and in laws for their belief, good will and support all through my life.

Vikram Sagar

PUBLICATIONS

Thesis:

1. *Exact analysis of particle dynamics in combined field of finite duration laser pulse and static axial magnetic field* , Vikram Sagar,Sudip Sengupta and P Kaw, Phys. Plasmas **19**, 113117 (2012);

2. *Adiabatic Formulation For Charged Particle Motion Inhomogeneous Electromagnetic Field*; Vikram Sagar, Sudip Sengupta, P Kaw, Journal Laser And Particle Beams, Vol. **31**, issue 03, pp. 439-455 (2013);

3. *Effect of Laser Pulse Polarization and Focusing On Particle Acceleration By Cyclotron Auto-Resonance* Vikram Sagar, Sudip Sengupta, P Kaw, Journal Laser And Particle Beams **to be submitted**.

Abstract

This thesis is devoted to the study of laser driven acceleration of charged particles in vacuum. The following two schemes of particle acceleration namely:"the laser driven auto-resonant acceleration" and "direct acceleration of particles by a focused laser field" have been theoretically investigated. It has been further shown that these two schemes of particle acceleration can be easily combined together to enhance the efficiency of the acceleration scheme.

The scheme of laser driven auto-resonant particle acceleration is of great interest, as in this scheme the acceleration rate is higher and radiation losses are lower as compared to other schemes of particle acceleration. In the laser driven auto-resonant scheme, the particle is subjected to the combined field of laser and a static axial magnetic field. The particle acceleration is achieved as a result of self sustained initial resonance between the wave frequency and cyclotron frequency of the particle. This resonance is maintained due to a precise cancellation of the relativistic mass effect due to the motion along the transverse direction which lowers the cyclotron frequency of the particle and a Doppler effect along the longitudinal direction, as result of which the frequency of the wave as seen by the particle is lower than the actual wave frequency. The renewed interest in this scheme is due to the observation of ultra high magnetic fields in the simulations as well as in the laboratory experiments pertaining to intense laser solid interaction. The observed magnetic fields are typically of the order of hundreds of mega-gauss and in general are found to be in turbulent state. However, in some of the cases, the fields are found to be coherent for a longer duration time compared to the time of interaction between the laser pulse and particle. Thus a detailed analytical as well as numerical understanding of the scheme is required to optimize the use of these magnetic field for experimental realization of the scheme. In this thesis, the particle acceleration is analytically and numerically studied using a "Gaussian" shaped temporal profile for the first time; this profile allows an unambiguous comparison between the analytical and numerical results. It is shown that particle with significant energy gain can be obtained for an optimum choice of parameters in terms of axial magnetic field, pulse width and peak laser intensity.

In the other scheme, the particle is accelerated by subjecting it to a focused laser field. For a focused laser, there is asymmetry in configuration of electric as

well as the magnetic fields, which are found to be strongest near the focal point and grows weaker while moving away from it. As a result of this asymmetry, the weaker laser field far away from the focus is not able to extract back the energy transfered to the particle by the laser closer to the focus and hence a net energy is imparted to the particle along the direction of propagation of laser. For a range of parameters the energy gain is obtained by numerically solving the equation of motion. These numerical results are compared with the analytical results which are obtained using a newly derived adiabatic formulation. The adiabatic formulation is derived using canonical transformation and Lie-transform perturbation method. It is shown that the analytical description provides good quantitative estimates of the numerical results. From these estimates, the optimum conditions for maximum energy gain of the particle are determined.

The theoretical understanding of the above two acceleration schemes is used to describe a new scheme of particle acceleration. In this scheme the particle is subjected to the combined field of focused finite duration laser and static axial magnetic field. It is shown that for suitable choice of parameters, the scheme results in efficient acceleration of particles.

Contents

List of Figures

1

Introduction

This chapter contains the brief history and review of different schemes of particle acceleration in vacuum. The motivation and methodology for each of the works has been outlined in the respective chapters.

1.1 Brief History and Review of Earlier Works

The area of particle acceleration has been a topic of intense scientific research for several decades. These accelerated charged particles have wide range of applications in diverse fields such as the study of fundamental constituents of matter, high-resolution radiography for non destructive material inspection, radiotherapy, ultrafast chemistry, radio-biology, material science, industrial applications, medical field etc. In recent years, the area of laser driven particle acceleration has received considerable attention due to a giant leap in laser technology caused by the advent of Chirped Pulse Amplification [CPA][1, 2, 3] technique. The optical beams produced using this technique have peak focused intensities of the order of $10^{21} - 10^{22} W cm^{-2}$. The corresponding electric fields produced by such high powered laser systems is of the order of $10^{12} V cm^{-1}$, which surpass those produced in the conventional RF linear accelerators by several orders of magnitude. Therefore, these laser driven accelerators with such high intensities and large accelerating gradients offers a compact, economical and efficient alternative to conventional accelerators for accelerating particles to relativistic energies. In 1961, Shimoda [4] first proposed the use of lasers as a clean and simple physical system to accelerate particles. Since then the laser driven acceleration of charged particles has been studied in plasma, gases and vacuum[5, 6, 7, 8, 9, 10, 11, 12, 13].

The problem of relativistic interactions of free electron with continuous and pulsed EM fields of laser has been a topic of great interest. In the past, the orbit solutions have been investigated for the problem of a charged particle moving under the influence of a laser pulse[14, 15, 16]. The force equation was integrated by Krüger and Bovyn [14], for a particle driven by a plane wave of arbitrary amplitude, in terms of the co-moving and inertial times. An exact solution was found by Shebalin [15], as a function of the phase of the wave, for the position and velocity of a particle interacting with an electromagnetic wave. Acharya and Saxena[16], solved the problem of a particle embedded in an elliptically polarized wave. Landau and Lifshitz [17], examined the problem in terms of an average rest frame drifting at a particular velocity with respect to the laboratory frame. Bardsley *et al.* [18], studied the nonlinear dynamics of electrons in intense laser fields by numerically solving the relativistic equation of motion of single electron in a pulse of very strong plane-wave interaction, taking account of space-charge effects and spatial variations in laser intensity. The further works on this topic are contained in the following references [20, 21, 22]. It is well known from these studies, that in vacuum a particle oscillating in the field of either a continuous plane monochromatic wave or a finite duration pulse is symmetrically accelerated and decelerated by the laser field resulting in no net energy transfer. The lack of energy transfer is a consequence of phase slippage of the particle from the laser field.

A number of studies have been reported over the years to overcome the issue of particle phase slippage from laser fields and thus accelerating charged particles in vacuum. All these works have made the laser driven acceleration of charged particle in vacuum as one of the intensely researched area of particle accelerations. Some of the schemes of accelerating the charged particles in vacuum are laser driven auto-resonant acceleration [23, 24, 25, 26, 27, 28, 29, 34, 35, 36, 37, 38, 39, 40, 41, 42, 33], direct laser acceleration by the focused laser field [46, 58, 56, 59, 60, 61, 62, 65, 48, 49, 50, 51, 52, 53, 54, 55, 57], Vacuum Beat Wave Acceleration(VBWA) [70, 71, 72, 73, 74], Inverse Free-Electron Laser (IFEL) [75, 78, 79, 80, 81, 82, 83] and particle acceleration by chirped laser frequency [84, 85, 86, 87, 88, 89, 90, 91]. The physical principles underlining these schemes along with the brief description of the earlier works on the topics is given below.

The mechanism for auto resonance scheme which is of great interest was discovered by KolomenskiÏ and Lebedev [23, 24] and, independently, by DavydovskiÏ [25]. The laser driven auto-resonant scheme provides a high acceleration rate and sufficiently low radiation losses [26]. In this scheme the charged particle is subjected to the combined field of laser and homogeneous static axial magnetic field. The particles are accelerated as a result of self-sustained resonance between the particle and the laser field, as result the particle remains phase locked with the laser pulse. The condition for the phase locking i.e $\omega - kv_x = \frac{\Omega_c}{\Gamma}$, where ω is the laser frequency and $\Omega_c (= \frac{eB_o}{mc})$ is the cyclotron frequency, v_x is the longitudinal particle velocity, is a consequence of conservation of $\frac{\Omega_c}{\omega\Delta}$; $\Delta = \Gamma - P_x/mc$, Γ and P_x respectively being the relativistic factor and x component of the momentum. The mechanism of auto-resonant particle scheme can be described in a following way: the particle initially at rest and satisfying the initial resonance condition ($\omega = \Omega_c$) is accelerated along the electric field of a wave. The gain in the energy along the transverse direction leads to the relativistic mass effect which in turn lowers the cyclotron frequency of the particle. As result of the transverse velocity gain, the particle is acted upon by the magnetic field component of the wave, which pushes the particle along the direction of the propagation of the wave. The relativistic velocity acquired by the particle along the longitudinal direction results in a Doppler shift to a lower frequency of the wave as "seen" by the particle. In this case, the Doppler shift in the wave frequency to the lower frequency equals the reduction in the cyclotron frequency, and the particle remains "synchronously" in cyclotron-resonance condition. Thus resulting in a continuous increase in particle energy and momentum along the direction of propagation of the wave. A brief account of the studies based on this scheme has been given below. An exact $``synchronous''$ solution to the equation of motion for the case of circular polarization was obtained by Roberts and Buchsbaum [27]. From the solution it was shown that when the index of refraction of the medium is not unity, the energy of the particle is periodic in time, and when that index is unity, the effect of the magnetic field compensates for the change in mass with energy and the energy increases indefinitely at resonance. An exact expression for the particle energy as a function of time was obtained. Bourdier and Gond [28, 29] studied the dynamics of a relativistic charged particle in both a linearly and circularly polarized EM plane wave with and without a constant axial magnetic field using Hamiltonian formalisms. For a particle initially at rest, they obtained a scaling law for the energy gain at resonance condition. They also examined the case with an external magnetic field gradient and some interesting results were obtained on particle acceleration mechanisms. Qian [30], has reported exact solutions, for certain initial conditions, for the motion of a charged particle driven by a circularly polarized wave propagating along a constant magnetic field. Qian [31], also considered the same problem with the superposition of circularly polarized waves and showed that this increases the chance for resonance. Ondarza-Rovira [32], solved the REM for an electron in an elliptically polarized wave along a constant axial magnetic field using a potential representing a traveling wave with constant amplitude. The method of solution allowed to integrate in exact form the Lorentz equation yielding to analytical expressions for the electron trajectories and drift velocities of the particles. These solutions exhibit resonance effects between the wave frequency and the cyclotron frequency associated with the axial magnetic field. Ondarza and Gomez [33], extended this work to include an elliptically polarized wave with a Gaussian-like shape propagating along a constant axial magnetic field. They used a sin^2 representation for the pulse shape and reported finding two new resonance conditions in the solution. The further works on the topic can be found in the following references [34, 35, 36, 37, 38, 39, 40, 41, 42].

Alternatively, the charged particle can be accelerated in vacuum by subjecting it directly to the field of focused laser, this scheme has been refereed to as the direct laser acceleration (DLA) in the literature [46, 47, 48, 49, 50, 51, 52, 53, 54, 55, 56, 57, 58, 59, 60, 61, 62, 65, 63]. The physical mechanism underlining this scheme can be described in a following way; on focusing the strength of electric field component of laser increases along the direction of propagation and reaching maximum at the focal spot, this region is termed as the focused region. The region beyond the focal point along the propagation direction is termed as the defocused region, the strength of electric field component decreases in this region. Thus the focusing of a laser field causes the asymmetry in the acceleration and deceleration phase of the laser field. At the beginning of the interaction, considering the particle to be positively charged and initially at rest is overtaken by the laser, which accelerates it along the electric field component of the laser. The particle acquires a relativistic velocity along the direction of electric field component of laser. As result of this, the force due to the magnetic field component becomes significant and the particle is subjected to strong $\vec{v} \times \vec{B}$ force which pushes the particle along direction of propagation of the laser into de-focused region. As described above the electric field component of the laser is weaker in this region and decays further while moving away from the focus, thus the laser is not able to extract the energy back from the particle. This asymmetry in energy exchange between the particle and laser field due to the focusing leads to the net transfer of energy to it along the direction of propagation. The earlier works on this scheme are briefly described below.

The particle dynamics in the focused laser field was earlier analytically studied by Kaw *et al.* in ref.[46] using an one dimensional model. The slow spatial modulation along the direction of laser propagation was used to model the focused laser field and optimum conditions for maximizing the energy gain by the particle were obtained. In ref.[47], it was pointed out that the two and three dimensional focused laser fields are associated with a longitudinal component of electric field which play a significant role in the acceleration of particle acceleration. Thus an improved description of fields is required for the detailed analysis of the direct particle acceleration in vacuum. Several theoretical studies on the vacuum electron acceleration have been based on the quasi-geometrical optics (paraxial) approximation or on its higher-order generalization [48, 49, 50, 51, 52, 53, 54, 55, 56]. In ref.[57] a more realistic focal laser field that satisfies Maxwell's equations has been employed ; however, this work involved idealized boundary conditions for a tightly focused laser beam. The further description of the works on the topic can be found in the following references [58, 59, 60, 61, 62, 65, 66]. The other aspects such as the effect of laser polarization of the laser pulse on the particle energy gain was studied by Singh *et al.* in ref [63] and from the numerical studies it was shown that the circularly polarized laser enhances the energy gain in comparison to the linearly polarized one. The particle dynamics in the overlapping field of two focused linearly polarized finite duration laser pulses was studied in [64] and based on numerical simulation it was concluded that energy gained by the particle can be enhanced considerably by suitable choice of pulse lengths.

Esarey *et.al* [67] proposed the Vacuum Beat Wave Accelerator [VBWA] scheme for accelerating charged particle by intense laser fields. This scheme does not require gas, plasma, or other proximate material medium to achieve a net energy gain. The scheme relies on the ponderomotive acceleration resulting from the beat wave produced by the interaction of two laser beams. In the VBWA, two laser beams of different frequencies are co-propagated in the presence of an injected electron beam. The beat term in the $\vec{v} \times \vec{B}$ force results in an axial acceleration of properly phased electrons, traveling essentially along the same axis as the two laser beams. By suitable choice of the frequencies, focal spot sizes and/or the focal points of the two beams, the phase velocity of the beat wave can be adjusted such that $v_{ph} \leq c$. Hence the phase velocity can be tuned to the electron velocity and the problem of phase slippage can be reduced. The acceleration mechanism in the VBWA is similar to that of the inverse free-electron laser (IFEL), wherein a propagating electromagnetic wave interacts with an electron beam in the presence of a periodic magneto-static field, and the resulting beat wave produces acceleration. In this effect, the wiggler field in the IFEL is replaced by one of the lasers in the VBWA. Hafizi *et.al* [68] extended the previously considered models [67, 69] of the interaction to obtain improved estimates for the energy gain. It was demonstrated through simulations that the energy gain can be improved significantly by employing a converging particle beam that was focused at the same location as the laser beams. Further progress on the topic can be found in the following references [70, 71, 72, 73, 74].

The inverse free-electron laser (IFEL) is one of the schemes of laser acceleration which has been studied over several years. The basic principles of the IFEL accelerator, although that name was given later, were proposed by Palmer[75]. The scheme is result of successful experiments [76, 77] with the free-electron laser which have shown that there is indeed a transfer of energy between the laser and electron beams in the presence of the undulator magnetic field. In a free-electron laser the energy is transferred from electrons to the laser beam. In the IFEL accelerator the energy transfer is in the opposite direction, from the laser beam to electrons. The IFEL can be used to accelerate electrons to energies of the order of 100-GeV regime. In an IFEL, relativistic particles are moving through an undulator magnet; a plane electromagnetic wave is propagating parallel to the beam. The undulator magnet produces a small transverse velocity (wiggling motion) in a direction parallel to the electric vector of the wave, so that energy can be transferred between the particle and the wave. In this scheme the magnetic fields is tailored in a way so that the electron's wiggling motion and the EM wave are always in the same relative phase. The sign of transverse electron velocity is changed synchronously with the laser field to compensate for the phase slippage of the electron due to which it falls behind the wave. The following references [78, 79, 80, 81, 82, 83] contains some of the detailed studies on the topic.

Several schemes have been described above for laser driven acceleration of charged particles in vacuum. In most of these schemes the laser frequency has been kept fixed, however particle can also be efficiently accelerated using the chirped laser pulses, for which the instantaneous frequency varies with time. The instantaneous variation of frequency of the laser with time forms the basis for the collapse of symmetry between acceleration and deceleration of charged particle by planer electromagnetic fields of the laser in vacuum. Several schemes [84, 85, 86, 87, 88, 89, 90, 91] have been proposed using chirped laser pulses for acceleration of particles in vacuum and it is shown that the use of chirped laser pulses could dramatically enhance the acceleration effect. In the chirped laser acceleration scheme, an electron with a low initial energy is injected into the high phase velocity region, but the variation in the instantaneous frequency of the chirped laser pulses versus the space-time coordinates affects the phase variation of the chirped laser. Due to the chirp effect, a region exists where the laser wave phase experienced by the electron will vary slowly, as a result the electron can be trapped in the acceleration phase for a long time. This leads to the violent acceleration of the electrons to a very high energy in the main acceleration stage, and when the electron enters the weak field region in the deceleration phase, the lost energy of the electron is insignificant when compared to its gain in the main acceleration stage.

From the above described various schemes for accelerating the charged particles in vacuum using high intensity laser field, the following two schemes of particle acceleration are found to be very promising namely: "the laser driven auto-resonant acceleration" and "direct acceleration of particle by a focused laser field". These schemes are analytically and numerically studied in this thesis and it is shown that the these two schemes of particle acceleration can be easily combined together to enhance the overall efficiency of the acceleration scheme.

The scheme of laser driven auto-resonant particle acceleration is of great interest, as in this scheme the acceleration rate is higher and radiation [92] losses are lower as compared to other schemes of particle acceleration. The renewed interest in this scheme is due to the observation of ultra high magnetic fields in the simulations as well as in the laboratory experiments pertaining to intense laser solid interaction[116, 117, 118, 119, 120, 121]. The observed magnetic fields are typically of the order of hundreds of mega-gauss and in general are found to be in the turbulent state. However in some cases, these fields are found to be coherent for a time duration much greater than that of the time of interaction between the laser pulse and particle. Thus a detailed analytical as well as numerical understanding of the scheme is required to optimize the use of these magnetic field for its experimental realization. The auto-resonant acceleration scheme has been previously studied by several authors in the past. The earlier studies on the scheme were reported using a monochromatic plane electromagnetic wave and it is found that even though these are good for academic interest as well as for basic understanding of the phenomenon, but they lack experimental realization due to the dual requirement of simultaneously maintaining the high intensity lasers as well as static axial magnetic field for long durations. Also, the choice of monochromatic wave is unphysical, as it has no-building or slowing down phase which corresponds to infinite energy. A more realistic approach is thus the use of finite duration laser pulse, which has a build-up as well as slowing-down phase and hence contains a finite amount of energy. In this study, it is reasonably good approximation to consider the particle to be at rest before the onset of interaction. The earlier theoretical studies of the scheme with finite duration laser pulse have used a Sin^2 modulation to describe the temporal shape of the pulse envelope [33, 41, 42]. In these studies, the analytical work has been carried using a periodically self repeating envelope pulse in an infinite modulated wave train. Such an envelope pulse has a discrete frequency spectra in the Fourier space, comprising two additional side band frequencies around the central frequency. Whereas a single period Sin^2 envelope has been used for the numerical study, which has a continuum of frequencies in the Fourier space. This leads to inconsistency in some of the numerical and analytical results such as continuous dependence of energy spectra on the parameter "r($=\frac{\Omega_c}{\omega\Delta}$)", where Ω_c is the cyclotron frequency, ω is the wave frequency and $\Delta(=\Gamma - P_x)$ is a constant of motion associated with the particle motion. Further, in the numerical study the modulation factor is chosen such that an integral number of oscillations are present inside the envelope, which is another restriction to obtain physically acceptable solutions. In the present study, a Gaussian envelope has been used for analytical as well as numerical study of the scheme and it is shown that the choice of this profile circumvent the above problems to give unambiguous comparison between these two results.

The direct particle acceleration by focused laser field is another promising scheme of particle acceleration, which has been studied by many authors in the past. In these studies, it has been shown that the electric and magnetic fields can have a very complicated structure near the focus and lot of work has been done in the description of these fields. The complicated structure of the fields near the focus restricts the analytical description of particle orbits, which are of fundamental importance to understand the mechanism of particle acceleration. Earlier Kaw *et.al*[46] have analytically studied the particle dynamics in the focused laser field using a simplified one dimensional model for focused field. In their study the slow spatial modulation in the laser intensity along the direction of propagation was used to describe the focused laser field. In this thesis, the particle dynamics is numerically studied using an one-dimensional model to determine the quantitative limit of the earlier analytical work and to find the optimum conditions in terms of peak laser intensity(A_0^2), pulse length $(1/\delta)$and (F) focal length for maximum energy gain by the particle. From the comparison of analytical and numerical results it is found that the earlier analytical work is unable to account for the energy gain in the tight focusing regime, in which the contribution due to fast motion becomes important. Thus a higher order adiabatic theory is derived using Lie transformation perturbation method which suitably takes this into account and gives better understanding of the mechanism.

The theoretical understanding of the above two acceleration schemes is used to describe new scheme of particle acceleration. In this scheme the particle is subjected to the combined field of a focused finite duration laser and static axial magnetic field. It is shown that for the suitable choice of parameters, the scheme leads to efficient acceleration of particles. The details of the work has been described in the following chapters.

1.2 Thesis outline

Chapter 2: Particle dynamics in the field of a relativistically intense laser field

This chapter is devoted to the comprehensive review of previous works in the area encompassing the study of particle dynamics in a relativistically intense continuous and pulsed laser field in vacuum [14, 15, 16, 19, 20, 21, 22]. The outline of the chapter is following: First, restricting to a case of continuous laser field, the exact analytical expressions are derived for arbitrary initial conditions describing the particle dynamics in the field of an elliptically polarized laser. The analytical expressions for particle position, momentum and energy are expressed in terms of constants of motion and laser vector potential which is a function of laser phase. These exact analytical expressions have been used to validate the output of the test particle code and to study the particle dynamics in the co-moving frame of average rest and Lorentz boosted frame for different laser polarizations.

The highly non-linear particle dynamics has been segregated into a secular phase averaged guiding center drift and fast oscillating motion. The removal of secular guiding center motion from complete dynamics results in the particle motion in the average frame of rest. The particle dynamics in the co-moving average rest frame has been thoroughly illustrated for different initial conditions. Next, the particle dynamics in the Lorentz boosted frame is studied by deriving a Lorentz transformations utilizing the phase averaged secular motion relating the particle dynamics in the lab frame with proper frame of reference of a particle. A set of different initial conditions have been chosen for illustrating the particle orbits in the proper frame of particle. The study of relativistic effects apart from being of great academic interest also finds an application in the study of accelerator physics.

Alternatively, the particle dynamics has been derived solving the corresponding Hamilton-Jacobi[17, 18, 43] equation for an elliptically polarized continuous as well as pulsed laser field. All the three constants of motion derived above have been obtained. The complete solution of the Hamilton-Jacobi equation makes the problem integrable and provides the information of the spatial and temporal symmetries associated with the system. The general expressions derived solving the Hamilton-Jacobi equation have been used for analytical and numerical study of particle dynamics in a finite duration laser pulse with $Gaussian$ and

$Sech$ temporal envelope profiles. These functions have been chosen for the theoretical study of the pulse particle interaction due to the following reasons. The frequency spectrum of the pulse corresponding to these profiles has a continuum in the Fourier space. The derivatives of these functions are continuous to all orders and the functions together with their respective derivatives vanish identically at the infinities($\pm\infty$) [93]. Moreover for these profiles, the choice of value of modulation factor is not restricted to be an integer for representing the number of oscillations inside a finite duration laser pulse. Thus these profiles suitably takes care of the above specified anomalies associated with Sin^2 temporal envelope for the theoretical study of pulse particle interaction.

Chapter 3: Exact analysis of particle dynamics in the combined field of finite duration laser pulse and static axial magnetic field

This chapter is devoted to the theoretical study of the laser driven auto-resonant acceleration scheme using finite duration laser pulse. As mentioned above, in the earlier work ref.[33, 41, 42] on the topic the analytical results were unable to account for some of the characteristics of the numerical work such as the continuous dependence of the energy gain on the ratio "$r(=\Omega_c/\omega\Delta)$". It is to be point out that the work presented in reference [33] and others references [41, 42] had used a single period Sin^2 envelope pulse for numerical calculation whereas the analytical work has been done with the envelope pulse repeating itself periodically in an infinite train of modulated envelope pulses. Thus whereas the numerical work has been done with a pulse which is made of a continuum spectrum of frequencies in Fourier space, the analytical expressions are derived with a spectral pulse made of three delta function frequencies, the central peak and the two side bands. In this thesis the analytical and numerical work is carried out using a Gaussian temporal modulation for pulse, which gives an unambiguous comparison between the numerical and analytical results.

The major findings of the interaction are the following: the resonant time of interaction between the particle and the pulse has been shown to be finite, unlike for a monochromatic case, the particle in this case can resonate with the laser pulse for a range of frequencies due to the finite width of the pulse, the final energy gain of the particle saturate and the dependence of the gain on "r", has been found to be consistent with the frequency spectrum of the temporally shaped Gaussian laser pulse. In the later part of chapter, the particle dynamics has been studied in the combined field of elliptically polarized finite duration laser pulse and static axial magnetic field. The aim of study is to determine the effect of polarization on the energy gain by the particle. The energy gain of the positively charged particle test particle has been found to be maximum for the right circular polarization and no energy gain was observed for the left circularly polarized laser field. The energy gain corresponding to the right circular polarization has been found to be twice that of the linear polarization for the same parameters of laser pulse viz. pulse length and power.

Chapter 4: Particle dynamics in a focused laser field

This chapter has been devoted to comprehensive numerical validation as well as for determining the quantitative limit of the earlier reported analytical work in ref.[46] describing the particle dynamics in a focused continuous and finite duration pulsed laser field. The focused laser field has been described by a slow spatial variation in the laser intensity along the direction of propagation of the laser. The numerical study of the particle dynamics in a focused continuous laser field has been used for verifying the earlier reported analytical condition of the optimum initial position of the particle resulting in its maximum energy gain at same peak power of the laser. The numerical study has been extended to a more realistic case of focused finite duration laser pulse which is aimed at determining the optimum initial conditions in terms of peak laser intensity, pulse length and focal length for the maximizing the energy gain by the particle. From numerical observations it can be reasoned that, the energy gain by a particle results in the increase of gyration length which can become comparable to the scale length of intensity variation and thus cannot be explained by the analytical results reported in ref.[46]. Thus an improved adiabatic theory is required for analytically obtaining the energy estimates of the particle.

The knowledge of Lie-transformation perturbation method which is based upon Hamiltonian dynamics and canonical transformation [94, 95, 96, 97, 98, 104] is required for deriving the improved adiabatic theory. The details of the method has been described in the following references [99, 100, 101, 102, 103, 104] and working methodology is given in the appendix of the thesis.

Chapter 5: Adiabatic formulation of charged particle dynamics in an inhomogeneous electromagnetic field

This chapter has been devoted to the study of charged particle dynamics in the relativistically intense inhomogeneous electromagnetic field of laser. It has been shown that in an inhomogeneous laser field the particle dynamics is devoid of the longitudinal constant of motion. As a result the total number of constants of motion is reduced by one which in turn makes the problem non-integrable. Thus the particle dynamics cannot be described in terms of constants of motion and vector potential, as was possible previously. However, it has been shown that for the slow variation in the laser intensity, the particle dynamics can be expressed in terms of an adiabatic invariant. Slowness in the variation of laser intensity is parameterized in terms of adiabaticity parameter "ϵ", which is defined as the ratio of gyration length of particle to scale length of variation in laser intensity. In the adiabatic approximation ($\epsilon << 1$), one can separate the particle dynamics in terms of fast varying quiver motion and phase averaged slow motion. Particle dynamics corresponding to the fast motion is associated with an adiabatic invariant, which is evaluated up to 2^{nd} order in the adiabaticity parameter using the Lie transform perturbation method [99, 100, 101, 102, 103, 104].

As an application of above derived adiabatic theory the problem of acceleration of a charged particle in vacuum by focused laser field(inhomogeneous laser field) is revisited which was earlier analytically investigated by Kaw *et.al.* in ref.[46]. The previously considered analysis corresponds to first order of the present adiabatic theory, however the first order contribution from the fast dynamics was no taken into account. The energy estimates obtained by numerically solving the relativistic equation of motion for a focused light field are compared with the results of adiabatic theory. It is shown that the energy estimates improve with the inclusion of higher order terms of the series.

Chapter 6: Particle acceleration by cyclotron auto-resonance with a focused finite duration laser pulse

In this chapter, a new scheme has been described based upon the cyclotron auto-resonant technique for acceleration of the charged particle in vacuum. In this mechanism a particle is subjected simultaneously to the combined field of a static axial magnetic field and a focused linearly polarized finite duration pulse whose temporal envelope shape is described by a Gaussian profile. The focused laser field is described by a slow spatial variation in the laser intensity along the direction of its propagation. In this mechanism the particle acceleration is achieved in two stages, at first an initially non-resonant particle is accelerated by the focused field of a pulse which drives it to a cyclotron resonance and thus subjecting it to a second stage resonant acceleration. It is shown that the use of static axial magnetic field leads to significant increase in energy gain by the particle in comparison to the un-magnetized focused finite duration laser pulse [45, 46, 105]. It is further shown that the initial energy gain of the particle by the focused field significantly lowers the required strength of the static axial magnetic field as well as of the laser intensity and hence making it an efficient scheme for particle acceleration.

Chapter 7: Summary and Conclusions

This chapter contains the summary of all the results described in the thesis and outline of the future work in the area.

2

Particle dynamics in the field of a relativistically intense laser

In this chapter the problem of a charged particle interacting with a continuous and pulsed electro-magnetic field of a laser has been reviewed from a general point of view using the constants of motion. The study elucidate some important characteristics regarding the trajectory, momentum and energy of a charged particle interacting with such high intensity laser fields in vacuum. The methodology described in this chapter for deriving the dynamics of a particle is to be used in the succeeding chapters. Further, the exact analytical solutions are derived for the first time describing the dynamics of a particle in a finite duration laser pulse, which give unambiguous comparison of the numerical and analytical results. The understanding of all these aspects lays foundation to the study of various schemes of laser driven particle acceleration.

2.1 Introduction

The study of particle dynamics in the field of a relativistically intense electromagnetic wave in vacuum has been one of the extensively investigated research topics in plasma physics. The diversity of the topic has led to numerous studies in the areas ranging from astrophysics to the generation of accelerated charged particles in the laboratory. To mention a few the wave-particle interaction forms the basis for understanding the phenomenon such as particle motion in Van Allen radiation belts [106], wave particle resonances [107], particle scattering by waves [108], Thomson scattering [18, 109, 110], free electron lasers[111], stochastic acceleration [112, 113, 114], stochastic heating[115], microwave generation, laser-matter interaction, particle acceleration, etc. In particular the topic of laser driven particle acceleration has been of great interest for last so many years, which has got further enhanced due to the experimental generation of accelerated charged particles in the laboratories. The success of these laser driven particle accelerators can be attributed to rapid advances in the optical technology such advent of CPA technique[1, 2, 3], which has lead to the availability of the table top high powered lasers in laboratories. The dynamics of a particle in such strong laser fields becomes relativistic with in one laser field, which in turn makes its study fundamental for the understanding of various acceleration schemes.

In this chapter, the dynamics of a charged particle has been analytically and numerically studied in the field of a relativistically intense continuous as well as finite duration laser field[14, 15, 16, 19, 20, 21, 22]. The methodology described here for obtaining the solutions encompasses the review of the earlier works on the topic. At first, the particle dynamics in the field of a continuous elliptically polarized laser is derived solving the relativistic equation of motion for a set of arbitrary initial conditions. The exact analytical expressions describing the particle position, momentum as well as the energy are expressed in terms of constants of motion and the vector potential only. These analytical expressions describing the non-linear dynamics of the particle are used to study the particle dynamics in the average rest frame and Lorentz boosted frame. The particle dynamics in the average rest frame is derived by integrating the exact expressions for particle position over fast varying oscillatory motion, which yields phase averaged expressions for the guiding center co-ordinates of the particle position and then subsequently subtracting them from the exact expressions. The phase averaged guiding center velocity is obtained by differentiating the corresponding phase averaged particle position. The Lorentz transformations are derived using phase averaged velocity connecting the particle trajectories in the lab to the Lorentz boosted frame of reference. A set of different initial conditions as well as laser polarizations are used to throughly illustrate the particle trajectories in all the three different frames viz., lab, average rest and Lorentz boost.

Alternatively, the general expressions describing the particle dynamics in a continuous as well finite duration laser have been derived by solving the corresponding Hamilton-Jacobi equation[17, 18, 43]. The method of solution of Hamilton-Jacobi equation provides an insight into the various symmetries associated with dynamics and the corresponding constants of motion. The dynamical variables viz. position, momentum and energy obtained are expressed in terms of constants of motion and vector potential.

Further, a set of new exact analytical expressions has been reported describing the particle dynamics in the field of a finite duration laser choosing $Gaussian$ and $Sech$ shaped temporal profiles. The choice of these profiles provides the correct analytical as well as numerical description of the particle dynamics. For the numerical studies these profiles can accommodate arbitrary number of oscillations, which is in contrast to the previously used Sin^2 temporal envelope which can only be used for the integral number of laser oscillations. For the non-integral number of laser wave periods the higher order derivatives of the vector potential for the Sin^2 envelope do not vanish at the boundaries and results in finite contribution, which can lead to unphysical results, whereas these profiles along with their derivatives to all orders vanish smoothly at the infinity. In the analytical description, the expressions describing the particle dynamics for Sin^2 modulation are derived representing it as a single pulse in the self repeating continuous wave train of pulses, which can lead to anomalous results. This anomaly in the description of the particle dynamics is circumvented by the choice of these profiles.

The organization of the chapter is the following: Section (2.2), contains the classical description of charged particle dynamics in a relativistically intense laser field obtained by solving the equation of motion. Sub-sections (2.2.1) and (2.2.2), contains the study of particle dynamics in the average rest frame and Lorentz boosted frame of reference using the above derived exact analytical expressions. Section (2.3), contains the methodology of solution of Hamilton-Jacobi equation for deriving the dynamics of a charged particle in relativistically intense laser field. The exact analytical expressions for the particle dynamics corresponding to the $Gaussian$ and $Sech$ shaped temporal profiles are derived using the general solutions obtained solving Hamilton-Jacobi equation. Section (2.4), contains the summary and conclusions of the chapter.

2.2 Classical relativistic dynamics of a charged particle in the field of an elliptically polarized plane electromagnetic wave

In this section the particle dynamics is studied in the field of a relativistically intense elliptically polarized continuous laser in vacuum. The vector potential describing the monochromatic elliptically polarized electromagnetic wave is given by,

$$\vec{A} = a_1 cos(\xi)\hat{y} + a_2 sin(\xi)\hat{z} \tag{2.1}$$

here the symbols have the following meaning: $\xi = (kx - \omega t)$ is the invariant phase, A_0 is the maximum amplitude of the wave with $a1 = \kappa A_0$, $a2 = (1-\kappa^2)^{1/2} A_0$, κ is the polarization factor, which for linear polarization has a value $\kappa \to 0, \pm 1$ and for circular case takes value $\kappa \to \pm\frac{1}{\sqrt{2}}$.

From here on the following normalization have been used in this chapter: $\vec{r} \to k\vec{r}, t \to \omega t, \vec{P} \to \frac{\vec{P}}{mc}, \Gamma \to \frac{\Gamma}{mc^2}, B \to \frac{qB}{m\omega c}, E \to \frac{qE}{mc\omega}, \hat{A} \to \frac{eA}{mc^2}$.

The normalized Electric and Magnetic Field are defined as

$$\vec{E} = -\frac{\partial \vec{A}}{\partial t} = a_1 sin(\xi)\hat{y} - a_2 cos(\xi)\hat{z}; \qquad \vec{B} = \nabla \times \vec{A} = a_2 cos(\xi)\hat{y} + a_1 sin(\xi)\hat{z}$$

The normalized momentum and energy equations are given by

$$\frac{d\vec{P}}{dt} = [\vec{E} + \frac{\vec{P}}{\Gamma} \times \vec{B})] \tag{2.2}$$

$$\frac{d\Gamma}{dt} = \frac{\vec{P}.\vec{E}}{\Gamma} \tag{2.3}$$

Writing equations in component form

$$\frac{dP_x}{dt} = \frac{1}{\Gamma}(P_y B_z - P_z B_y) \tag{2.4}$$

$$\frac{dP_y}{dt} = E_y - \frac{P_y}{\Gamma} B_z \tag{2.5}$$

$$\frac{dP_z}{dt} = E_z + \frac{P_x}{\Gamma} B_y \tag{2.6}$$

$$\frac{d\Gamma}{dt} = \frac{1}{\Gamma}(P_y E_y + P_z E_z) \tag{2.7}$$

P_x, P_y, P_z are four momentum components. The relativistic factor is given by $\Gamma = (1 + P_x^2 + P_y^2 + P_z^2)^{1/2}$.

From the above definition of electric and magnetic field it can be seen that $E_y = B_z$ and $E_z = -B_y$, using this a constant of motion $\Delta (= \Gamma - P_x)$ can be obtained by subtracting the Eq.(2.4) from Eq.(2.7). The invariant phase is related to the constant of motion as $\dot{\xi} = \frac{\Delta}{\Gamma}$, which can be used to express the momentum and energy of a particle as

$$P_x = \frac{1 - \Delta^2}{2\Delta} + \frac{P_y^2 + P_z^2}{2\Delta} \tag{2.8}$$

$$P_y = \alpha - a_1 cos(\xi) \tag{2.9}$$

$$P_z = \alpha_1 - a_2 sin(\xi) \tag{2.10}$$

$$\Gamma = \frac{1 + \Delta^2}{2\Delta} + \frac{P_y^2 + P_z^2}{2\Delta} \tag{2.11}$$

In the above equations α and α_1 are the exact constants of motion.

The particle position can be obtained as,

$$\vec{r} - \vec{r_0} = \frac{1}{\Delta} \int_{\xi_0}^{\xi} \vec{P} d\xi. \tag{2.12}$$

In terms of co-ordinates the position of the particle is given by

$$\begin{aligned} x - x_0 = & \frac{1}{2\Delta^2}[1 - \Delta^2 + \alpha^2 + {\alpha_1}^2 + \frac{{a^2}_1 + {a^2}_2}{2}](\xi - \xi_0) - \\ & \frac{1}{\Delta^2}[a_1 \alpha (sin(\xi) - sin(\xi_0)) - \alpha_1 a_2 (cos(\xi) - cos(\xi_0))] + \\ & \frac{{a_1}^2 - {a_2}^2}{8\Delta^2}[sin(2\xi) - sin(2\xi_0)] \end{aligned} \tag{2.13}$$

$$y - y_0 = \frac{1}{\Delta}[\alpha(\xi - \xi_0) - a_1(sin(\xi) - sin(\xi_0))] \tag{2.14}$$

$$z - z_0 = \frac{1}{\Delta}[\alpha_1(\xi - \xi_0) + a_2(cos(\xi) - cos(\xi_0))] \tag{2.15}$$

In the equations from Eq.(2.13) to Eq.(2.15), ξ_0 is the initial phase of the wave as seen by the particle. The above equations describe the momentum, energy and position of a particle in an exact form. The dynamical variables for particle dynamics in the field of relativistically intense, elliptically polarized continuous laser have been represented in terms of constants of motions and vector potential only. These solutions provides insight into the dynamics of the particle and can be used to understand its different physical aspects, some of which have been described in the following subsections.

2.2.1 Particle dynamics in an average rest frame

The exact solutions derived above on solving the relativistic equation of motion describes the dynamics of a particle in the lab frame for an arbitrary initial conditions. From these solution it is evident that the dynamics of particle in a relativistically intense laser fields is highly non-linear and results in a complicated particle trajectories. Thus making it worthwhile to examine the particle dynamics in a frame of reference in which there is no average displacement of the particle over one period. In order to do this the expression describing the dynamics of the particle dynamics are separated into expressions for the phase averaged slow guiding center motion and fast oscillatory motion. The position coordinates of the guiding center are obtained by integrating the particle position over one oscillation (i.e averaging over ξ and $\bar{\xi} = (t - \bar{x})$), which gives $\delta x = x - x_0$ and $\xi - \xi_0 = t - \delta x$. The detailed methodology is described below and on averaging the exact co-ordinates of the particle position over one laser period

$$\bar{\delta x} = \frac{1 - \Delta^2 + \alpha^2 + \alpha_1^2 + \frac{a_1^2+a_2^2}{2}}{1 + \Delta^2 + \alpha^2 + \alpha_1^2 + \frac{a_1^2+a_2^2}{2}} t - 2\frac{(\alpha_1 a_2 cos(\xi_0) - \alpha a_1 sin(\xi_0))}{1 - \Delta^2 + \alpha^2 + \alpha_1^2 + \frac{a_1^2+a_2^2}{2}} \tag{2.16}$$
$$- \frac{(a_1^2 - a_2^2)}{4(1 - \Delta^2 + \alpha^2 + \alpha_1^2 + \frac{a_1^2+a_2^2}{2})} sin(2\xi_0).$$
$$\bar{\delta y} = \frac{1}{\Delta}[\alpha(t - \bar{\delta x}) + a_1 sin(\xi_0)] \tag{2.17}$$
$$\bar{\delta z} = \frac{1}{\Delta}[\alpha_1(t - \bar{\delta x}) - a_2 cos(\xi_0)]. \tag{2.18}$$

The corresponding guiding center velocity is given by,

$$v_{gx} = \frac{1 - \Delta^2 + \alpha^2 + \alpha_1^2 + \frac{a_1^2+a_2^2}{2}}{1 + \Delta^2 + \alpha^2 + \alpha_1^2 + \frac{a_1^2+a_2^2}{2}} \tag{2.19}$$

$$v_{gy} = \frac{2\alpha\Delta}{1 + \Delta^2 + \alpha^2 + \alpha_1^2 + \frac{a_1^2+a_2^2}{2}} \tag{2.20}$$

$$v_{gz} = \frac{2\alpha_1\Delta}{1 + \Delta^2 + \alpha^2 + \alpha_1^2 + \frac{a_1^2+a_2^2}{2}} \tag{2.21}$$

The particle coordinates in the oscillation center frame can be derived by subtracting the guiding center coordinates from lab frame co-ordinates of the particle. Thus corresponding oscillation center particle position is given by,

$$x_{osc} = \delta x - \bar{\delta x} \tag{2.22}$$

$$y_{osc} = \delta y - \bar{\delta y} \tag{2.23}$$

$$z_{osc} = \delta z - \bar{\delta z} \tag{2.24}$$

The relativistic velocity factor (γ) is given by $\beta = (v_{gx}^2 + v_{gy}^2 + v_{gz}^2)^{1/2}$ and $\gamma = 1/\sqrt(1-\beta^2)$. In this chapter, the relativistic factor corresponding to phase averaged motion is given by '$gamma$', to distinguish it from previously defined '$Gamma$' factor. Thus the non-linear particle dynamics in the lab frame has been be separated into a phase averaged slow $``guiding''$ center and fast varying $``oscillation''$ center motion. The motion in the fast varying $``oscillation''$ center corresponds to a reference frame, in which there is no net displacement of the particle over gyration. In the following figures, the particle dynamics in the configuration space is described by separating it in terms of lab, guiding center and oscillation center co-ordinates for the linear, circular as well as elliptical polarizations. A different sets of initial conditions are used for the thorough illustrations of the particle dynamics.

Linear Polarization

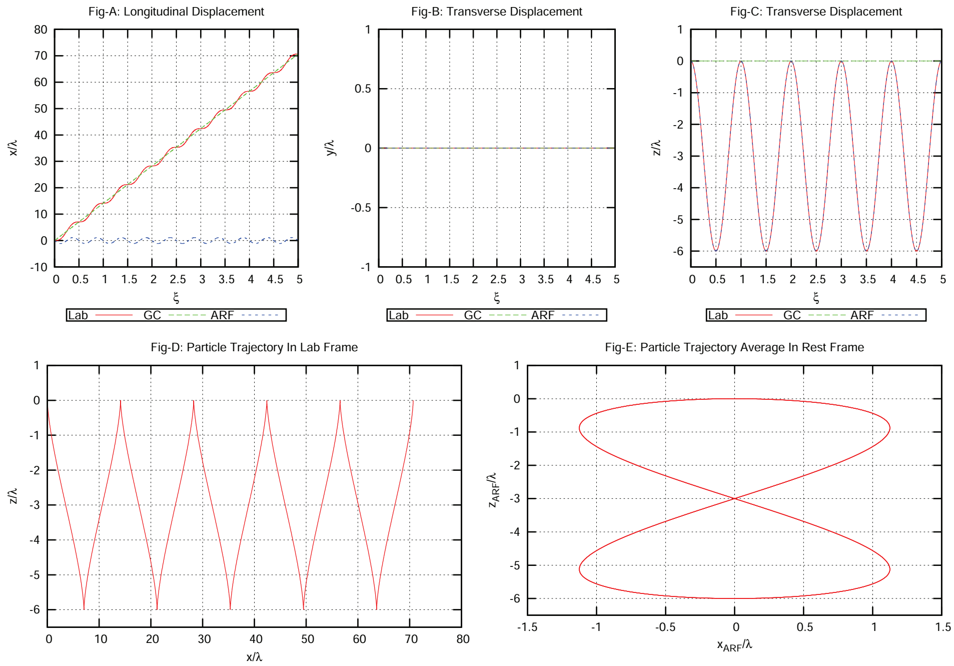

Figure 2.1: Particle Displacement(Linear Polarization): Subplot(A-B-C), plot for the evolution of components of particle position along the three co-ordinates in the lab, guiding center and average rest frame. Subplot:(D-E): Particle trajectory in the lab and average rest frame.

At first the particle dynamics is studied in the field of linearly polarized continuous electromagnetic wave for a particle starting initially at rest and subjected to the laser at minimum of the wave is shown in Fig.(2.1). The evolution of the particle in the configuration space along the co-ordinates is shown in the subplots (A-B-C) and particle dynamics is divided into phase averaged slow $``guiding''$ center and fast varying $``oscillation''$ center, which is compared to the exact evolution in lab. It can be seen that the particle has slow secular drift along the direction of propagation of the laser and there is no net displacement of the particle in the transverse direction. It can be further inferred that the particle oscillates at twice the frequency along the direction of propagation in comparison to the transverse direction. The exact particle trajectory is shown in the subplots (D-E) which is compared to that in the fast varying $``oscillation''$ center. In this fast varying average rest frame the particle trajectory resembles the numeric number eight and is also know as the figure of eight motion.

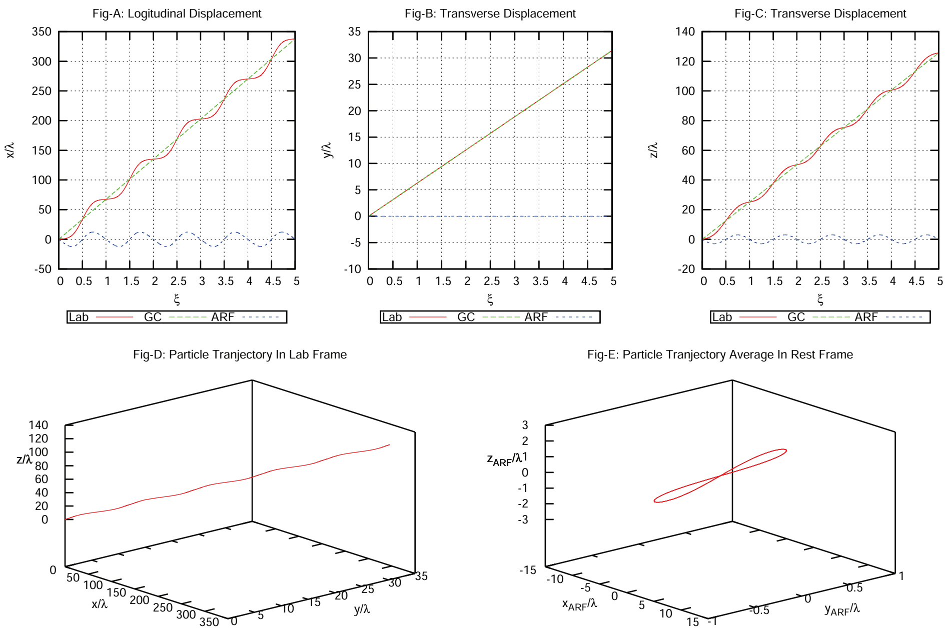

Figure 2.2: Particle Displacement(Linear Polarization): Subplot(A-B-C), plot for the evolution of components of particle position along the three co-ordinates in the lab, guiding center and average rest frame. Subplot:(D-E): Particle trajectory in the lab and average rest frame.

In the above figure Fig.(2.2), the evolution of the position co-ordinates correspond to the case, when it has initial velocity and interaction with the wave starts at initial phase($\pi/4$) different from the minimum. It can be seen that the particle has non-zero secular displacement along all three co-ordinates, which is shown in subplots (A-B-C) of the figure. The corresponding particle trajectory has been shown in the sub-plot (D-E) of the figure. It can be seen that in the average rest frame particle follows a figure of eight trajectory which is tilted at angle to the direction of propagation of the wave.

Circular Polarization

In the subplots (A-B-C) of the following figure Fig.(2.3), the evolution of the particle position is described as a function of invariant phase (ξ) for a circularly polarized laser along the three co-ordinates of the configuration space. The particle is considered to be initially at rest and initial interaction begins at ($\xi_0 = 0$) phase of the wave. It can be seen that the particle is displaced in the longitudinal as well as transverse directions. The corresponding trajectories of the particle in the lab and average rest frame are shown in the subplots (D-E) of the figure. From the figure it can be seen that the particle comes back to rest at the end of each successive gyration and it traces out a circular trajectory in the average rest frame.

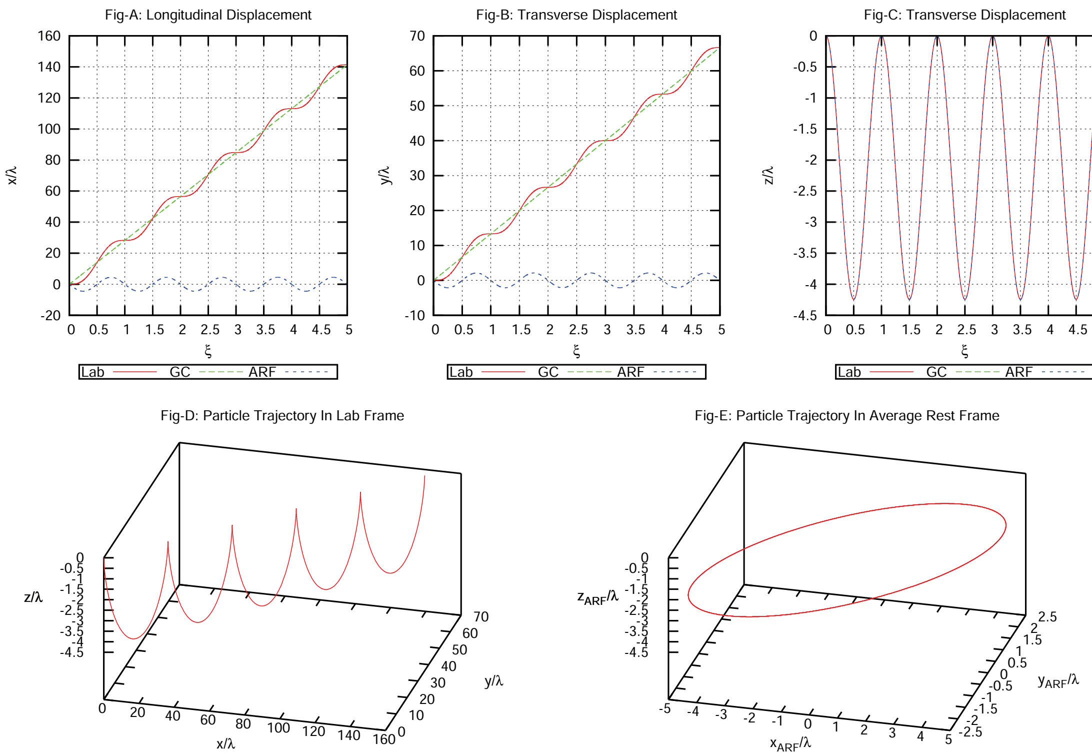

Figure 2.3: Particle Displacement(Circular Polarization): Subplot(A-B-C), plot for the evolution of components of particle position along the three co-ordinates in the lab, guiding center and average rest frame. Subplot:(D-E): Particle trajectory in the lab and average rest frame.

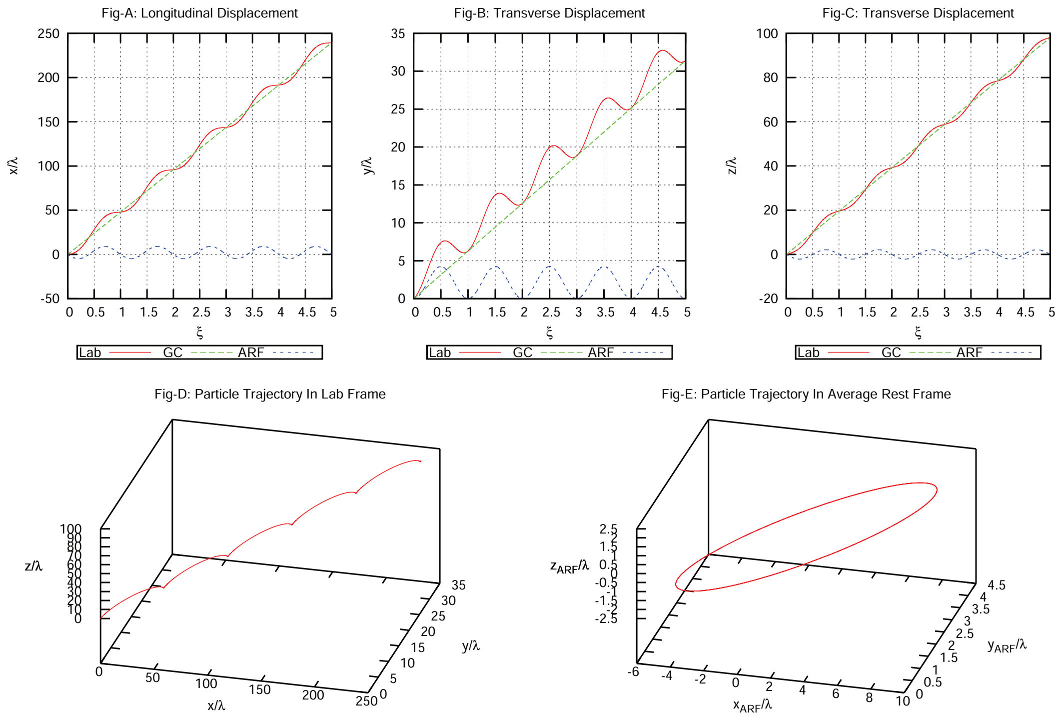

Figure 2.4: Particle Displacement(Circular Polarization): Subplot(A-B-C), plot for the evolution of components of particle position along the three co-ordinates in the lab, guiding center and average rest frame. Subplot:(D-E): Particle trajectory in the lab and average rest frame.

In the Fig.(2.4), the evolution of the particle position in the field of circularly polarized laser is shown along the configuration space. The subplot(A-B-C) and subplots(D-E), describes the particle trajectories in the lab and average rest frame respectively. These correspond to initial conditions that the particle interacting with the laser field has a finite initial velocity and at the onset of the interaction with wave the initial phase is given by ($\xi_0 = \pi/4$). The particle trajectory is composed of fast oscillatory motion along with the finite displacement in the longitudinal and transverse directions. The finite secular drift corresponds to phase averaged guiding center motion and in the average rest frame the particle follows closed orbit, which signifies that it comes back to initial velocity at the end of each successive gyration. The diameter of the circular particle trajectory in the average rest frame is increased as a result of initial energy and is tilted at angle to the horizontal(x-y)plane.

Elliptical Polarization

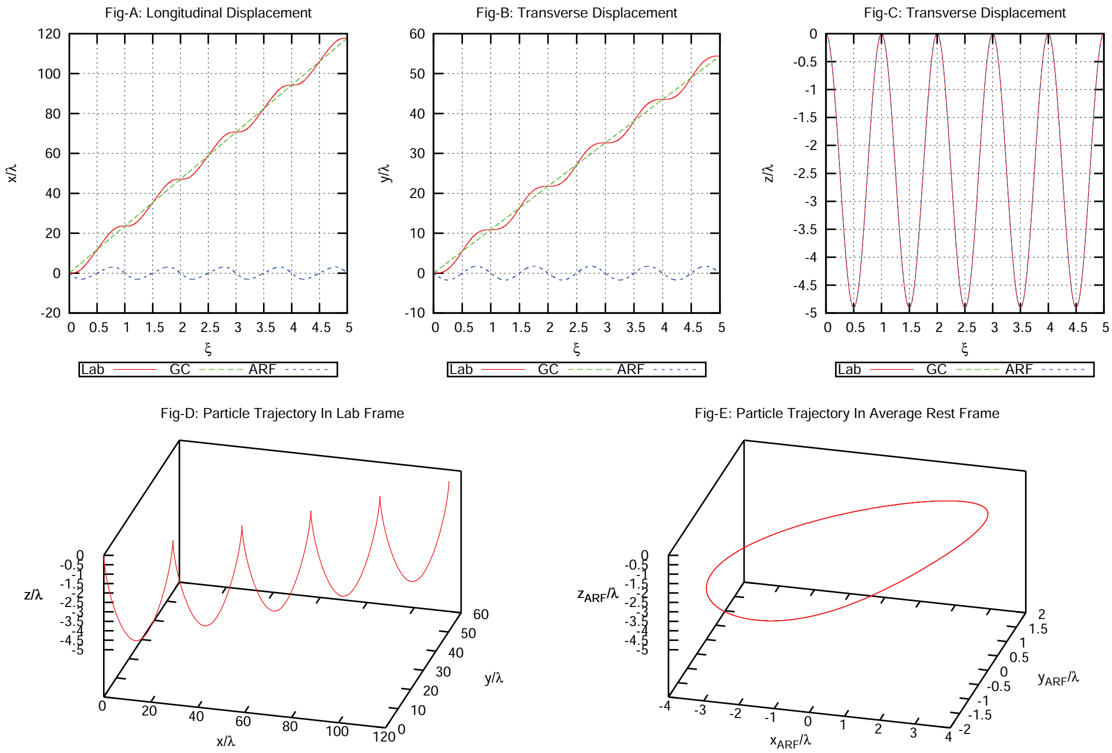

Figure 2.5: Particle Displacement(Elliptical Polarization): Subplot(A-B-C), plot for the evolution of components of particle position along the three co-ordinates in the lab, guiding center and average rest frame. Subplot:(D-E): Particle trajectory in the lab and average rest frame.

In the subplots(A-B-C) of the figure Fig.(2.5), the evolution of the particle position is described along the three co-ordinates in an elliptically polarized wave and its corresponding trajectories in the lab as well as average rest frame are shown in subplots(D-E). In this figure, the polarization of the wave is defined by choosing $\kappa = 1/\sqrt{3}$ and the particle is considered to be at rest at the onset of interaction, which begins at initial phase $\xi_0 = 0$. The particle has a finite displacement along the longitudinal as well as in transverse directions, which is shown in the phase averaged motion described in the subplot(A-B). The particle follows an elliptical trajectory in the average rest frame which is shown in the subplot(E) of the figure.

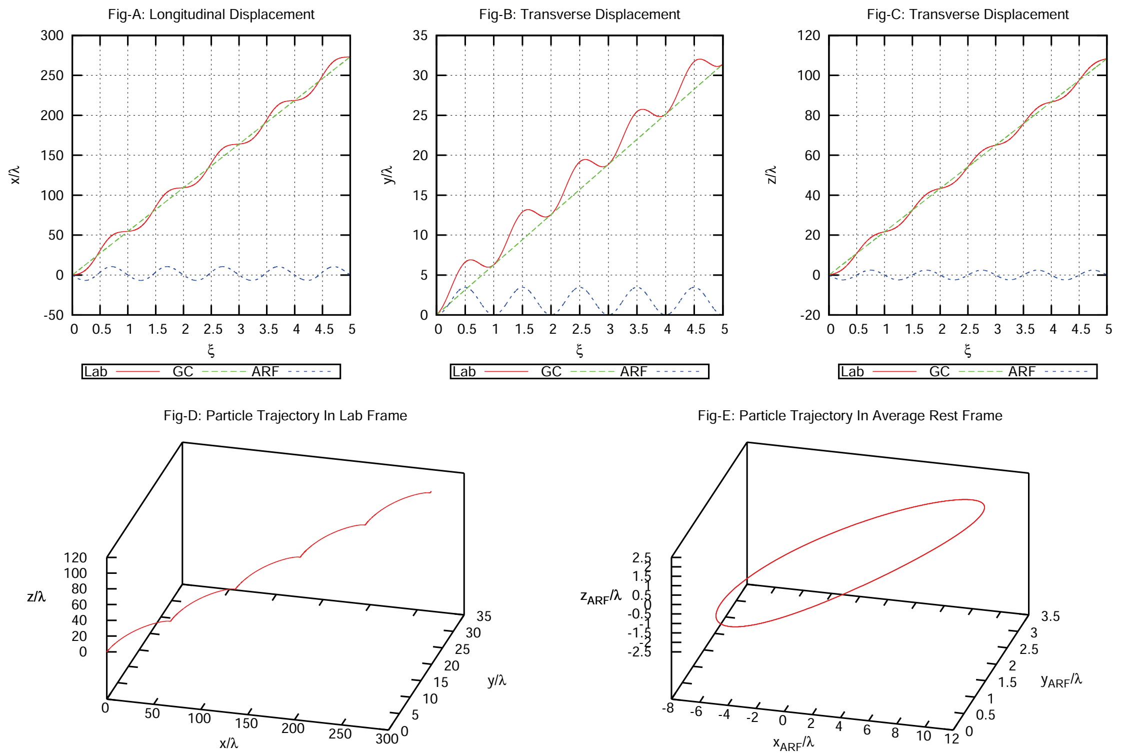

Figure 2.6: Particle Displacement(Elliptical Polarization): Subplot(A-B-C), plot for the evolution of components of particle position along the three co-ordinates in the lab, guiding center and average rest frame. Subplot:(D-E): Particle trajectory in the lab and average rest frame.

In the subplot(A-B-C) of the following figure Fig(2.6), the evolution of the particle position along the three co-ordinates is shown in the lab, average rest frame as well as in guiding center for a continuous elliptically polarized wave. These corresponds to the initial condition that the particle interacts with the wave with an initial velocity and at an initial phase of ($\xi_0 = \pi/4$). The lab motion is divided into the phase averaged slow guiding center motion and fast varying phased averaged motion. The guiding center of the particle has phase averaged secular drift along the longitudinal as well as transverse directions. The particle trajectory in the lab frame and average rest is shown in the subplots(D-E), where it can be seen that the particle traces out a bigger ellipse and is at an angle to (xy) plane in the frame of average rest. In this the figure similar to the previous the figure Fig.(2.5) above, the polarization of the particle is given by $\kappa = 1/\sqrt{3}$.

2.2.2 Particle dynamics in a Lorentz boost frame

In this section the above derived exact analytical results are used to study the particle motion in the Lorentz boosted frame of reference. The Lorentz transformations have been derived relating the particle dynamics in the lab frame with Lorentz boost frame. These studies are important in the study of the accelerated charged particles. The methodology can be described in a following way, consider two reference frames k and $k^{'}$, whose axis are parallel to each other, but the velocity $\vec{v}$ of the frame $k^{'}$ in the frame k is in arbitrary direction. If frame $k^{'}$ moves parallel to the $x-axis$, then transformation equations are

$$x_0{'} = \gamma(x_0 - \beta x) \tag{2.25}$$
$$x^{'} = \gamma(x - \beta x_0) \tag{2.26}$$
$$y^{'} = y \tag{2.27}$$
$$z^{'} = z \tag{2.28}$$

For arbitrary direction of $\vec{v}$

$$x_0 = \gamma(x_0 - \vec{\beta}\vec{x})$$

. As in the Lorenz transformation the perpendicular coordinates remain invariant therefore

$$\vec{x^{'}} \times \vec{\beta} = \vec{x} \times \vec{\beta}.$$

Relation for $\vec{x^{'}}$, is obtained as

$$\vec{\beta} \times (\vec{x^{'}} \times \vec{\beta}) = \vec{\beta} \times (\vec{x} \times \vec{\beta}).$$

On re-arranging:

$$\vec{x^{'}} = \vec{x} + \frac{\vec{\beta}(\vec{x^{'}}.\vec{\beta}) - \vec{\beta}(\vec{x}.\vec{\beta})}{\beta^2}.$$

Using Eq.(2.26) and simplifying the above expression yields:

$$\vec{x^{'}} = \vec{x} + \frac{(\gamma-1)(\vec{\beta}.\vec{x})\vec{\beta}}{\beta^2} - \gamma\vec{\beta}x_0. \tag{2.29}$$

In the following figures the trajectories of the particle in the lab frame are compared with that in the Lorentz boosted frame of reference using Eq.(2.29), for different polarizations of the laser field.

Linear Polarization

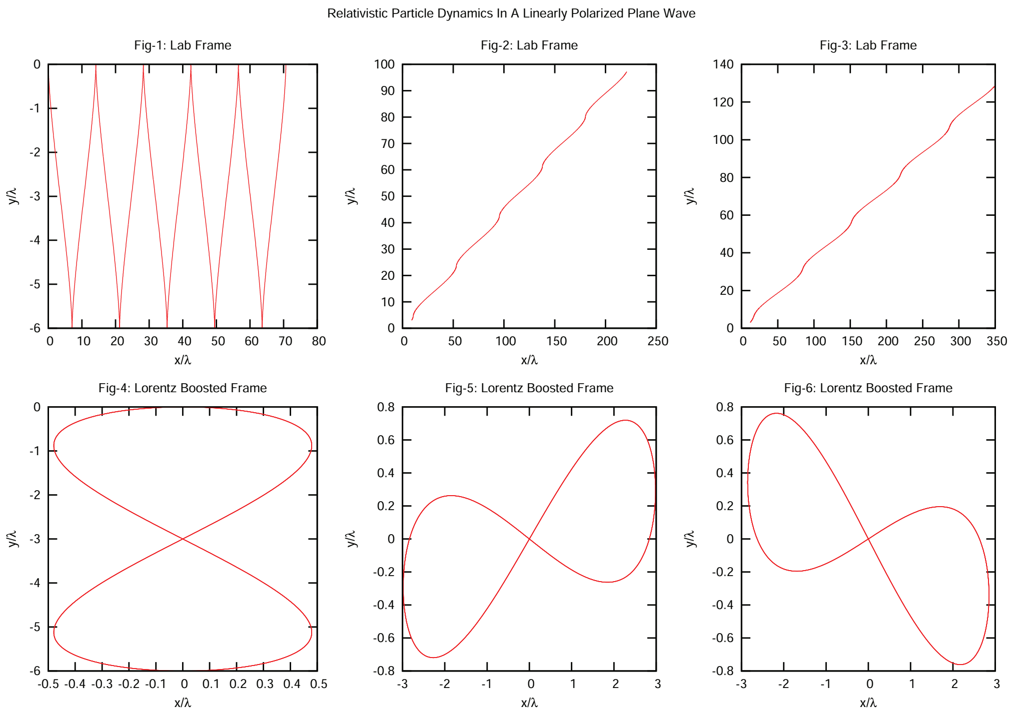

Figure 2.7: Particle motion in average rest frame and Lorentz boost frame for different parameters

In the above figure Fig.(2.7), the trajectories of the particle in a linearly polarized wave in lab and corresponding Lorenz boosted frame are described in subplot(1-2-3) and subplot(4-5-6) respectively. For a linearly polarized wave the particle traces out a figure of eight trajectory in the Lorentz boosted frame. The different trajectories corresponds to the different initial conditions to which the particle is subjected to at the onset of the wave particle interaction. In subplot(1,4), the particle is considered to be initially at rest at the onset of the interaction with the wave, which begins at an initial phase ($\xi_0 = 0$) of the wave. Further in subplot (2,5), the particle has an initial velocity at the onset of the interaction which results in the relativistic effect such as length contraction when seen from the lab frame. In the last subplots (3,6), the particle has initial velocity and the interaction with the wave starts at initial phase ($\xi_0 = \pi/4$).

Circular Polarization

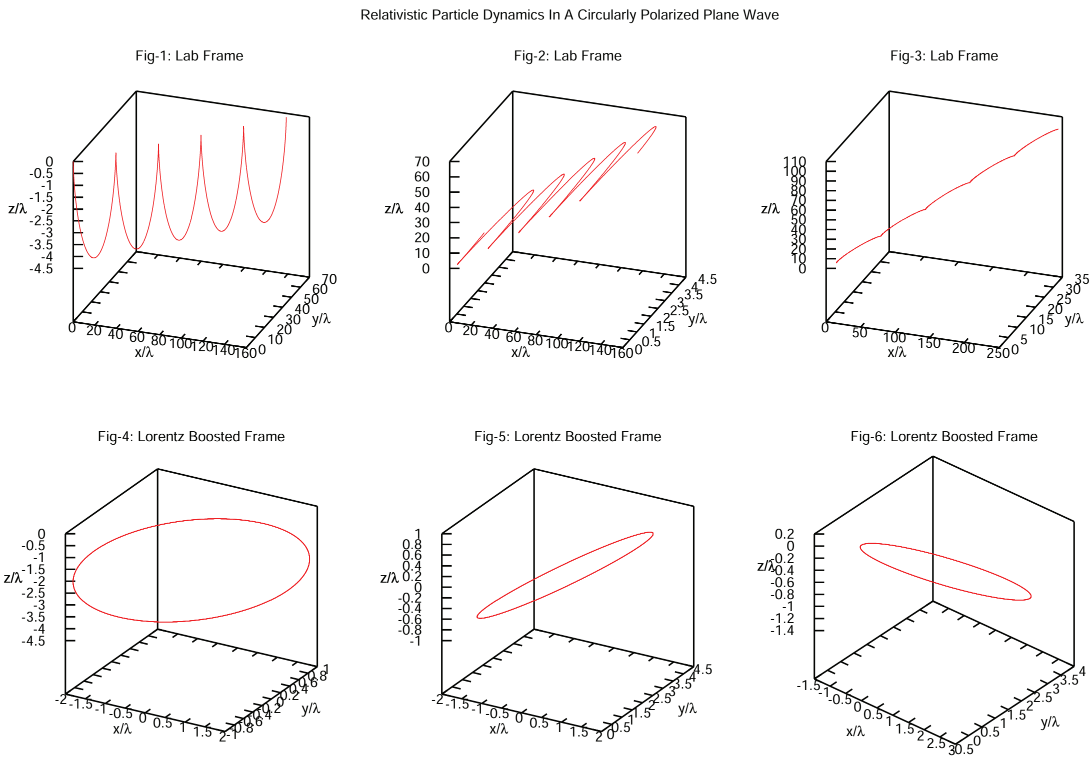

Figure 2.8: Particle motion in average rest frame and Lorentz boost frame for different parameters

In the above figure Fig.(2.8), the particle trajectories are shown in the circularly polarized wave in lab as well as in the Lorentz boost frame of reference which are described in subplots(1-2-3) and subplots (4-5-6) respectively. The trajectory of the particle is circular for the circular polarization of the wave in the Lorentz boost frame of reference. The different trajectories corresponds to the different initial conditions such as in subplot(1,4) at the onset of interaction with pulse the particle is initially at rest and the interaction begins at initial phase ($\xi_0 = 0$) of the wave. The relativistic effect such length contraction are shown by giving initial velocity to the particle, which interacts with the wave at initial phase ($\xi_0 = 0$) and ($\xi_0 = \pi/4$) described in subplots(2,5) and subplots(3,6) respectively.

Elliptical Polarization

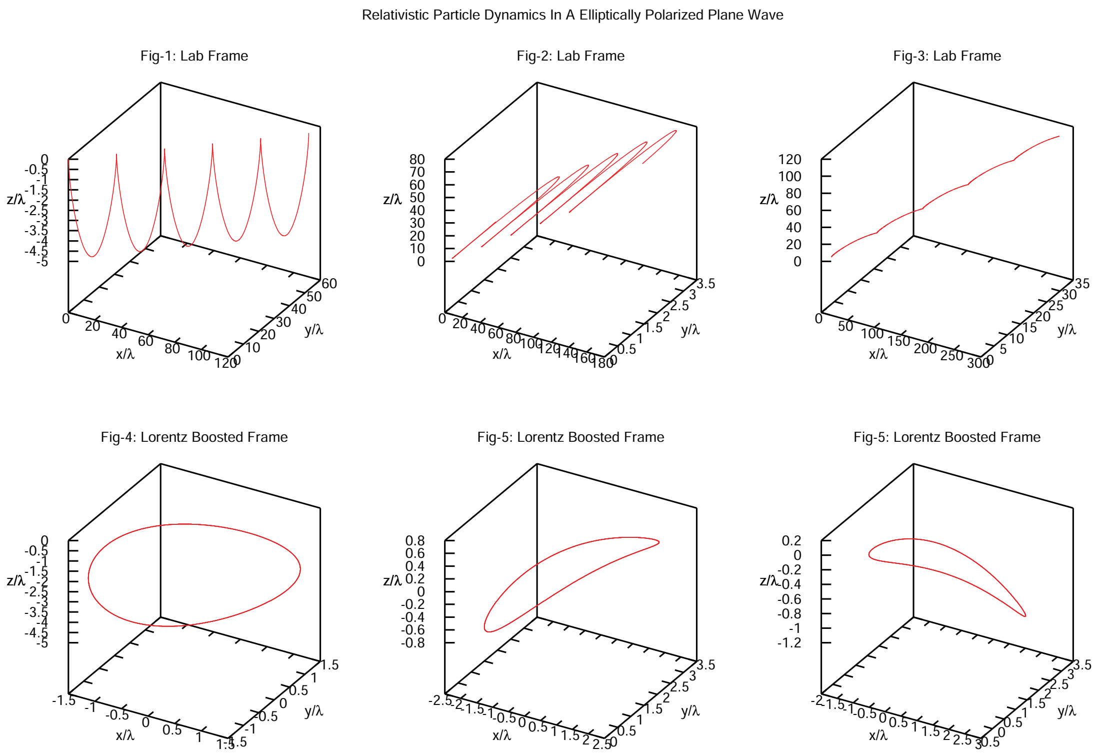

Figure 2.9: Particle motion in average rest frame and Lorentz boost frame for different parameters

In the above figure Fig.(2.9), the trajectories of the particle in the lab and Lorentz boosted frame are shown in subplots(1-2-3) and subplots(4-5-6). The electromagnetic wave is considered to be elliptically polarized and the polarization factor has a value ($\kappa = 1/\sqrt{3}$), in such a polarization the particle traces out an elliptical trajectory in the Lorentz boosted frame of reference. The relativistic effects have been demonstrated by choosing different set of initial conditions, in the subplots(1,4) the particle is considered to be initially at rest with the initial phase of a wave having a value($\xi_0 = 0$). In the subsequent subplot(2,5) and the subplot(3,6) the particle starts interacting with the wave with finite velocity and the wave particle interaction starts at the initial phase of the wave given by ($\xi_0 = 0$) and ($\xi_0 = \pi/4$).

2.3 Hamilton-Jacobi equation for charged particle in relativistically intense laser field

In the previous section, the exact analytical expressions have been derived solving the relativistic equation of motion. It is shown that the particle dynamics is associated with three constants of motion and the dynamical variables viz. position, momentum and energy are expressed in terms of these constants of motion and vector potential only. Alternatively, the dynamics of the particle can also be derived solving the Hamilton-Jacobi[17, 18, 43]equation of motion. The method of solution provides deeper insight into the particle dynamics, such the understanding of the various symmetries associated with the particle dynamics and the corresponding constants of motion. The methodology of the solution is the following,

Starting with the Lagrangian of the charged particle in the electromagnetic field which is given by

$$L = -\sqrt{1-u^2} + \vec{u}.\vec{A} - \phi \tag{2.30}$$

where ϕ is the electrostatic potential and is equal to zero in vacuum.

The normalized canonical conjugate momentum is

$$\vec{P} = \frac{\partial L}{\partial u} = \Gamma \vec{u} + \vec{A} \tag{2.31}$$

In Eq.(2.31) describing the canonical particle momentum which is composed of kinetic momentum $\vec{p} = \Gamma\vec{u}$ and the field momentum $\vec{A}$

Hence re-writing the conjugate momentum

$$\vec{P} = \vec{p} + \vec{A} \tag{2.32}$$

The particle velocity is given by

$$\vec{u} = \frac{\vec{p}}{\Gamma} \tag{2.33}$$

Using the above expression

$$\Gamma = \sqrt{1+p^2} \tag{2.34}$$

and hence

$$\vec{u} = \frac{(\vec{P} - \vec{A})}{\sqrt{(\vec{P} - \vec{A})^2 + 1}}. \tag{2.35}$$

The Hamiltonian is defined as

$$H = \vec{u}.\vec{P} - L. \tag{2.36}$$

On substituting the values of Γ and $\vec{u}$ in the above expression results in

$$H = \sqrt{(\vec{P} - \vec{A})^2 + 1} \tag{2.37}$$

Let us consider the equation of the motion of an electron, initially at rest at the origin, under the action of a laser beam incident on it. The incident beam is assumed to be transverse, plane, and arbitrarily elliptically polarized, and to be characterized by a wave vector **K** with frequency $\omega = c \mid \mathbf{k} \mid = \mathbf{ck}$.

On multiplying by a pulse shaping factor the vector potential becomes

$$\vec{A}(\vec{r}, t) = \vec{A}_0 \times P(\xi) \times \Theta(\xi) \tag{2.38}$$

where $\vec{A}_o$ is the amplitude ,$P(\xi)$ is the oscillatory factor, $\Theta(\xi)$ is the envelope part and $\xi = t - \vec{r}$ is the phase of the wave.

Neglecting the radiative reaction effects. The Hamilton-Jacobi equation for the problem is

$$[\nabla s(\vec{r}, t) - \vec{A}(\xi)]^2 - [\frac{\partial s(\vec{r}, t)}{\partial t}]^2 + 1 = 0 \tag{2.39}$$

$s(\vec{r}, t)$, is the Hamilton principal function.

The Hamiltonian has no explicit dependence upon the co-ordinates x, y, z, t and it depends only upon the invariant phase of the laser, therefore corresponding to the cyclic co-ordinates the four momenta's are constants of motion. Thus the above equation Eq.(2.4) has the solution of the form

$$s(\vec{r}, t) = \vec{\alpha}.\vec{r} + \beta t + \Phi(\xi) \tag{2.40}$$

where $\vec{\alpha}$ and β are constants to be determined by the boundary conditions and

$\Phi(\xi)$ is a function determined from equation Eq.(2.39). On substituting Eq.(2.40) in Eq.(2.39) and re-arranging gives

$$\Phi(\xi) = \frac{1}{2}(\vec{\alpha}.\vec{k} + \beta k)^{-1} \int_{\xi_o}^{\xi} [\alpha^2 - \beta^2 + 1 - 2\vec{\alpha}.\vec{A}(\xi) + A_0^2 P^2(\xi)\Theta^2(\xi)]. \tag{2.41}$$

On substituting the value of Eq.(2.41) in Eq.(2.40) gives the principle function

$$\begin{aligned} s(\vec{r}, t) = \vec{\alpha}.\vec{r} + \beta ct + \frac{1}{2}(\vec{\alpha}.\vec{k} + \beta k)^{-1} \\ \int_{\xi_o}^{\xi} \left[\alpha^2 - \beta^2 + 1 \; -2\vec{\alpha}.\vec{A}(\xi) + A_0^2 P^2(\xi)\Theta^2(\xi)\right] d\xi. \end{aligned} \tag{2.42}$$

The equation of motion can be derived by differentiating the principal function w.r.t new momenta i.e (α) and equating to the initial co-ordinates

$$\begin{aligned} \vec{r}(\xi) = \nabla_\alpha s = \vec{r_o} - \int_{\xi_o}^{\xi} \frac{\vec{\alpha} - \vec{A}}{\vec{\alpha}.\vec{k} + \beta k} d\xi + \\ 2\vec{k} \int_{\xi_o}^{\xi} \frac{[\alpha^2 - \beta^2 + 1 - 2\vec{\alpha}.\vec{A}(\xi) + A_0^2 P^2(\xi)\Theta^2(\xi)]}{(\vec{2\alpha}.\vec{k} + 2\beta k)^2} d\xi \end{aligned} \tag{2.43}$$

$$\begin{aligned} t = \frac{\partial s}{\partial \beta} = t_0 + \frac{\vec{k}}{2(\vec{\alpha}.\vec{k} + k\beta)^2} \\ \int_{\xi_0}^{\xi} [\alpha^2 - \beta^2 + 1 - 2\vec{\alpha}.\vec{A}(\xi) + A_0^2 P^2(\xi)\Theta^2(\xi)] d\xi \\ + \frac{1}{2(\vec{\alpha}.\vec{k} + k\beta)} \int_{\xi_0}^{\xi} (2\beta) d\xi \end{aligned} \tag{2.44}$$

Canonical momentum and energy are given by

$$\vec{P}_{can}(= \vec{p} + \vec{A}) = \nabla s = \vec{\alpha} - \vec{k} \left[\frac{\alpha^2 - \beta^2 - 2\vec{\alpha}.\vec{A} + A_0^2 P^2(\xi)\Theta^2(\xi) + 1}{2(\vec{\alpha}.\vec{k} + k\beta)}\right] \tag{2.45}$$

$$\Gamma = -\frac{\partial s}{\partial t} = -\left[\beta + \frac{\vec{k}}{k}.(\vec{\alpha} - \vec{P}_{can})\right] \tag{2.46}$$

where initial momentum of the particle is given by $\vec{\alpha} = p_\parallel + p_\perp$ and the constant of motion is derived using relation described by Eq.(2.46).

$$\Gamma - p_x = \Delta = -(p_{\parallel} + \beta) \tag{2.47}$$

In terms of the constant of motion the dynamical variables can be written as

$$p_x = P_{x(can)} = \frac{1-\Delta^2}{2\Delta} + \left[\frac{p_\perp^2 - 2p_\perp A + A_0^2 P^2(\xi)\Theta^2(\xi)}{2\Delta}\right] \tag{2.48}$$

$$p_y = \alpha_y - A_y \tag{2.49}$$

$$p_z = \alpha_z - A_z \tag{2.50}$$

$$\Gamma = \frac{1+\Delta^2}{2\Delta} + \left[\frac{p_\perp^2 - 2p_\perp A + A_0^2 P^2(\xi)\Theta^2(\xi)}{2\Delta}\right] \tag{2.51}$$

The co-ordinates of the particle position can be obtained as,

$$x(\xi) = x_0 + \int_{\xi_o}^{\xi} \frac{1-\Delta^2}{2\Delta^2} d\xi + \int_{\xi_o}^{\xi} \left[\frac{p_\perp^2 - 2p_\perp A + A_0^2 P^2(\xi)\Theta^2(\xi)}{2\Delta^2}\right] d\xi \tag{2.52}$$

$$y(\xi) = \int_{\xi_o}^{\xi} \frac{\alpha_y - A_y}{\Delta} d\xi \tag{2.53}$$

$$z(\xi) = \int_{\xi_o}^{\xi} \frac{\alpha_z - A_z}{\Delta} d\xi \tag{2.54}$$

$$t = t_0 + \int_{\xi_o}^{\xi} \frac{1+\Delta^2}{2\Delta^2} d\xi + \int_{\xi_o}^{\xi} \left[\frac{p_\perp^2 - 2p_\perp A + A_0^2 P^2(\xi)\Theta^2(\xi)}{2\Delta^2}\right] d\xi \tag{2.55}$$

2.3.1 Particle Dynamics in The Field Of Finite Duration Laser Pulse

In this section, the dynamics of a charged particle is studied in the field of a finite duration laser pulse. The exact analytical expressions of the particle position, momentum and energy as a function of invariant phase(ξ) for $Sech$ and $Gaussian$ shaped temporal profiles are obtained using the general results derived by solving the corresponding Hamilton-Jacobi equation for a particle interacting with the field of an elliptically polarized, arbitrarily long homogeneous laser pulse. These exact expressions are reported for the first time, which gives the unambiguous comparison for the analytical and numerical results. This serves as an considerable improvement to the earlier derived results in the literature using Sin^2 shaped temporal envelope, in which the numerical study is restricted to the use of integral number of oscillations inside the pulse and the analytical work has been done with the envelope pulse repeating itself periodically in an infinite train of modulated envelope pulses. Such a description of the particle dynamics can lead to the ambiguous results. The exact analytical expressions for the particle co-ordinates in the $Sech$ shaped envelope corresponding to the $\Theta(\delta\xi) = Sech[\delta\xi - \phi]$ and $Gaussian$ shaped envelope corresponding to $\Theta(\delta\xi) = Exp[-\frac{(\delta\xi-\phi)^2}{2}]$ have been described below. These expressions are obtained by integrating the Eq-(2.52)-Eq.(2.54) and the variable (ϕ) is used to be consistent with the initial conditions that the particle interacts with the rising edge of the finite duration laser pulse. The expressions Eq-(2.48)-Eq.(2.50) and Eq-(2.51) are used to obtain the corresponding expression for the components of momentum and energy of the particle respectively.

Sech profile

$$
\begin{aligned}
Z = {} & \frac{1}{2\Delta} e^{-i\xi} \Bigg(2e^{i\xi}(z_o\Delta + \alpha_1\xi) + ia_2 \Bigg(\text{H2F1}\left[1, -\frac{i}{\delta}, \frac{-i+\delta}{\delta}, -ie^{\delta\xi-\phi}\right] - \\
& \text{H2F1}\left[1, -\frac{i}{\delta}, \frac{-i+\delta}{\delta}, ie^{\delta\xi-\phi}\right] + e^{i\xi} \Bigg(-\text{H2F1}\left[1, -\frac{i}{\delta}, \frac{-i+\delta}{\delta}, -ie^{-\phi}\right] + \\
& \text{H2F1}\left[1, -\frac{i}{\delta}, \frac{-i+\delta}{\delta}, ie^{-\phi}\right] + e^{i\xi} \Bigg(\text{H2F1}\left[1, \frac{i}{\delta}, \frac{i+\delta}{\delta}, -ie^{\delta\xi-\phi}\right] - \\
& \text{H2F1}\left[1, \frac{i}{\delta}, \frac{i+\delta}{\delta}, ie^{\delta\xi-\phi}\right] \Bigg) - \text{H2F1}\left[1, \frac{i}{\delta}, \frac{i+\delta}{\delta}, -ie^{-\phi}\right] + \\
& \text{H2F1}\left[1, \frac{i}{\delta}, \frac{i+\delta}{\delta}, ie^{-\phi}\right] \Bigg) \Bigg) \Bigg)
\end{aligned}
\tag{2.56}
$$

$$
\begin{aligned}
Y = {} & \frac{1}{(1+\delta^2)\,\Delta} e^{-\phi} \Bigg(-a_1 e^{(-i+\delta)\xi}(i+\delta)\text{H2F1}\left[1, \frac{-i+\delta}{2\delta}, \frac{3}{2} - \frac{i}{2\delta}, -e^{2\delta\xi-2\phi}\right] + \\
& a_1(i+\delta)\text{H2F1}\left[1, \frac{-i+\delta}{2\delta}, \frac{3}{2} - \frac{i}{2\delta}, -e^{-2\phi}\right] + (-i+\delta) \\
& \Bigg(e^{\phi}(i+\delta)(y_o\Delta + \alpha\xi) + a_1 \Bigg(-e^{(i+\delta)\xi}\text{H2F1}\left[1, \frac{i+\delta}{2\delta}, \frac{3}{2} + \frac{i}{2\delta}, -e^{2\delta\xi-2\phi}\right] + \\
& \text{H2F1}\left[1, \frac{i+\delta}{2\delta}, \frac{3}{2} + \frac{i}{2\delta}, -e^{-2\phi}\right] \Bigg) \Bigg) \Bigg)
\end{aligned}
\tag{2.57}
$$

$$
\begin{aligned}
X = &-\frac{1}{8\delta\Delta^2}\left(\frac{-1}{(e^{2\delta\xi}+e^{2\phi})}4ia_2e^{-2\phi}\alpha_1\text{Cosh}[\phi]\,(A)+\frac{1}{(e^{2\delta\xi}+e^{2\phi})}4a_1e^{-2\phi}\alpha\text{Cosh}[\phi]\,(B)-\right.\\
&a_1^2\,(C)+a_2^2\,(D)-a_1^2\,(E)+a_2^2\,(F)-\left(2e^{-3\phi}\left(-2\left(1+e^{2\phi}\right)(a_1\alpha+ia_2\alpha_1)(-i+\delta)^2\right.\right.\\
&\left(-1+4i\delta+3\delta^2\right)\text{H2F1}\left[1,\frac{3}{2}-\frac{i}{2\delta},\frac{5}{2}-\frac{i}{2\delta},-e^{-2\phi}\right]+(-i+3\delta)\left(-2\left(1+e^{2\phi}\right)\right.\\
&(a_1\alpha-ia_2\alpha_1)(-i+\delta)(i+\delta)^2\text{H2F1}\left[1,\frac{3}{2}+\frac{i}{2\delta},\frac{5}{2}+\frac{i}{2\delta},-e^{-2\phi}\right]+e^{\phi}(i+3\delta)\\
&\left(2e^{\phi}\left(1+e^{2\phi}\right)(a_1\alpha+ia_2\alpha_1 i)(i+\delta)^2\text{H2F1}\left[1,\frac{-i+\delta}{2\delta},\frac{3}{2}-\frac{i}{2\delta},-e^{-2\phi}\right]+\right.\\
&\left(a_1^2-a_2^2\right)\left(1+e^{2\phi}\right)(1-i\delta)\text{H2F1}\left[1,\frac{-i+\delta}{\delta},2-\frac{i}{\delta},-e^{-2\phi}\right]+(-i+\delta)\\
&\left(e^{\phi}(i+\delta)\left(a_1^2e^{\phi}\left(-3+e^{2\phi}\right)+4a_1\left(1+e^{2\phi}\right)\alpha+e^{\phi}\left(a_2^2\left(1+e^{2\phi}\right)+\right.\right.\right.\\
&\left.\left.\left(-1+e^{2\phi}\right)\alpha^2-\alpha_1^2+e^{2\phi}\alpha_1^2+4x_o\delta\Delta^2+4e^{2\phi}x_o\delta\Delta^2\right)\right)+\\
&2e^{\phi}\left(1+e^{2\phi}\right)(a_1\alpha-ia_2\alpha_1)(-i+\delta)\text{H2F1}\left[1,\frac{i+\delta}{2\delta},\frac{3}{2}+\frac{i}{2\delta},-e^{-2\phi}\right]+\\
&\left.\left.\left.\left.\left.i\left(a_1^2-a_2^2\right)\left(1+e^{2\phi}\right)\text{H2F1}\left[1,\frac{i+\delta}{\delta},2+\frac{i}{\delta},-e^{-2\phi}\right]\right)\right)\right)\right)\right)/\\
&\left(\left(1+e^{2\phi}\right)(-i+\delta)(i+\delta)(-i+3\delta)(i+3\delta)\right)-\frac{1}{(e^{2\delta\xi}+e^{2\phi})}\\
&4a_1e^{-2\phi}\alpha\,(G)\,\text{Sinh}[\phi]+\frac{1}{(e^{2\delta\xi}+e^{2\phi})}4ia_2e^{-2\phi}\alpha_1\,(H)\,\text{Sinh}[\phi]+\\
&2\alpha^2\left(1+2\text{Cosh}[\phi]^2\text{Log}[\text{Cosh}[\delta\xi-\phi]]-\text{Cosh}[\delta\xi+\phi]\text{Sech}[\delta\xi-\phi]+\right.\\
&\left.4\delta\xi\text{Cosh}[\phi]\text{Sinh}[\phi]+2\text{Log}[\text{Cosh}[\delta\xi-\phi]]\text{Sinh}[\phi]^2\right)\text{Sinh}[2\phi]+\\
&2\alpha_1^2\left(1+2\text{Cosh}[\phi]^2\text{Log}[\text{Cosh}[\delta\xi-\phi]]-\text{Cosh}[\delta\xi+\phi]\text{Sech}[\delta\xi-\phi]+\right.\\
&\left.4\delta\xi\text{Cosh}[\phi]\text{Sinh}[\phi]+2\text{Log}[\text{Cosh}[\delta\xi-\phi]]\text{Sinh}[\phi]^2\right)\text{Sinh}[2\phi]-\\
&(2a_1^2+2a_2^2+2\alpha^2+2\alpha_1^2)\text{Tanh}[\delta\xi-\phi]+\alpha^2\text{Cosh}[\phi]^2\left(2\delta\xi-4\delta\xi\text{Cosh}[\phi]^2-\right.\\
&\left.2\text{Log}[\text{Cosh}[\delta\xi-\phi]]\text{Sinh}[2\phi]+\text{Sech}[\delta\xi-\phi]\text{Sinh}[\delta\xi+\phi]+\text{Tanh}[\delta\xi-\phi]\right)+\alpha_1^2\text{Cosh}[\phi]^2\\
&\left(2\delta\xi-4\delta\xi\text{Cosh}[\phi]^2-2\text{Log}[\text{Cosh}[\delta\xi-\phi]]\text{Sinh}[2\phi]+\text{Sech}[\delta\xi-\phi]\text{Sinh}[\delta\xi+\phi]+\text{Tanh}[\delta\xi-\phi]\right)\\
&+\alpha^2\text{Sinh}[\phi]^2\left(2\delta\xi-4\delta\xi\text{Cosh}[\phi]^2-2\text{Log}[\text{Cosh}[\delta\xi-\phi]]\text{Sinh}[2\phi]+\text{Sech}[\delta\xi-\phi]\text{Sinh}[\delta\xi+\phi]+\right.\\
&\left.\text{Tanh}[\delta\xi-\phi]\right)+\alpha_1^2\text{Sinh}[\phi]^2\left(2\delta\xi-4\delta\xi\text{Cosh}[\phi]^2-2\text{Log}[\text{Cosh}[\delta\xi-\phi]\text{Sinh}[2\phi]+\text{Sech}[\delta\xi-\phi]\right.\\
&\left.\text{Sinh}[\delta\xi+\phi]+\text{Tanh}[\delta\xi-\phi]\right)-2\alpha^2\text{Cosh}[2\phi](\delta\xi\text{Cosh}[2\phi]+\text{Log}[\text{Cosh}[\delta\xi-\phi]]\text{Sinh}[2\phi]\\
&-\text{Sech}[\delta\xi-\phi]\text{Sinh}[\delta\xi]\text{Sinh}[\phi]\text{Tanh}[\phi])-2\alpha_1^2\text{Cosh}[2\phi](\delta\xi\text{Cosh}[2\phi]+\\
&\text{Log}[\text{Cosh}[\delta\xi-\phi]]\text{Sinh}[2\phi]-\text{Sech}[\delta\xi-\phi]\text{Sinh}[\delta\xi]\text{Sinh}[\phi]\text{Tanh}[\phi]))
\end{aligned}
\tag{2.58}
$$

In the above equations $H2FC$ is a short hand notion used for the mathematical function $Hypergemetric2FC$ and the values of variables (A-H) used in the longitudinal component of position is given in the Annexure at the end of chapter. Following are the components of the particle position in a finite duration laser pulse with $Gaussian$ shaped temporal envelope.

Gaussian Profile

$$Z = \frac{1}{4\delta\Delta}e^{-\frac{1+2i\delta\phi}{2\delta^2}}\left(4e^{\frac{1+2i\delta\phi}{2\delta^2}}\delta(z_o\Delta+\alpha_1\xi)+a_2\sqrt{2\pi}\left(ie^{\frac{2i\phi}{\delta}}\right.\right.$$
$$\left.\left.\left(\text{Erf}\left[\frac{-i+\delta^2\xi-\delta\phi}{\sqrt{2}\delta}\right]+\text{Erf}\left[\frac{i+\delta\phi}{\sqrt{2}\delta}\right]\right)+\text{Erfi}\left[\frac{1-i\delta(\delta\xi-\phi)}{\sqrt{2}\delta}\right]-\text{Erfi}\left[\frac{1+i\delta\phi}{\sqrt{2}\delta}\right]\right)\right) \tag{2.59}$$

$$Y = \frac{1}{4\delta\Delta}e^{-\frac{1+2i\delta\phi}{2\delta^2}}\left(4e^{\frac{1+2i\delta\phi}{2\delta^2}}\delta(y_o\Delta+\alpha\xi)+a_1\sqrt{2\pi}\left(\text{Erf}\left[\frac{i-\delta\phi}{\sqrt{2}\delta}\right]-\text{Erf}\left[\frac{i+\delta^2\xi-\delta\phi}{\sqrt{2}\delta}\right]+\right.\right.$$
$$\left.\left.ie^{\frac{2i\phi}{\delta}}\left(\text{Erfi}\left[\frac{1+i\delta(\delta\xi-\phi)}{\sqrt{2}\delta}\right]-\text{Erfi}\left[\frac{1-i\delta\phi}{\sqrt{2}\delta}\right]\right)\right)\right) \tag{2.60}$$

$$X = \frac{1}{16\delta\Delta^2}e^{-\frac{1+2i\delta\phi}{\delta^2}}\left(2e^{\frac{1+2i\delta\phi}{\delta^2}}\left(8x_o\delta\Delta^2+4\left(\alpha^2+\alpha1^2\right)\delta\xi+\left(\text{a1}^2+\text{a2}^2\right)\sqrt{\pi}\right.\right.$$
$$\left.(\text{Erf}[\delta\xi-\phi]+\text{Erf}[\phi])\right)+4e^{\frac{1+2i\delta\phi}{2\delta^2}}\sqrt{2\pi}(a_1\alpha+ia_2\alpha_1)\left(\text{Erf}\left[\frac{i-\delta\phi}{\sqrt{2}\delta}\right]-\text{Erf}\left[\frac{i+\delta^2\xi-\delta\phi}{\sqrt{2}\delta}\right]\right)$$
$$+(a_1^2-a_2^2)e^{\frac{4i\phi}{\delta}}\sqrt{\pi}\left(-\text{Erfc}\left[\frac{i}{\delta}+\phi\right]+\text{Erfc}\left[\frac{i}{\delta}-\delta\xi+\phi\right]\right)+$$
$$(a_1^2-a_2^2)\sqrt{\pi}\left(\text{Erf}\left[\frac{i+\delta^2\xi-\delta\phi}{\delta}\right]-i\text{Erfi}\left[\frac{1}{\delta}+i\phi\right]\right)+$$
$$\left.4e^{\frac{1+6i\delta\phi}{2\delta^2}}\sqrt{2\pi}(i\text{a1}\alpha+\text{a2}\alpha 1)\left(\text{Erfi}\left[\frac{1+i\delta(\delta\xi-\phi)}{\sqrt{2}\delta}\right]-\text{Erfi}\left[\frac{1-i\delta\phi}{\sqrt{2}\delta}\right]\right)\right) \tag{2.61}$$

In the above expressions the function Erfi is imaginary error function which is related to the error function as $Erfi(z) = -iErf(iz)$. It is evident that the above derived exact analytical expressions have a complicated mathematical structure. Thus a comparative analytical and numerical results have been presented in the following figures to gain insight into the dynamics described by these expressions.

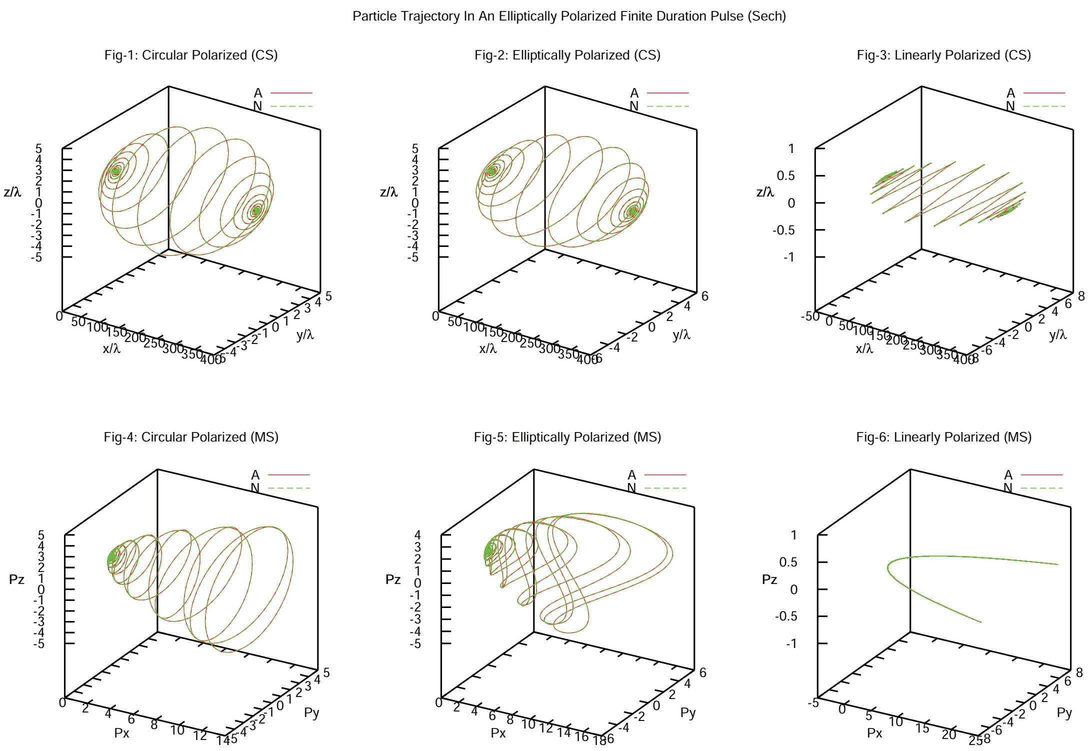

Figure 2.10: Description of evolution of particle position and momentum in the field of a finite duration laser pulse as a function of invariant phase(ξ) for a $Sech(\delta\xi)$ envelope. Subplot-(1)-(3) The numerically (N) and analytically (A) obtained particle trajectory in the configuration space for different laser polarizations. Subplot (d)-(f): the momentum space trajectory on the particle for different laser polarizations.

In the subplots (1-2-3) of the figures Fig.(2.10) and Fig.(2.11), the trajectory of the particle is shown in the configuration space for the circular, elliptical and linear polarizations which are defined by the value of polarization factor[$\kappa(= 1/\sqrt{2}; 1/\sqrt{3}; 0)$]. The trajectory of the particle is resultant of oscillatory motion along the longitudinal and transverse direction coupled with a secular drift along the direction of propagation. The corresponding shape of particle orbit over one laser cycle, depends upon the polarization state which can be circular, elliptical and in figure of the number eight shapes when viewed in an average frame of reference drifting with the particle for the above specified values of κ. It is further shown that the gyration length and transverse excursion amplitude increases with each successive gyration. This corresponds to the accelerating phase of the laser pulse reaching the maximum at the center of the pulse. Beyond this point, the particle due to its finite mass is out run by the wave and goes into retarding phase of the laser pulse. In the retarding phase of a laser pulse the particle decelerates and comes back to rest while returning all its energy back to the laser pulse.

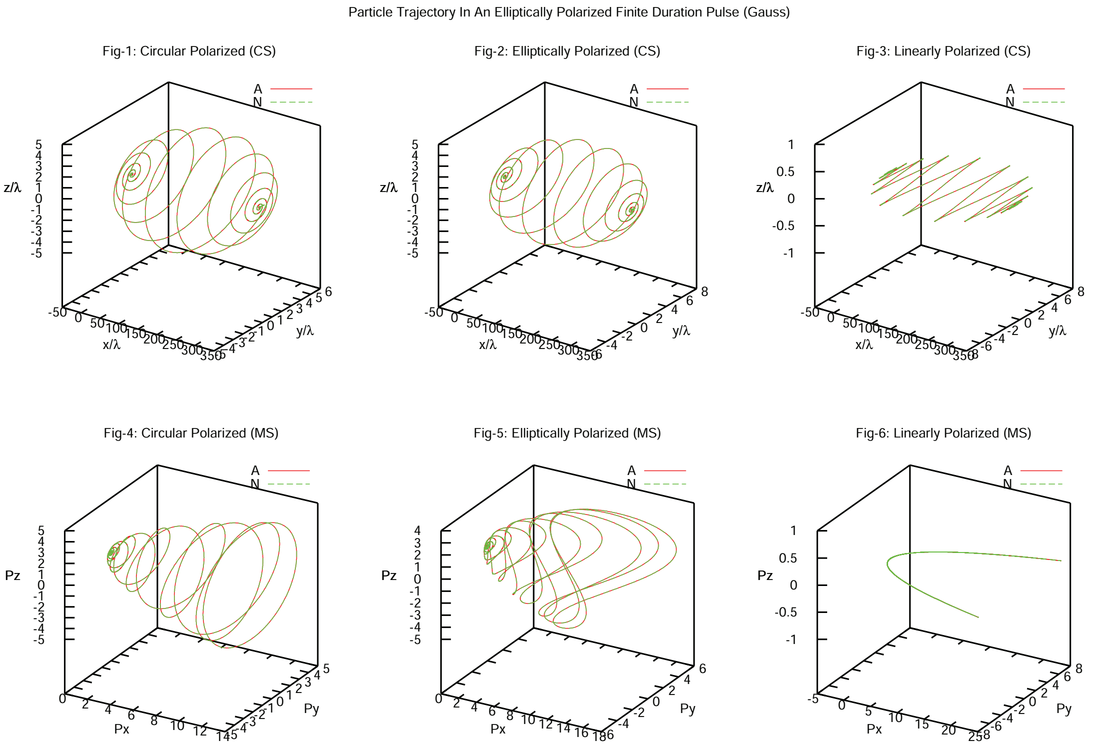

Figure 2.11: Description of evolution of particle position and momentum in the field of a finite duration laser pulse as a function of invariant phase(ξ) for a $Gaussian(\delta\xi)$envelope. Subplot-(1)-(3) The numerically (N) and analytically (A) obtained particle trajectory in the configuration space for different laser polarizations. Subplot (4)-(6): the momentum space trajectory on the particle for different laser polarizations.

The momentum space trajectory of the particle is shown in subplots(4-5-6) of the figures Fig.(2.10) and Fig.(2.11). It can be seen from the figure that for a circular and elliptical polarizations the particle has non-zero net momentum along the direction of propagation which increases and decreases symmetrically in the build up and slowing down phases of the laser pulse in comparison to the linear polarization in which is parabolic in shape. Thus for a linearly polarization the average longitudinal momentum is zero over each gyration. From the above figures it is evident that there is a very good matching between the analytical and numerical results describing the particle trajectories in the configuration as well as momentum space. Thus the analytical results expressed here can be used for the further study involving interaction of particle with finite duration laser pulse.

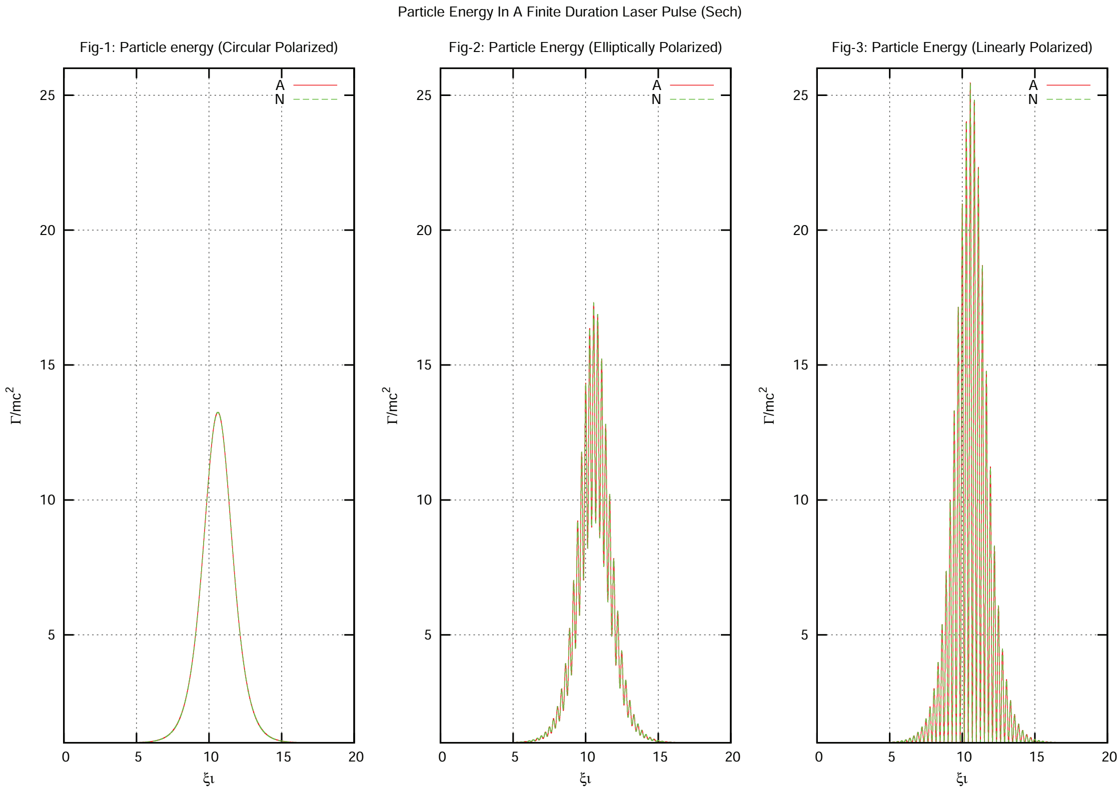

Figure 2.12: Analytical(A) and Numerical (N) plot for the total energy of the particle as function of invariant phase(ξ) for different polarization of the laser using $Sech$ profile for temporal shape. Subplot(a):Circular Polarization: Subplot (b):Elliptical Polarization Subplot (c):Linear Polarization

The total particle energy for $Sech$ and $Gaussian$ profiles is shown in Fig.(2.12) and Fig.(2.13). From these figure and momentum space trajectory it is evident that the total energy of the particle over one gyration during the pulse-particle interaction is non-zero for circular and elliptical polarization, whereas for linear polarization the particle energy is zero over one gyration. Further the maximum energy of the particle at the center of the pulse for linear polarization is twice that of circular polarization. At the end of pulse particle interaction the energy of particle interaction is equal to its initial value and there is no net transfer of energy to the particle.

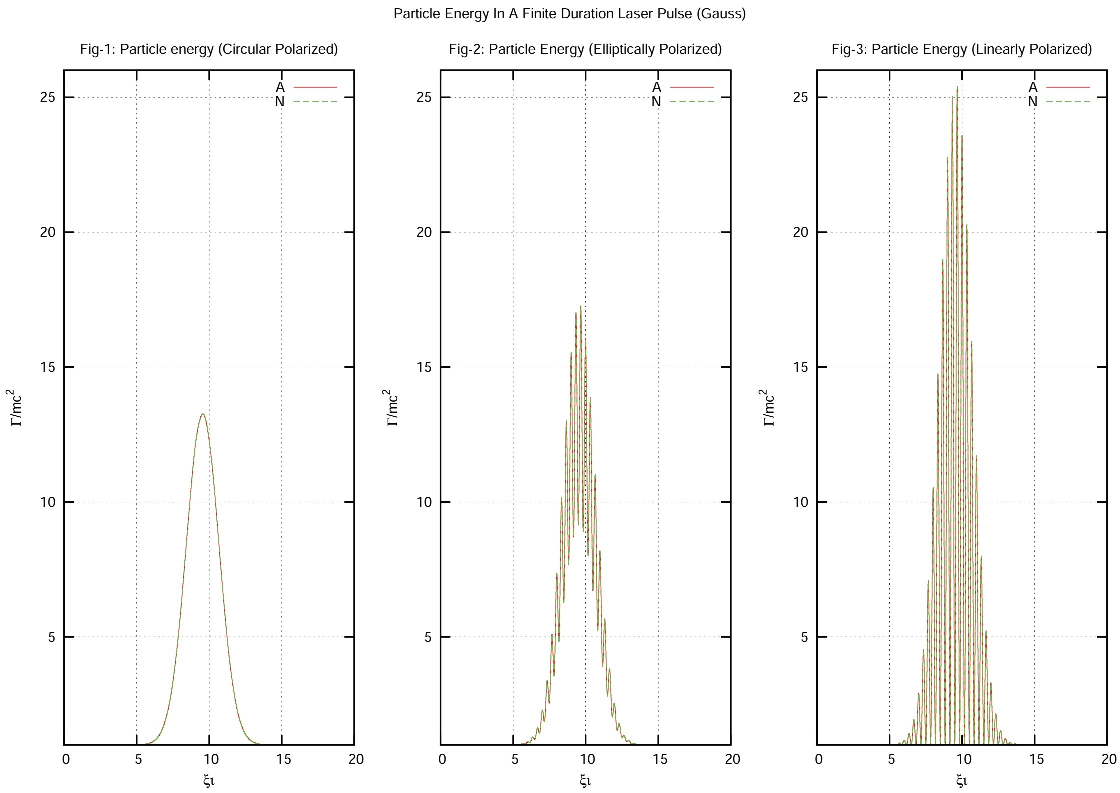

Figure 2.13: Analytical(A) and Numerical (N) plot for the total energy of the particle as function of invariant phase(ξ) for different polarization of the laser using $Gaussian$ profile for temporal shape. Subplot(a):Circular Polarization: Subplot (b):Elliptical Polarization Subplot (c):Linear Polarization

2.4 Summary

Using the above derived results, we summarize the physical aspects of particle interaction with a continuous and pulsed laser. At first, the particle motion in a monochromatic plane wave can be described in the following way. At the beginning of the interaction, the particle, which is initially at rest is accelerated along the electric field component of the laser field. It acquires a relativistic velocity along the field direction in a time much shorter than the period of the wave and is acted upon by the magnetic field component of the laser field. Under the effect of $\vec{v} \times \vec{B}$ force, the particle drifts with a relativistic velocity along the direction of laser propagation. But due to its finite mass the particle gets slowly phase lagged from the laser field and eventually the direction of field is reversed which brings the particle back to rest. At the end of each successive gyration the particle is displaced along the direction of propagation without any net energy transfer from the laser.

For a continuous laser pulse, it is shown that the particle motion can be divided into secular guiding center motion and fast oscillation center motion. The study of particle motion in the fast oscillation center provides better physical insight of the particle trajectories. The secular guiding center motion is used to derive the Lorenz transformation connecting the particle dynamics in the rest frame to the lab frame. These transformations enhances the understanding of relativistic effects, which is fundamental to the study of laser particle interaction.

The general solutions are derived describing the motion of the particle in the field of an elliptically polarized and arbitrarily long finite duration laser pulse. Using these general solutions the exact analytical expressions are derived using $Sech$ and $Gaussian$ shaped temporal envelopes for the position, momentum and energy of the particle. These solutions give unambiguous comparison of the analytical and numerical results. On the basis of these results the analytical and numerical the particle motion can be physically described in a following way: for a finite duration laser pulse which includes the light pressure effects, at the onset of pulse particle interaction, the particle is acted upon by a radiation pressure in the rising front of pulse, which pushes the particle forward along the direction of propagation. In the trailing part of the pulse, the direction of field is reversed, as a result of this, the radiation pressure retards the motion of a particle. So, in this, process there is no transfer of energy to the particle takes places as the pulse slips past it.

2.5 Annexure

$$A = \frac{e^{(-i+3\delta)\xi}\left(e^{2\phi}(i-3\delta)+\left(e^{2\delta\xi}+e^{2\phi}\right)(-i+\delta)\mathrm{H2F1}\left[1,\frac{3}{2}-\frac{i}{2\delta},\frac{5}{2}-\frac{i}{2\delta},-e^{2\delta\xi-2\phi}\right]\right)}{-i+3\delta}+ \frac{e^{(i+3\delta)\xi}\left(e^{2\phi}(i+3\delta)-\left(e^{2\delta\xi}+e^{2\phi}\right)(i+\delta)\mathrm{H2F1}\left[1,\frac{3}{2}+\frac{i}{2\delta},\frac{5}{2}+\frac{i}{2\delta},-e^{2\delta\xi-2\phi}\right]\right)}{i+3\delta}- \frac{e^{(-i+\delta)\xi}\left(e^{2\phi}(-i+\delta)+\left(e^{2\delta\xi}+e^{2\phi}\right)(i+\delta)\mathrm{H2F1}\left[1,\frac{-i+\delta}{2\delta},\frac{3}{2}-\frac{i}{2\delta},-e^{2\delta\xi-2\phi}\right]\right)}{-i+\delta}+ \frac{e^{(i+\delta)\xi}\left(e^{2\phi}(i+\delta)+\left(e^{2\delta\xi}+e^{2\phi}\right)(-i+\delta)\mathrm{H2F1}\left[1,\frac{i+\delta}{2\delta},\frac{3}{2}+\frac{i}{2\delta},-e^{2\delta\xi-2\phi}\right]\right)}{i+\delta}$$

$$B = -\frac{e^{(-i+3\delta)\xi}\left(e^{2\phi}(i-3\delta)+\left(e^{2\delta\xi}+e^{2\phi}\right)(-i+\delta)\mathrm{H2F1}\left[1,\frac{3}{2}-\frac{i}{2\delta},\frac{5}{2}-\frac{i}{2\delta},-e^{2\delta\xi-2\phi}\right]\right)}{-i+3\delta}+ \frac{e^{(i+3\delta)\xi}\left(e^{2\phi}(i+3\delta)-\left(e^{2\delta\xi}+e^{2\phi}\right)(i+\delta)\mathrm{H2F1}\left[1,\frac{3}{2}+\frac{i}{2\delta},\frac{5}{2}+\frac{i}{2\delta},-e^{2\delta\xi-2\phi}\right]\right)}{i+3\delta}+ \frac{e^{(-i+\delta)\xi}\left(e^{2\phi}(-i+\delta)+\left(e^{2\delta\xi}+e^{2\phi}\right)(i+\delta)\mathrm{H2F1}\left[1,\frac{-i+\delta}{2\delta},\frac{3}{2}-\frac{i}{2\delta},-e^{2\delta\xi-2\phi}\right]\right)}{-i+\delta}+ \frac{e^{(i+\delta)\xi}\left(e^{2\phi}(i+\delta)+\left(e^{2\delta\xi}+e^{2\phi}\right)(-i+\delta)\mathrm{H2F1}\left[1,\frac{i+\delta}{2\delta},\frac{3}{2}+\frac{i}{2\delta},-e^{2\delta\xi-2\phi}\right]\right)}{i+\delta}$$

$$C = \frac{e^{2(-i+\delta)\xi}\left(-1+e^{2i\xi}\right)^2}{e^{2\delta\xi}+e^{2\phi}}+\frac{e^{2(-i+\delta)\xi-2\phi}\mathrm{H2F1}\left[1,\frac{-i+\delta}{\delta},2-\frac{i}{\delta},-e^{2\delta\xi-2\phi}\right]}{-1-i\delta}+ \frac{e^{2(i+\delta)\xi-2\phi}\mathrm{H2F1}\left[1,\frac{i+\delta}{\delta},2+\frac{i}{\delta},-e^{2\delta\xi-2\phi}\right]}{-1+i\delta}$$

$$D = \frac{e^{2(-i+\delta)\xi}\left(-1+e^{2i\xi}\right)^2}{e^{2\delta\xi}+e^{2\phi}}+\frac{e^{2(-i+\delta)\xi-2\phi}\mathrm{H2F1}\left[1,\frac{-i+\delta}{\delta},2-\frac{i}{\delta},-e^{2\delta\xi-2\phi}\right]}{-1-i\delta}+ \frac{e^{2(i+\delta)\xi-2\phi}\mathrm{H2F1}\left[1,\frac{i+\delta}{\delta},2+\frac{i}{\delta},-e^{2\delta\xi-2\phi}\right]}{-1+i\delta}$$

$$E = \frac{e^{2(-i+\delta)\xi}\left(1+e^{2i\xi}\right)^2}{e^{2\delta\xi}+e^{2\phi}} + \frac{e^{2(-i+\delta)\xi-2\phi}\mathrm{H2F1}\left[1, \frac{-i+\delta}{\delta}, 2-\frac{i}{\delta}, -e^{2\delta\xi-2\phi}\right]}{-1-i\delta} + \frac{e^{2(i+\delta)\xi-2\phi}\mathrm{H2F1}\left[1, \frac{i+\delta}{\delta}, 2+\frac{i}{\delta}, -e^{2\delta\xi-2\phi}\right]}{-1+i\delta}$$

$$\begin{aligned} G = &-\frac{e^{(-i+3\delta)\xi}\left(e^{2\phi}(i-3\delta)+\left(e^{2\delta\xi}+e^{2\phi}\right)(-i+\delta)\mathrm{H2F1}\left[1, \frac{3}{2}-\frac{i}{2\delta}, \frac{5}{2}-\frac{i}{2\delta}, -e^{2\delta\xi-2\phi}\right]\right)}{-i+3\delta} + \\ &\frac{e^{(i+3\delta)\xi}\left(e^{2\phi}(i+3\delta)-\left(e^{2\delta\xi}+e^{2\phi}\right)(i+\delta)\mathrm{H2F1}\left[1, \frac{3}{2}+\frac{i}{2\delta}, \frac{5}{2}+\frac{i}{2\delta}, -e^{2\delta\xi-2\phi}\right]\right)}{i+3\delta} - \\ &\frac{e^{(-i+\delta)\xi}\left(e^{2\phi}(-i+\delta)+\left(e^{2\delta\xi}+e^{2\phi}\right)(i+\delta)\mathrm{H2F1}\left[1, \frac{-i+\delta}{2\delta}, \frac{3}{2}-\frac{i}{2\delta}, -e^{2\delta\xi-2\phi}\right]\right)}{-i+\delta} - \\ &\frac{e^{(i+\delta)\xi}\left(e^{2\phi}(i+\delta)+\left(e^{2\delta\xi}+e^{2\phi}\right)(-i+\delta)\mathrm{H2F1}\left[1, \frac{i+\delta}{2\delta}, \frac{3}{2}+\frac{i}{2\delta}, -e^{2\delta\xi-2\phi}\right]\right)}{i+\delta} \end{aligned}$$

$$\begin{aligned} H = &\frac{e^{(-i+3\delta)\xi}\left(e^{2\phi}(i-3\delta)+\left(e^{2\delta\xi}+e^{2\phi}\right)(-i+\delta)\mathrm{H2F1}\left[1, \frac{3}{2}-\frac{i}{2\delta}, \frac{5}{2}-\frac{i}{2\delta}, -e^{2\delta\xi-2\phi}\right]\right)}{-i+3\delta} + \\ &\frac{e^{(i+3\delta)\xi}\left(e^{2\phi}(i+3\delta)-\left(e^{2\delta\xi}+e^{2\phi}\right)(i+\delta)\mathrm{H2F1}\left[1, \frac{3}{2}+\frac{i}{2\delta}, \frac{5}{2}+\frac{i}{2\delta}, -e^{2\delta\xi-2\phi}\right]\right)}{i+3\delta} + \\ &\frac{e^{(-i+\delta)\xi}\left(e^{2\phi}(-i+\delta)+\left(e^{2\delta\xi}+e^{2\phi}\right)(i+\delta)\mathrm{H2F1}\left[1, \frac{-i+\delta}{2\delta}, \frac{3}{2}-\frac{i}{2\delta}, -e^{2\delta\xi-2\phi}\right]\right)}{-i+\delta} - \\ &\frac{e^{(i+\delta)\xi}\left(e^{2\phi}(i+\delta)+\left(e^{2\delta\xi}+e^{2\phi}\right)(-i+\delta)\mathrm{H2F1}\left[1, \frac{i+\delta}{2\delta}, \frac{3}{2}+\frac{i}{2\delta}, -e^{2\delta\xi-2\phi}\right]\right)}{i+\delta} \end{aligned}$$

3

Exact analysis of particle dynamics in the combined field of finite duration laser pulse and static axial magnetic field

This chapter is devoted to the theoretical study of relativistic dynamics of a charged particle interacting with a combined field of finite duration laser pulse and static axial magnetic field in vacuum. In this study the Gaussian shaped envelope has been used for describing the temporal profile of finite duration laser pulse. The understanding of the mechanism of interaction is of fundamental importance as it forms the underlining principle for laser driven Auto-Resonant acceleration scheme of particle acceleration in vacuum. A significant part of this chapter have been published in the Ref. **Sagar *et.al.***[45]

3.1 Introduction

The relativistic equation of motion for a charged particle interacting with a continuous as well as pulsed laser and its methods of solution have been described in the previous chapter. From the theoretical study, it has been concluded that the interaction of charged particle with a continuous as well as pulsed laser does not result in the net transfer of energy to the particle. This happens so because of the symmetrical acceleration and deceleration of the particle by laser field. The scheme of laser driven auto-resonance acceleration is theoretically studied in this chapter for accelerating the charged particle initially at rest to relativistic velocities. The mechanism for this scheme was discovered in the study of particle dynamics interacting simultaneously with continuous laser and static axial magnetic field [23, 24, 25]. The historical developments of the scheme can be traced in the following references [26, 27, 28, 29, 34, 35, 36, 37, 38, 39, 40, 41, 42, 33].

The scheme of laser driven auto-resonant acceleration is a consequence of purely relativistic effect. In this scheme the particle moving in the combined field of a laser and axial magnetic field ($\vec{B}_0$) is associated with two relativistic effects along the transverse and longitudinal directions; the relativistic mass effect along the transverse direction which lowers the cyclotron frequency of the particle and a Doppler effect along the longitudinal direction caused by the magnetic field of the wave, as result of which the frequency of a wave as seen by the particle is lower than the actual wave frequency. In this scheme, the initial resonance condition is itself preserved due to the precise cancellation of these two effects, which leads to the locking of the particle in the accelerating phase of the wave and thus resulting in a continuous energy gain.

The physical picture of this interaction can be described in the following way: a particle initially at rest is accelerated along the electric field component of the wave and it begins to gyrate about the propagation direction with a cyclotron frequency $\Omega_c(= qB_0/mc; m = m_0\Gamma)$. The energy gain along the transverse direction causes the relativistic mass effect which lowers the cyclotron frequency. The particle is simultaneously accelerated in the direction of $\vec{B}_0$ (and $\vec{k}$) by the magnetic field of the wave, and as the particle acquires some velocity in this direction it sees the wave at a Doppler-shifted frequency which is lower than the wave frequency ω. In the resonant case, the magnetic and mass effects just cancel one another, and the condition $\Gamma - P_x - \Omega_{c0}(= qB_0/m_0c) = 0$ is true throughout the particle's motion. Thus at the resonance, what happens is that as the particle gains energy and the cyclotron frequency consequently decreases, the magnetic field of the wave produces just the right velocity along $\vec{B}_0$ (and $\vec{k}$) to Doppler-shift the wave frequency to the value necessary to maintain resonance. This effect is similar to a synchrotron which maintains its synchronism automatically.

However, the requirement of large input laser power together with generation and sustaining of static magnetic fields of the order of laser magnetic field makes the use of continuous laser very limited for experimental realization of the auto-resonant particle acceleration scheme. Another principal objection is that a monochromatic wave has no building-up or slowing-down phase, and is infinite in time. Thus it contains an infinite amount of energy. A laser pulse is finite in time and carries a finite energy. Thus it is reasonable to consider particles initially at rest (at the origin), as there are no forces.

The scheme of laser driven auto-resonant particle acceleration was earlier theoretically studied in using a linearly polarized finite duration laser pulse with a Sin^2 temporal modulation[41, 42]. The position, momentum and energy of the particle were analytically obtained as function of laser phase. Later, using the same temporal modulation the problem was analytically and numerical studied by Ondazara *et.al*[33] for an elliptically polarized laser pulse. In these studies, the analytical work has been carried out using a periodically self repeating envelope pulse in an infinite train of modulated envelope pulses. Such a pulse envelope has a discreet frequency spectrum in the Fourier space, with an additional side band frequencies on the either side of the central maxima. However, the numerical work was done using a single pulse considered over one period, the frequency spectra for the pulse has a continuum in the Fourier space. Thus analytical results are unable to account for some of the numerical results such as the continuous dependence of energy spectra on the previously defined parameter $``r(=\frac{\Omega_c}{\omega\Delta})''$. An improved mathematical description of the envelope is therefore required for physical understanding the mechanism.

In this chapter, the interaction of the charged particle with the combined field of a finite duration laser and static axial magnetic field is analytically and numerically studied by choosing the Gaussian profile for describing the temporal shape of the pulse envelope. The exact analytical expressions are derived for the position, momentum and energy of the particle. This study is motivated to gain insight into mechanism of resonant interaction of the particle with the laser field. It is further intended to determine the optimum conditions in terms for laser intensity, pulse length, strength of axial magnetic field and laser polarization for maximizing the energy gain by the particle.

The organization of the chapter is the following: In section (3.2), the relativistic equation of motion and its solutions are analytically derived for a particle interacting simultaneously with the finite duration laser pulse and static axial magnetic field. Further, the results are first derived for the linear polarization in subsection (3.2.1) and are generalized for the elliptical polarization in subsection (3.2.2). The results of numerical study has been described in this section (3.3) and are compared with the analytical results. In section (3.4), the results of analytical and numerical study are discussed in detail for optimizing the energy gain of the particle in terms of various parameters.

3.2 Particle motion in the combined field of a finite duration laser pulse and static axial magnetic field

In this section, we present the method of solution of relativistic equation of motion describing the particle dynamics in the combined field of finite duration laser pulse and static axial magnetic field. The expression for the particle position, momentum and energy are expressed in terms of constants of motion and vector potential as function of laser phase. In this work vector potential description has been used for specifying the finite duration laser pulse and corresponding electric as well as magnetic fields are derived from it. Due to the complicated form, the analytical expressions are first described explicitly for the linearly polarized finite duration laser pulse and solutions corresponding to the elliptical polarization are presented in the subsequent subsection.

3.2.1 Linear Polarization

The vector potential of a finite duration laser pulse traveling along $\hat{x}$ direction in the presence of a constant homogeneous axial magnetic field is given by,

$$\vec{A} = A_0\Theta(\delta\xi)P(\xi)\hat{y} - \frac{B_0 z}{2}\hat{y} + \frac{B_0 y}{2}\hat{z} \tag{3.1}$$

where the symbols represents the following: $\xi = (\omega t - kx)$ is the phase of the laser, $\Theta(\delta\xi)$ is pulse envelope, $P_1(\xi)$ is the oscillatory part, factor $\delta(=\frac{\lambda}{L})$ is ratio of the laser wavelength to the pulse length, A_0 is the peak laser amplitude, B_0 is the magnitude of the external magnetic field.

The electric and magnetic fields corresponding to the above described vector potential of the laser are defined as,

$$\vec{E} = -\frac{1}{c}\frac{\partial \vec{A}}{\partial t} \qquad\qquad \vec{B} = \nabla \times \vec{A} \tag{3.2}$$

. The variables can be expressed in the dimensionless form by using the following normalizations: $\vec{r} \rightarrow k\vec{r}, t \rightarrow \omega t, \vec{P} \rightarrow \frac{\vec{P}}{mc}, \Gamma \rightarrow \frac{\Gamma}{mc^2}, B \rightarrow \frac{qB}{m\omega c}, E \rightarrow \frac{qE}{mc\omega}, \hat{A} \rightarrow \frac{eA}{mc^2}, \Omega_c \rightarrow \frac{qB_0}{mc\omega}$.

The normalized relativistic momentum and energy equation are given by

$$\frac{d\vec{P}}{dt} = [\vec{E} + \frac{\vec{P}}{\Gamma} \times (\vec{B} + \vec{\Omega}_c)] \tag{3.3}$$

$$\frac{d\Gamma}{dt} = \frac{\vec{P}.\vec{E}}{\Gamma} \tag{3.4}$$

Here Γ is the relativistic factor defined as,

$$\Gamma = (1 + P_x^2 + P_y^2 + P_z^2)^{1/2}$$

and P_x, P_y, P_z are the four momentum components.

On re-writing the equations in component form

$$\frac{dP_x}{dt} = -\frac{P_y}{\Gamma}\frac{\partial A}{\partial \xi} \tag{3.5}$$

$$\frac{dP_y}{dt} = -\frac{(\Gamma - P_x)}{\Gamma}\frac{\partial A}{\partial \xi} + \frac{P_z\Omega_c}{\Gamma} \tag{3.6}$$

$$\frac{dP_z}{dt} = -\frac{P_y\Omega_c}{\Gamma} \tag{3.7}$$

$$\frac{d\Gamma}{dt} = -\frac{P_y}{\Gamma}\frac{\partial A}{\partial \xi} \tag{3.8}$$

Subtracting equation Eq.(3.5) from Eq.(3.8) results in a constant of motion Δ defined as,

$$\Delta = \Gamma - P_x \tag{3.9}$$

.

The phase of the laser and the constant of motion Δ are related as $\dot{\xi} = \frac{\Delta}{\Gamma}$.

On expressing the above equations Eq.(3.5 to 3.7) in terms of null coordinates of laser phase ξ and using Eq.(3.9) the components of particle momentum takes the following form,

$$P_x = \frac{1-\Delta^2}{2\Delta} + \frac{P_y^2 + P_z^2}{2\Delta} \tag{3.10}$$

$$P_y = \alpha_1 - A + Z\Omega_c \tag{3.11}$$

$$P_z = \alpha_2 - Y\Omega_c \tag{3.12}$$

in the above expressions α_1 and α_2 are two exact constants of motion which corresponds to the conservation of transverse canonical momentum. The total energy of the particle given below is derived using Eq.(3.9) and Eq.(3.10),

$$\Gamma = \frac{1+\Delta^2}{2\Delta} + \frac{P_y^2 + P_z^2}{2\Delta} \tag{3.13}$$

The particle position is obtained by integrating particle momentum as

$$\vec{R} - \vec{R}_0 = \frac{1}{\Delta}\int_{\xi_0}^{\xi} \vec{P} d\xi \tag{3.14}$$

Transverse momentum as well as the position of a particle can be obtained either by representing them as first order complex differential equation or by decoupling the equations and writing them as second order differential equations,

$$\frac{d^2Y}{d\xi^2} + r^2 Y = \frac{r}{\Delta}\alpha_2 - \frac{1}{\Delta}\frac{dA}{d\xi} \tag{3.15}$$

$$\frac{d^2Z}{d\xi^2} + r^2 Z = \frac{rA}{\Delta} \tag{3.16}$$

The equations Eq.(3.15) and Eq.(3.16) describe the cyclotron motion of the particle in the combined field of laser and static axial magnetic field. As the laser pulse has a continuous frequency spectra in the Fourier space, the tuning of cyclotron frequency with the characteristic frequency in the spectrum can lead to the resonant energy gain by the particle.

The explicit form of the temporal envelope and the oscillatory part describing the vector potential of a finite duration laser pulse is specified below,

$$\Theta(\xi) = exp(-\frac{(\delta\xi - \phi)^2}{2}) \tag{3.17}$$

$$P(\xi) = sin(\xi) \tag{3.18}$$

.

Here ϕ, is the initial phase which corresponds to the assumption that the laser pulse is at an infinite distance away from the particle before the onset of interaction and the particle is acted upon by the rising edge of the laser pulse. In this work the particle is assumed to be initially at rest (and at the origin), which corresponds to the following initial conditions: initial particle position is given by $X = Y = Z = 0$, the components of canonical momenta are given by $\alpha 1 = \alpha 2 = 0$, the constant of motion resulting from the spatio-temporal symmetry of the vector potential in variables x and t is given by $\Delta = 1$. The solution of equations Eq.(3.15) and Eq.(3.16) describing the cyclotron motion gives the transverse coordinates of the particle position. The position and momentum of the particle are related to each other by the following relation

$$\frac{d\vec{R}}{d\xi} = \frac{\vec{P}}{\Delta} \tag{3.19}$$

here as specified earlier $\vec{P}$ represents the normalized four momentum of the particle.

The co-ordinates for transverse particle position are given below.

Particle position

$$Y = \frac{1}{8r\delta}A_0 e^{-\frac{1+r(2+r+2i\xi\delta^2)+2i(1+r)\delta\phi}{2\delta^2}}\sqrt{\frac{\pi}{2}}(2e^{2ir\xi}r\text{Erf}[\frac{i+ir+\xi\delta^2-\delta\phi}{\sqrt{2}\delta}]+e^{\frac{2i(1+r)\phi}{\delta}}$$
$$(-1+i\delta\phi+e^{2ir\xi}(1+i\delta\phi))\text{Erf}[\frac{i(1+r)+\delta\phi}{\sqrt{2}\delta}]+e^{\frac{2i(1+r)\phi}{\delta}}\text{Erf}[\frac{i+ir+\delta(-\xi\delta+\phi)}{\sqrt{2}\delta}]$$
$$-ie^{\frac{2i(1+r)\phi}{\delta}}\delta\phi\text{Erf}[\frac{i+ir+\delta(-\xi\delta+\phi)}{\sqrt{2}\delta}]-2ie^{\frac{2r(1+i\delta\phi)}{\delta^2}}r\text{Erfi}[\frac{1-r-i\delta(\xi\delta-\phi)}{\sqrt{2}\delta}]$$
$$-ie^{\frac{2i(1+r)\phi}{\delta}}\text{Erfi}[\frac{1+r+i\delta(\xi\delta-\phi)}{\sqrt{2}\delta}]-2ie^{\frac{2i(1+r)\phi}{\delta}}r\text{Erfi}[\frac{1+r+i\delta(\xi\delta-\phi)}{\sqrt{2}\delta}]$$
$$-e^{\frac{2i(1+r)\phi}{\delta}}\delta\phi\text{Erfi}[\frac{1+r+i\delta(\xi\delta-\phi)}{\sqrt{2}\delta}]+ie^{\frac{2i(1+r)\phi}{\delta}}\text{Erfi}[\frac{1+r-i\delta\phi}{\sqrt{2}\delta}]+2ie^{\frac{2i(1+r)\phi}{\delta}}r$$
$$\text{Erfi}[\frac{1+r-i\delta\phi}{\sqrt{2}\delta}]+e^{\frac{2i(1+r)\phi}{\delta}}\delta\phi\text{Erfi}[\frac{1+r-i\delta\phi}{\sqrt{2}\delta}]+2ie^{\frac{2r(1+i\delta\phi)}{\delta^2}}r\text{Erfi}[\frac{1-r+i\delta\phi}{\sqrt{2}\delta}]+$$
$$e^{2ir\xi}(e^{\frac{2i(1+r)\phi}{\delta}}(-i+\delta\phi)(-i\text{Erf}[\frac{i+ir+\delta(-\xi\delta+\phi)}{\sqrt{2}\delta}]-\text{Erfi}[\frac{1+r+i\delta(t\delta-\phi)}{\sqrt{2}\delta}]+$$
$$\text{Erfi}[\frac{1+r-i\delta\phi}{\sqrt{2}\delta}])+2ir(e^{\frac{2(r+i\delta\phi)}{\delta^2}}(\text{Erfi}[\frac{1-r+i\delta(\xi\delta-\phi)}{\sqrt{2}\delta}]+\text{Erfi}[\frac{-1+r+i\delta\phi}{\sqrt{2}\delta}])$$
$$-\text{Erfi}[\frac{1+r+i\delta\phi}{\sqrt{2}\delta}]))) \tag{3.20}$$

$$Z = \frac{1}{8r^2\delta}A_0 e^{-\frac{1+r^2+4i\xi\delta^2+2\delta\phi(i+\delta\phi)+r(2+2i\delta(\xi\delta+\phi))}{2\delta^2}}(-4e^{\frac{1}{2}(4i\xi+\frac{(1+r)^2}{\delta^2}+\frac{2i(1+r)\phi}{\delta}+\phi^2)}(-1+e^{ir\xi})^2\delta+$$
$$\sqrt{2\pi}(-ie^{2i(1+r)\xi+\phi^2}r^2\text{Erf}[\frac{i+ir+\xi\delta^2-\delta\phi}{\sqrt{2}\delta}]+e^{2i\xi}(e^{\phi(\frac{2i(1+r)}{\delta}+\phi)}(\delta\phi\text{Erf}[\frac{i(1+r)+\delta\phi}{\sqrt{2}\delta}]-$$
$$\delta\phi\text{Erf}[\frac{i+ir+\delta(-\xi\delta+\phi)}{\sqrt{2}\delta}]+(r^2+i\delta\phi)(\text{Erfi}[\frac{1+r+i\delta(\xi\delta-\phi)}{\sqrt{2}\delta}]-\text{Erfi}[\frac{1+r-i\delta\phi}{\sqrt{2}\delta}]))+$$
$$e^{\phi^2+\frac{2r(1+i\delta\phi)}{\delta^2}}r^2(\text{Erfi}[\frac{1-r-i\delta(\xi\delta-\phi)}{\sqrt{2}\delta}]-\text{Erfi}[\frac{1-r+i\delta\phi}{\sqrt{2}\delta}]))+e^{2i(1+r)\xi}(-e^{\phi(\frac{2i(1+r)}{\delta}+\phi)}$$
$$\delta\phi\text{Erf}[\frac{i(1+r)+\delta\phi}{\sqrt{2}\delta}]+e^{\phi(\frac{2i(1+r)}{\delta}+\phi)}\delta\phi\text{Erf}[\frac{i+ir+\delta(-\xi\delta+\phi)}{\sqrt{2}\delta}]-ie^{\phi(\frac{2i(1+r)}{\delta}+\phi)}$$
$$\delta\phi\text{Erfi}[\frac{1+r+i\delta(\xi\delta-\phi)}{\sqrt{2}\delta}]+ie^{\phi(\frac{2i(1+r)}{\delta}+\phi)}\delta\phi\text{Erfi}[\frac{1+r-i\delta\phi}{\sqrt{2}\delta}]+e^{\frac{2r+\delta\phi(2i+\delta\phi)}{\delta^2}}r^2$$
$$(\text{Erfi}[\frac{1-r+i\delta(\xi\delta-\phi)}{\sqrt{2}\delta}]+\text{Erfi}[\frac{-1+r+i\delta\phi}{\sqrt{2}\delta}])-e^{\phi^2}r^2\text{Erfi}[\frac{1+r+i\delta\phi}{\sqrt{2}\delta}]))) \tag{3.21}$$

The corresponding transverse momentum component using Eq.(3.19) takes the following analytical form.

Particle Momentum

$$P_y = \frac{1}{8\delta}A_0 e^{-i(1+r)\xi-\frac{(1+r)^2+2i(1+r)\delta\phi+\delta^2\phi^2}{2\delta^2}}\sqrt{\frac{\pi}{2}}(-2e^{i(1+2r)\xi+\frac{4r+\delta\phi(4i+\delta\phi)}{2\delta^2}}r(\text{Erfi}[\frac{1-r+i\delta(\xi\delta-\phi)}{\sqrt{2}\delta}]+$$
$$\text{Erfi}[\frac{-1+r+i\delta\phi}{\sqrt{2}\delta}])+2e^{i\xi+\frac{\phi^2}{2}}r(e^{\frac{2r(1+i\delta\phi)}{\delta^2}}(-\text{Erfi}[\frac{1-r-i\delta(\xi\delta-\phi)}{\sqrt{2}\delta}]+\text{Erfi}[\frac{1-r+i\delta\phi}{\sqrt{2}\delta}])+$$
$$e^{2ir\xi}(i\text{Erf}[\frac{i+ir+\xi\delta^2-\delta\phi}{\sqrt{2}\delta}]+\text{Erfi}[\frac{1+r+i\delta\phi}{\sqrt{2}\delta}]))+2e^{i(1+r)\xi+\frac{2i(1+r)\phi}{\delta}+\frac{\phi^2}{2}}$$
$$(i\cos[r\xi]\text{Erf}[\frac{-i-ir+\xi\delta^2-\delta\phi}{\sqrt{2}\delta}]+i\delta\phi\text{Erf}[\frac{i+ir+\delta(-\xi\delta+\phi)}{\sqrt{2}\delta}]\sin[r\xi]+$$
$$i\text{Erf}[\frac{i(1+r)+\delta\phi}{\sqrt{2}\delta}](\cos[r\xi]-\delta\phi\sin[r\xi])-(\text{Erfi}[\frac{1+r+i\delta(\xi\delta-\phi)}{\sqrt{2}\delta}]-\text{Erfi}[\frac{1+r-i\delta\phi}{\sqrt{2}\delta}])$$
$$((1+r)\cos[r\xi]-(ir+\delta\phi)\sin[r\xi]))) \tag{3.22}$$

$$P_z = \frac{1}{8r\delta}A_0 e^{-\frac{1+r^2+4i\xi\delta^2+\xi^2\delta^4+2\delta\phi(i+\delta\phi)+r(2+2i\delta(\xi\delta+\phi))}{2\delta^2}}(4ie^{\frac{1+r(2+r)+2ir\delta\phi+\delta^2\phi^2+2i\delta(\xi\delta+\phi)}{2\delta^2}}(e^{\frac{1}{2}\xi(2i+\xi\delta^2)}$$
$$-e^{\frac{1}{2}\xi(2i+4ir+\xi\delta^2)}+e^{ir\xi+\xi\delta\phi}(-1+e^{2i\xi})r)\delta+e^{\frac{\xi^2\delta^2}{2}}\sqrt{2\pi}(e^{2i(1+r)\xi+\phi^2}r^2\text{Erf}[\frac{i+ir+\xi\delta^2-\delta\phi}{\sqrt{2}\delta}]$$
$$+e^{2i\xi}(e^{\phi(\frac{2i(1+r)}{\delta}+\phi)}(-i\delta\phi\text{Erf}[\frac{i(1+r)+\delta\phi}{\sqrt{2}\delta}]+i\delta\phi\text{Erf}[\frac{i+ir+\delta(-\xi\delta+\phi)}{\sqrt{2}\delta}]+$$
$$(-ir^2+\delta\phi)(\text{Erfi}[\frac{1+r+i\delta(\xi\delta-\phi)}{\sqrt{2}\delta}]-$$
$$\text{Erfi}[\frac{1+r-i\delta\phi}{\sqrt{2}\delta}]))-ie^{\phi^2+\frac{2r(1+i\delta\phi)}{\delta^2}}r^2(\text{Erfi}[\frac{1-r-i\delta(\xi\delta-\phi)}{\sqrt{2}\delta}]-\text{Erfi}[\frac{1-r+i\delta\phi}{\sqrt{2}\delta}]))$$
$$e^{2i(1+r)\xi}(-ie^{\phi(\frac{2i(1+r)}{\delta}+\phi)}\delta\phi\text{Erf}[\frac{i(1+r)+\delta\phi}{\sqrt{2}\delta}]+ie^{\phi(\frac{2i(1+r)}{\delta}+\phi)}\delta\phi\text{Erf}[\frac{i+ir+\delta(-\xi\delta+\phi)}{\sqrt{2}\delta}]+$$
$$e^{\phi(\frac{2i(1+r)}{\delta}+\phi)}\delta\phi\text{Erfi}[\frac{1+r+i\delta(\xi\delta-\phi)}{\sqrt{2}\delta}]-e^{\phi(\frac{2i(1+r)}{\delta}+\phi)}\delta\phi\text{Erfi}[\frac{1+r-i\delta\phi}{\sqrt{2}\delta}]+ie^{\frac{2r+\delta\phi(2i+\delta\phi)}{\delta^2}}$$
$$r^2(\text{Erfi}[\frac{1-r+i\delta(\xi\delta-\phi)}{\sqrt{2}\delta}]+\text{Erfi}[\frac{-1+r+i\delta\phi}{\sqrt{2}\delta}])-ie^{\phi^2}r^2\text{Erfi}[\frac{1+r+i\delta\phi}{\sqrt{2}\delta}]))) \tag{3.23}$$

Thus longitudinal component of the particle momentum as well as the energy can be simply obtained by substituting expressions Eq.(3.22) and Eq.(3.23) in the expressions Eq.(3.10) and Eq.(3.13) respectively. The longitudinal particle position can be obtained by integrating the expression (3.10). In the above expressions Erfi, is the imaginary error function which is related to the Erf, as Erfi(z)=-iErf(iz). The above derived analytical solutions, describing the particle dynamics in the combined field of a finite duration laser pulse and static axial magnetic field are in parametric form and thus can be used to study different aspects of pulse-particle interaction. The understanding of these solution enables us to explore the features of laser driven auto-resonant acceleration scheme of charged particles in the vacuum for the finite duration laser pulse.

3.2.2 Elliptical Polarization

In this subsection, we present the description of the method of solution to the relativistic equation of motion interacting simultaneously with the field of elliptically polarized finite duration laser pulse and static axial magnetic field. The methodology of the solution is similar to the one described above but have been explicitly specified for the ease of reading. The vector potential of an elliptically polarized finite duration laser pulse traveling along $\hat{x}$ direction in the presence of a constant homogeneous axial magnetic field is

$$\vec{A} = (A_0\Theta(\delta\xi)(1-\kappa^2)^{1/2}P(\xi) - \frac{B_0 z}{2})\hat{y} + (A_0\Theta(\delta\xi)\kappa P_1(\xi) + \frac{B_0 y}{2})\hat{z} \tag{3.24}$$

in the above expression κ defines the polarization state of the pulse and other terms as specified above are: the phase of the laser is given by $\xi = (\omega t - kx)$, $\Theta(\delta\xi)$ is pulse envelope, $P(\xi)$ and $P_1(\xi)$ are the oscillatory parts, factor $\delta(=\frac{\lambda}{L})$ is the ratio of the laser wavelength to the pulse length, A_0 is the peak laser amplitude, B_0 is the magnitude of the external magnetic field.

The corresponding electric and magnetic field corresponding to the above described vector potential of the laser are defined as,

$$\vec{E} = -\frac{1}{c}\frac{\partial\vec{A}}{\partial t} \qquad \vec{B} = \nabla\times\vec{A} \tag{3.25}$$

.

Using the above specified normalizations the relativistic momentum and energy equation are given by,

$$\frac{d\vec{P}}{dt} = [\vec{E} + \frac{\vec{P}}{\Gamma} \times (\vec{B} + \vec{\Omega}_c)] \tag{3.26}$$

$$\frac{d\Gamma}{dt} = \frac{\vec{P}.\vec{E}}{\Gamma} \tag{3.27}$$

Here Γ as defined above is the relativistic factor given by,

$$\Gamma = (1 + P_x^2 + P_y^2 + P_z^2)^{1/2}$$

and P_x, P_y, P_z are the four momentum components.

On re-writing the equations in component form,

$$\frac{dP_x}{dt} = -\frac{1}{\Gamma}\left(P_y\frac{\partial A_y}{\partial \xi} - P_z\frac{\partial A_z}{\partial \xi}\right) \tag{3.28}$$

$$\frac{dP_y}{dt} = -\frac{(\Gamma - P_x)}{\Gamma}\frac{\partial A_y}{\partial \xi} + \frac{P_z\Omega_c}{\Gamma} \tag{3.29}$$

$$\frac{dP_z}{dt} = -\frac{(\Gamma - P_x)}{\Gamma}\frac{\partial A_z}{\partial \xi} - \frac{P_y\Omega_c}{\Gamma} \tag{3.30}$$

$$\frac{d\Gamma}{dt} = -\frac{1}{\Gamma}\left(P_y\frac{\partial A_y}{\partial \xi} - P_z\frac{\partial A_z}{\partial \xi}\right) \tag{3.31}$$

From Eq.(3.28) and Eq.(3.31) as described above we get a constant of motion Δ defined as,

$$\Delta = \Gamma - P_x \tag{3.32}$$

.

The phase of the laser and the constant of motion Δ are related as $\dot{\xi} = \frac{\Delta}{\Gamma}$. On expressing the above equations Eq.(3.28) to Eq.(3.31) in terms of laser phase ξ and using Eq.(3.9), the components of particle momentum takes the following form,

$$P_x = \frac{1-\Delta^2}{2\Delta} + \frac{P_y^2 + P_z^2}{2\Delta} \tag{3.33}$$

$$P_y = \alpha_1 - A_y + Z\Omega_c \tag{3.34}$$

$$P_z = \alpha_2 - A_z - Y\Omega_c \tag{3.35}$$

where as described above α_1 and α_2 are constants of motion which correspond to the conservation of transverse canonical momentum.

Using Eq.(3.9) and Eq.(3.33) the total energy of a particle is given by,

$$\Gamma = \frac{1+\Delta^2}{2\Delta} + \frac{P_y^2 + P_z^2}{2\Delta} \tag{3.36}$$

As described above the particle position can be obtained by integrating particle momentum as,

$$\vec{R} - \vec{R}_0 = \frac{1}{\Delta}\int_{\xi_0}^{\xi} \vec{P} d\xi \tag{3.37}$$

Similar to above case, the transverse momentum as well as the position of a particle can be obtained either by representing them as first order complex differential equation or by decoupling the equations and writing them as second order differential equations describing the cyclotron motion,

$$\frac{d^2Y}{d\xi^2} + r^2 y = r(\frac{\alpha_2}{\Delta} - \frac{A_z}{\Delta}) - \frac{1}{\Delta}\frac{dA_y}{d\xi} \tag{3.38}$$

$$\frac{d^2Z}{d\xi^2} + r^2 z = -\frac{1}{\Delta}\frac{dA_z}{d\xi} - r(\frac{\alpha_1}{\Delta} - \frac{A_y}{\Delta}) \tag{3.39}$$

The temporal profile and the oscillatory part defining the vector potential of the finite duration laser pulse are given below.

$$\Theta(\xi) = exp(-\frac{(\delta\xi - \phi)^2}{2}) \tag{3.40}$$

$$P(\xi) = sin(\xi) \tag{3.41}$$

$$P_1(\xi) = cos(\xi) \tag{3.42}$$

As described above the position and momentum of the particle are related to each other as,

$$\frac{d\vec{R}}{d\xi} = \frac{\vec{P}}{\Delta} \tag{3.43}$$

here as specified earlier $\vec{P}$ represents the normalized four momentum of the particle. The transverse co-ordinates of the particle position derived by solving the equations of cyclotron motion given by Eq.(3.38) and Eq.(3.39) which are expressed symbolically in simplified form are given below. The various terms in the expression have been specified in the appendix. **Particle Position**

$$
\begin{aligned}
Z = {} & \\
& \frac{1}{\delta\Delta r} e^{\frac{\text{k1}}{\delta^2} - i\xi(-1+r)} \\
& \Big(e^{\text{k5}}\delta\left(-e^{\text{k6}+i\xi(-1+r)}\left((-1+\text{CS})\text{CS}+\text{Sn}^2\right)\alpha 1 + \text{A0Sn}\left(\left(0.25e^{\frac{\text{k11}}{\delta^2}} + 0.25e^{\text{k18}+i\xi(-1+r)} + \right.\right.\right. \\
& 0.25e^{\text{k19}+i\xi(-1+r)} + 0.25e^{\text{k21}+i\xi(-1+r)} - 0.25e^{\frac{\text{k12}}{\delta^2}+i\xi(-1+r)} + 0.25e^{\frac{\text{k13}}{\delta^2}+i\xi(-1+r)}\Big)\kappa - \\
& \text{A13}e^{i\xi(-1+r)}\left(\text{D1}\left(e^{\text{k14}} - e^{\text{k15}} - e^{\text{k16}} + e^{\text{k17}}\right) + \left(e^{\text{k14}} + e^{\text{k15}} + e^{\text{k16}} + e^{\text{k17}}\right)\kappa\right)\Big)\Big) + \\
& \text{A0A9}e^{\text{k5}+i\xi(-1+r)}\left(\text{CS}e^{\frac{\text{k7}}{\delta^2}}\kappa - ie^{\frac{\text{k20}}{\delta^2}}\text{Sn}\kappa - \text{CSD2}e^{\text{k29}+\text{k30}}r\right)\text{Erf[j1]} + \text{A0A9}e^{\text{k25}+\text{k5}+i\xi(-1+r)} \\
& \left(ie^{\text{k27}}\text{Sn}\kappa + \text{CS}e^{\text{k26}}(-\kappa + \text{D1}r)\right)\text{Erf[j11]} + \text{A0}e^{i\xi(-1+r)}\left(\text{A9}e^{\text{k28}+\text{k5}}\kappa\left(-ie^{\text{k4}}\text{Sn}(1+r) - \right.\right. \\
& \text{CS}e^{\text{k3}}(1+r+i\delta\phi)\Big)\text{Erf[j12]} + \text{A9}e^{\text{k2}}\kappa\left(ie^{\text{k4}}\text{Sn}(1+r) + \text{CS}e^{\text{k3}}(1+r+i\delta\phi)\right)\text{Erf[j2]} + \\
& e^{\text{k5}}\Big(\text{A9}\Big(\Big(e^{\frac{\text{k24}}{\delta^2}}\text{Sn}\kappa + i\text{CSD2}e^{\text{k26}+\text{k29}}r - \text{D2}e^{\text{k27}+\text{k29}}\text{Sn}r + \text{CS}e^{\frac{\text{k10}}{\delta^2}}\kappa(-i+\delta\phi)\Big)\text{Erfi[j10]} + \\
& \left(e^{\frac{\text{k22}}{\delta^2}}\text{Sn}(\text{D1}r + \kappa(-1+i\delta\phi)) + e^{\frac{\text{k8}}{\delta^2}}(-i\text{CS}(\text{D1}-\kappa)r - \text{Sn}\kappa(-1+r+i\delta\phi))\right)\text{Erfi[j3]} + \\
& i\text{CS}e^{\frac{\text{k7}}{\delta^2}}\kappa\text{Erfi[j4]} + e^{\frac{\text{k20}}{\delta^2}}\text{Sn}\kappa\text{Erfi[j4]} + \text{D1}e^{\frac{\text{k20}}{\delta^2}}\text{Sn}r\text{Erfi[j4]} + i\text{CS}e^{\frac{\text{k7}}{\delta^2}}\kappa r\text{Erfi[j4]} + e^{\frac{\text{k20}}{\delta^2}}\text{Sn}\kappa r\text{Erfi[j4]} + \\
& i\text{CSD1}e^{\frac{\text{k9}}{\delta^2}}r\text{Erfi[j5]} + \text{D1}e^{\frac{\text{k23}}{\delta^2}}\text{Sn}r\text{Erfi[j5]} - i\text{CS}e^{\frac{\text{k9}}{\delta^2}}\kappa r\text{Erfi[j5]} - e^{\frac{\text{k23}}{\delta^2}}\text{Sn}\kappa r\text{Erfi[j5]} + i\text{CS}e^{\frac{\text{k10}}{\delta^2}}\kappa\text{Erfi[j6]} \\
& -e^{\frac{\text{k24}}{\delta^2}}\text{Sn}\kappa\text{Erfi[j6]} - i\text{CSD1}e^{\frac{\text{k10}}{\delta^2}}r\text{Erfi[j6]} + \text{D1}e^{\frac{\text{k24}}{\delta^2}}\text{Sn}r\text{Erfi[j6]} - \text{CS}e^{\frac{\text{k10}}{\delta^2}}\delta\kappa\phi\text{Erfi[j6]} + e^{\frac{\text{k22}}{\delta^2}}\text{Sn}\kappa \\
& \text{Erfi[j7]} - e^{\frac{\text{k8}}{\delta^2}}\text{Sn}\kappa\text{Erfi[j7]} + i\text{CSD2}e^{\text{k29}+\text{k34}+\frac{2i\phi}{\delta}}r\text{Erfi[j7]} - \text{D2}e^{\text{k29}+\text{k35}+\frac{2i\phi}{\delta}}\text{Sn}r\text{Erfi[j7]} \\
& -i\text{CS}e^{\frac{\text{k8}}{\delta^2}}\kappa r\text{Erfi[j7]} + e^{\frac{\text{k8}}{\delta^2}}\text{Sn}\kappa r\text{Erfi[j7]} - ie^{\frac{\text{k22}}{\delta^2}}\text{Sn}\delta\kappa\phi\text{Erfi[j7]} + ie^{\frac{\text{k8}}{\delta^2}}\text{Sn}\delta\kappa\phi\text{Erfi[j7]} - i\text{CS}e^{\frac{\text{k7}}{\delta^2}}\kappa\text{Erfi[j8]} \\
& -e^{\frac{\text{k20}}{\delta^2}}\text{Sn}\kappa\text{Erfi[j8]} - \text{D2}e^{\text{k29}+\text{k32}}\text{Sn}r\text{Erfi[j8]} - i\text{CS}e^{\frac{\text{k7}}{\delta^2}}\kappa r\text{Erfi[j8]} - e^{\frac{\text{k20}}{\delta^2}}\text{Sn}\kappa r\text{Erfi[j8]} - \\
& i\text{CSD2}e^{\text{k29}+\text{k31}}r\text{Erfi[j9]} - \text{D2}e^{\text{k29}+\text{k33}}\text{Sn}r\text{Erfi[j9]} + i\text{CS}e^{\frac{\text{k9}}{\delta^2}}\kappa r\text{Erfi[j9]} + e^{\frac{\text{k23}}{\delta^2}}\text{Sn}\kappa r\text{Erfi[j9]}\Big) - \\
& \text{CS}e^{\frac{\text{k11}}{\delta^2}}\delta\kappa\text{Cos}[\xi]\text{Sin}[\xi r]\Big)\Big)\Big)
\end{aligned}
$$

$$Y = \frac{1}{\delta \Delta r} e^{\mathrm{d31}} \Big(0.25\mathrm{A0c1}e^{\mathrm{d10a}} i\mathrm{Sn}\delta - 0.25\mathrm{A0c1}e^{\mathrm{d11}} i\mathrm{Sn}\delta - 0.25\mathrm{A0c1}e^{\mathrm{d6}} i\mathrm{Sn}\delta + 0.25\mathrm{A0c1}e^{\mathrm{d7}} i\mathrm{Sn}\delta + 0.25\mathrm{A0c1}e^{\mathrm{d8}} i\mathrm{Sn}\delta - 0.25\mathrm{A0c1}e^{\mathrm{d9}} i\mathrm{Sn}\delta - \mathrm{CS}e^{\mathrm{d2}}\alpha 2\delta + \mathrm{CS}^2 e^{\mathrm{d2}}\alpha 2\delta - 0.125e^{\mathrm{d2}}\mathrm{Sn}^2\alpha 2\delta + 0.25\mathrm{A0}e^{\mathrm{d10a}} i\mathrm{Sn}\delta\kappa - 0.25\mathrm{A0}e^{\mathrm{d11}} i\mathrm{Sn}\delta\kappa + 0.25\mathrm{A0}e^{\mathrm{d6}} i\mathrm{Sn}\delta\kappa - 0.25\mathrm{A0}e^{\mathrm{d7}} i\mathrm{Sn}\delta\kappa + i\mathrm{A0a8c1CS}e^{\mathrm{d1}} r\mathrm{Erf}[\mathrm{e1}] - \mathrm{A0a8c1}e^{\mathrm{d12}}\mathrm{Sn}r\mathrm{Erf}[\mathrm{e1}] - i\mathrm{A0a8c1CS}e^{\mathrm{d4}}\mathrm{Erf}[\mathrm{e2}] - \mathrm{A0a8c1}e^{\mathrm{d13}}\mathrm{SnErf}[\mathrm{e2}] - \mathrm{A0a8CS}e^{\mathrm{d1}}\kappa r\mathrm{Erfi}[\mathrm{e10}] - i\mathrm{A0a8}e^{\mathrm{d12}}\mathrm{Sn}\kappa r\mathrm{Erfi}[\mathrm{e10}] - i\mathrm{A0a8c1}e^{\mathrm{d14}}\mathrm{SnErfi}[\mathrm{e3}] + i\mathrm{A0a8c1}e^{\mathrm{d3}}\mathrm{SnErfi}[\mathrm{e3}] - \mathrm{A0a8c1CS}e^{\mathrm{d3}} r\mathrm{Erfi}[\mathrm{e3}] - i\mathrm{A0a8c1}e^{\mathrm{d3}}\mathrm{Sn}r\mathrm{Erfi}[\mathrm{e3}] - \mathrm{A0a8CS}e^{\mathrm{d3}}\kappa r\mathrm{Erfi}[\mathrm{e3}] - i\mathrm{A0a8}e^{\mathrm{d14}}\mathrm{Sn}\kappa r\mathrm{Erfi}[\mathrm{e3}] - \mathrm{A0a8c1}e^{\mathrm{d14}}\mathrm{Sn}\delta\phi\mathrm{Erfi}[\mathrm{e3}] + \mathrm{A0a8c1}e^{\mathrm{d3}}\mathrm{Sn}\delta\phi\mathrm{Erfi}[\mathrm{e3}] + \mathrm{A0a8CS}e^{\mathrm{d3}}\kappa r\mathrm{Erfi}[\mathrm{e4}] + i\mathrm{A0a8}e^{\mathrm{d14}}\mathrm{Sn}\kappa r\mathrm{Erfi}[\mathrm{e4}] - \mathrm{A0a8c1CS}e^{\mathrm{d4}}\mathrm{Erfi}[\mathrm{e5}] + i\mathrm{A0a8c1}e^{\mathrm{d13}}\mathrm{SnErfi}[\mathrm{e5}] - \mathrm{A0a8c1CS}e^{\mathrm{d4}} r\mathrm{Erfi}[\mathrm{e5}] + i\mathrm{A0a8c1}e^{\mathrm{d13}}\mathrm{Sn} r\mathrm{Erfi}[\mathrm{e5}] + \mathrm{A0a8CS}e^{\mathrm{d4}}\kappa r\mathrm{Erfi}[\mathrm{e5}] - i\mathrm{A0a8}e^{\mathrm{d13}}\mathrm{Sn}\kappa r\mathrm{Erfi}[\mathrm{e5}] - \mathrm{A0a8CS}e^{\mathrm{d4}}\kappa r\mathrm{Erfi}[\mathrm{e6}] + i\mathrm{A0a8}e^{\mathrm{d13}}\mathrm{Sn}\kappa r\mathrm{Erfi}[\mathrm{e6}] - \mathrm{A0a8c1CS}e^{\mathrm{d5}} r\mathrm{Erfi}[\mathrm{e7}] + i\mathrm{A0a8c1}e^{\mathrm{d15}}\mathrm{Sn}r\mathrm{Erfi}[\mathrm{e7}] - \mathrm{A0a8CS}e^{\mathrm{d5}}\kappa r\mathrm{Erfi}[\mathrm{e7}] + i\mathrm{A0a8}e^{\mathrm{d15}}\mathrm{Sn}\kappa r\mathrm{Erfi}[\mathrm{e7}] + \mathrm{A0a8CS}e^{\mathrm{d5}}\kappa r\mathrm{Erfi}[\mathrm{e8}] - i\mathrm{A0a8}e^{\mathrm{d15}}\mathrm{Sn}\kappa r\mathrm{Erfi}[\mathrm{e8}] + \mathrm{A0c2}\left(e^{\mathrm{d16}}\left(-0.125e^{\mathrm{d17}} + 0.125e^{\mathrm{d18}} + e^{2i\xi r}\left(0.125e^{\mathrm{d17}} - 0.125e^{\mathrm{d18}}\right)\right)\delta + \mathrm{a8}e^{-i\xi}\left(e^{\mathrm{d19}}\left(-i\mathrm{CS}e^{\mathrm{d20}} + e^{\mathrm{d25}}\mathrm{Sn}\right) r\mathrm{Erf}[\mathrm{e11}] + \left(i\mathrm{CS}e^{\mathrm{d21}} + e^{\mathrm{d22}}\mathrm{Sn}\right)\mathrm{Erf}[\mathrm{e12}] + e^{\mathrm{d23}}\left(e^{\mathrm{d30}}\left(e^{\mathrm{d27}}\mathrm{Sn}(i + \delta\phi) + e^{\mathrm{d26}}(\mathrm{CS}r + i\mathrm{Sn}(-1 + r + i\delta\phi))\right)\mathrm{Erfi}[\mathrm{e4}] + \left(\mathrm{CS}e^{\mathrm{d28}} - ie^{\mathrm{d29}}\mathrm{Sn}\right)(1 + r)\mathrm{Erfi}[\mathrm{e6}] + e^{\mathrm{d24}}\left(\mathrm{CS}e^{\mathrm{d26}} - ie^{\mathrm{d27}}\mathrm{Sn}\right) r\mathrm{Erfi}[\mathrm{e8}]\right)\right)\right) + \mathrm{A0a8CS}e^{\mathrm{d1}}\kappa r\mathrm{Erfi}[\mathrm{e9}] + i\mathrm{A0a8}e^{\mathrm{d12}}\mathrm{Sn}\kappa r\mathrm{Erfi}[\mathrm{e9}]\Big)$$

In the following solutions symbol 'Ξ' and 'r ' represent the same. The other dynamical variables viz. momentum, energy and longitudinal position of the particle can be derived in the manner described above for the linear polarization. The analytical expression derived in this section have a complicated mathematical structure and thus an exhaustive numerical work has been carried out in the following section to gain comprehensive understanding of the particle dynamics.

3.3 Numerical Results

In this section, we present numerical solution of the relativistic equation of motion of the particle interacting with the linearly polarized finite duration laser pulse using R.K. method with adaptive step size control. The analytical expressions derived above are used to validate the numerical results. In the present analysis as specified earlier the particle is assumed to be at rest before the onset of interaction with the laser field. The initial conditions, $\Delta = 1$ and $\alpha_1 = \alpha_2 = 0$, correspond to the particle which is initially at rest before the onset of pulse particle interaction.

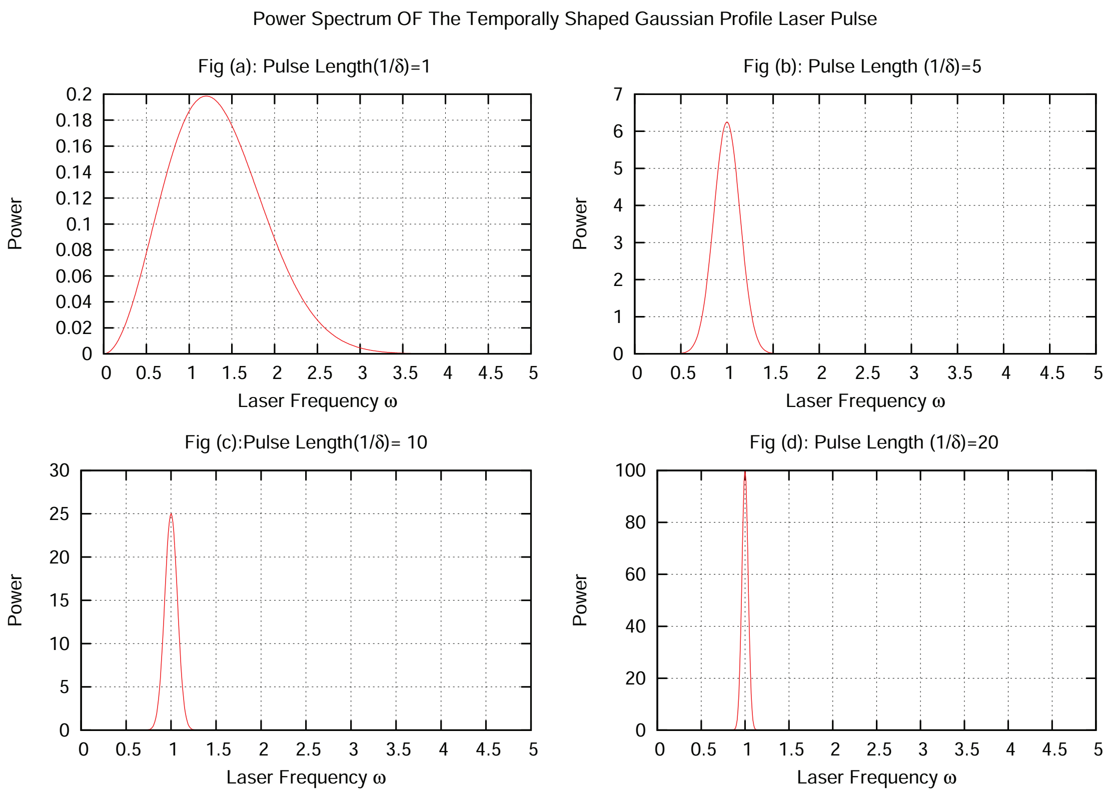

Figure 3.1: The power spectrum of a laser pulse corresponding to the different pulse lengths $(\frac{1}{\delta})$.

In Fig.3.1, the frequency spectrum of a finite duration laser pulse which has temporally shaped Gaussian envelope for different pulse lengths is plotted, it can be seen that frequency spectrum of the laser pulse is continuous. It has a finite width around the central frequency and the width of the spectrum decreases with increase in the length of the laser pulse.

The results of a single particle code are plotted in Fig.3.2 and Fig.3.3, along with the analytical results representing all the three components of momentum and position of a particle respectively. The results in these figure describe the non-resonant as well as resonant interaction of the particle with the laser pulse.

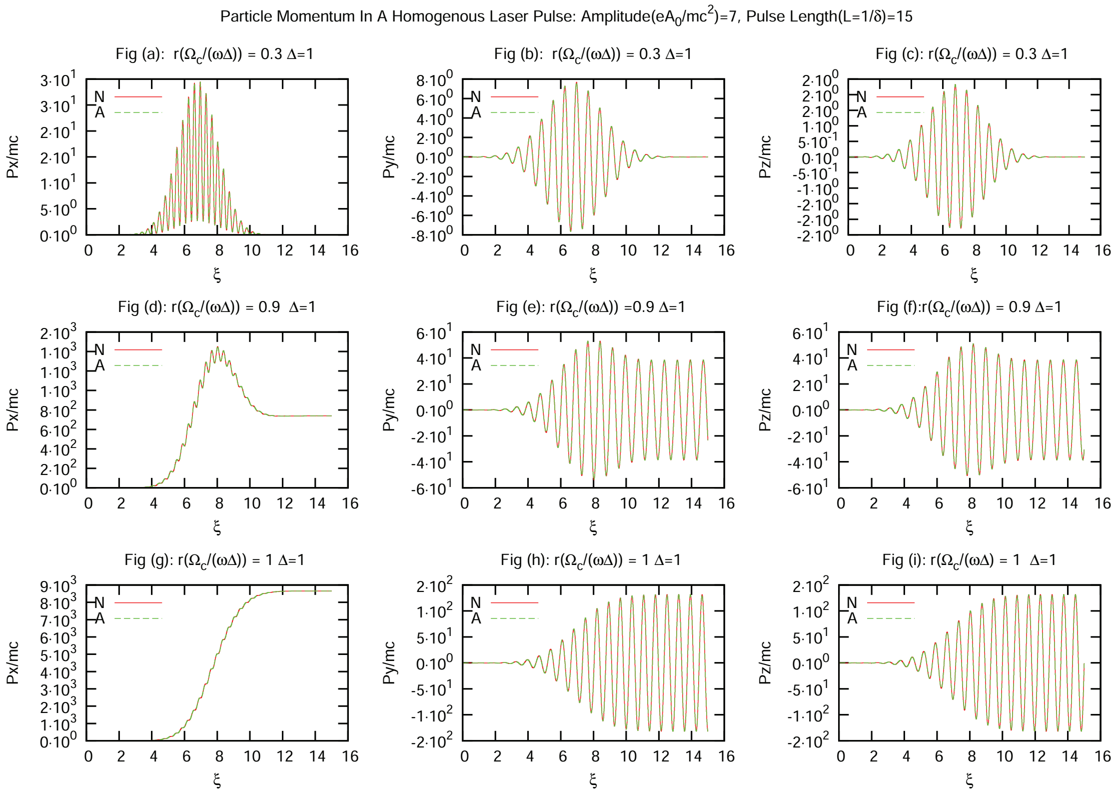

Figure 3.2: Analytical (A) and Numerical(N) description of evolution of particle momentum as a function of laser phase ξ for the amplitude $eA_0/mc^2 = 7$, $\delta = 1/15$ and $\Delta = 1$. Figs.2(a)-(c):The three momentum components for the particle corresponding to the non-resonant interaction with the pulse. In Figs.2(d)-(f): Momentum components corresponding to the resonant interaction with the laser pulse at frequency different for the central frequency. In Figs.2(g)-(i): Momentum components corresponding to the r=1 resonant case.

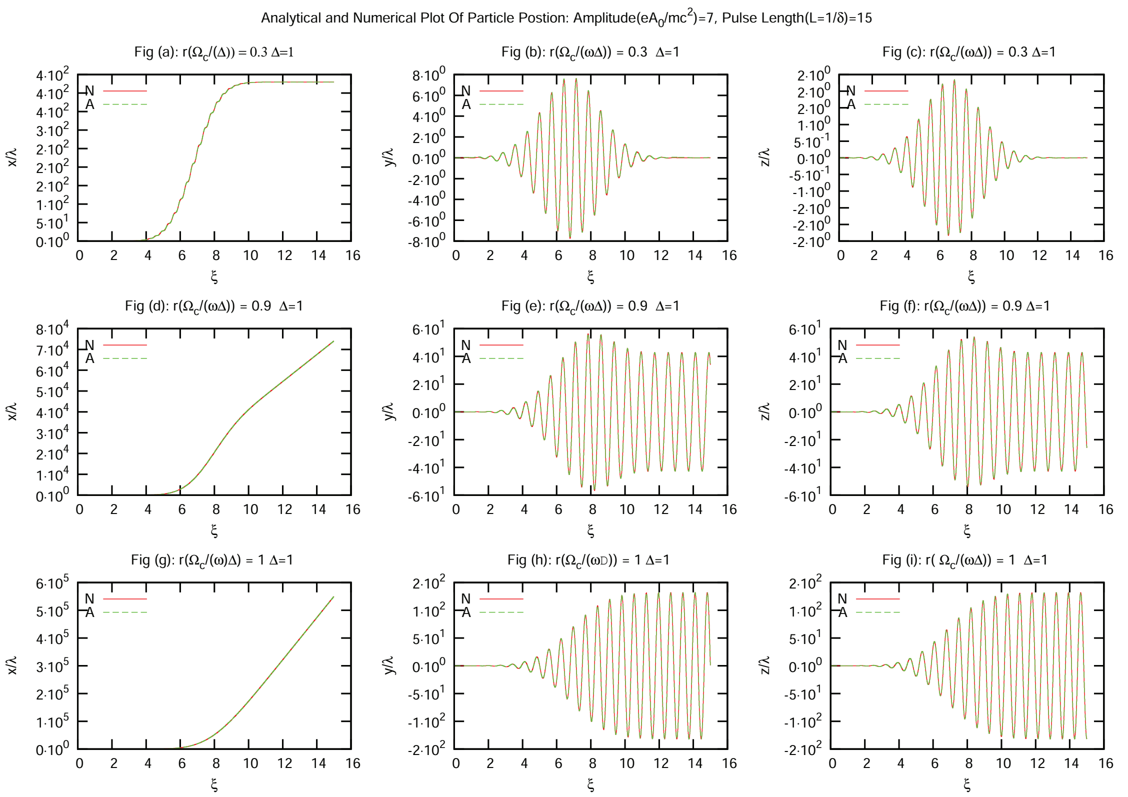

Figure 3.3: Analytical (A) and Numerical(N) description of evolution of particle position as a function of laser phase ξ for the amplitude $eA_0/mc^2 = 7$, $\delta = 1/15$ and $\Delta = 1$. Figs.3(a)-(c):The three position co-ordinates for the particle corresponding to the non-resonant interaction with the pulse. In Figs.3(d)-(f): Position co-ordinates corresponding to the resonant interaction with the laser pulse at frequency different for the central frequency. In Fig.-(g)-(i): Position coordinates corresponding to the r=1 resonant case.

In Figs.3.2 subplots (a-b-c), the three components of particle four momentum are plotted corresponding to the non-resonant interaction. It can be seen that for the case of a non-resonant interaction of the particle with a laser pulse i.e, when the cyclotron frequency of the particle does not correspond to any of the characteristic frequencies in a laser spectrum, no net energy is transfered to the particle and all the three components of momentum becomes zero after the interaction. In subplots (d-e-f), the momentum components for the resonant case are plotted by tuning the cyclotron frequency of the particle at a characteristic frequency in pulse spectrum different from central frequency. From the results it can be seen that for a resonant case, there is net energy transfer to the particle along the propagation direction of the laser pulse. In the transverse direction beyond the point of resonance matching, the particle momentum exhibits finite amplitude oscillations. In the subplots (g-h-i), momentum components correspond to resonant case for the central frequency. There is increase in the net energy gain by the particle along the direction of the laser propagation. The amplitude of the particle oscillations along the transverse direction increases as a consequence of increase in the net energy transfer to the particle.

In the Fig.3.3 subplots(a-b-c), the particle position is plotted for the non-resonant interaction of the particle with a laser pulse. The particle is at rest after the interaction with a laser pulse and is displaced along the direction of laser propagation with no side-wise displacement. In the subplots (d-e-f), the particle position for a resonant case are plotted at a frequency different from the central frequency. The continuous shift in the longitudinal position is due to finite energy gain along the longitudinal direction. Along the transverse direction beyond the point of resonance, the particle exhibits a finite amplitude oscillatory motion corresponding to the energy gain by a particle. In subplots (g-h-i), the position coordinates of particle corresponds to the resonant interaction of a particle with the laser pulse at central frequency. The particle is displaced by large distance along the direction of propagation of the laser pulse. At the onset of the pulse particle interaction there is increase in the transverse amplitude of particle oscillations that attains maximum value at the center of the laser pulse and corresponds to a resonant energy transfer beyond, which the amplitude of oscillations remains constant. From the position and momentum plots it can be seen that the results of a single particle code are in good agreement with the above derived analytical results.

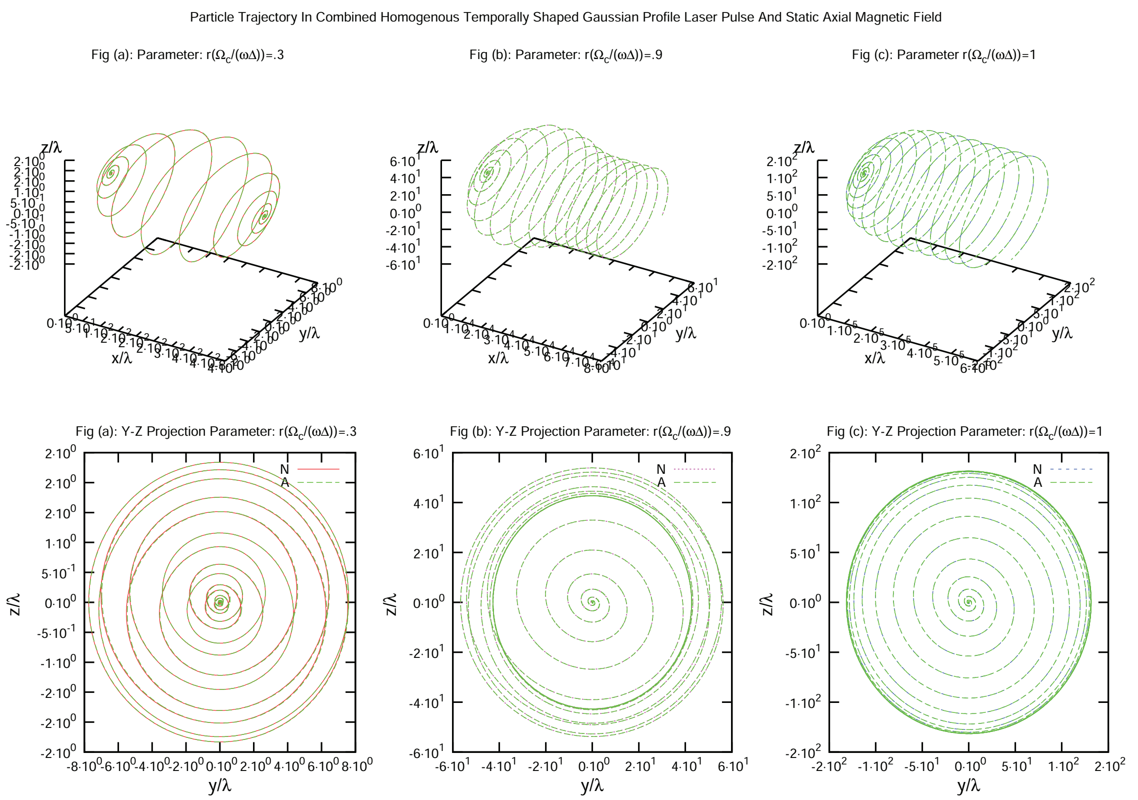

Figure 3.4: Analytical (A) and Numerical (N) 3-D particle trajectory along with the transverse projection in Y-Z plane for following parameters $eA_0/mc^2 = 7$, $\delta = 1/15$ and $\Delta = 1$.

In Fig.3.4, the 3-D trajectories of particle dynamics along with its transverse projection in the Y-Z plane are plotted for non-resonant and resonant interaction of a particle with laser pulse. For a non-resonant interaction subplot (a), the particle which is initially at rest is accelerated by the laser field in the rising edge of the laser pulse, particle carries out a cyclotron motion while moving in a helical path with increasing cyclotron radius along the direction of propagation. The cyclotron radius is maximum at the center of the pulse. Beyond this point the particle decelerates in the trailing part of the pulse and in the process it comes back to rest returning all its energy to the pulse. This symmetry in the acceleration and deceleration can be seen in the transverse projection of the particle trajectory, which is in the form of closed loops. For the resonant interaction subplots (b-c), the particle is at rest before the onset of the pulse particle interaction. It is initially accelerated by the rising edge of the laser pulse and corresponding to matching of cyclotron frequency of a particle with the characteristic frequency from the laser spectrum, net energy is transfered to it. After resonant interaction transverse radius of the particle gets fixed and particle moves in a helical path along the propagation direction. The symmetry in acceleration and deceleration is lost, as can be seen the 2-D transverse projection where the loops are no longer closed ones. It can be inferred from the plot that the cyclotron radius of the particle increases with an increase in the resonant frequency reaching maximum for the central resonance.

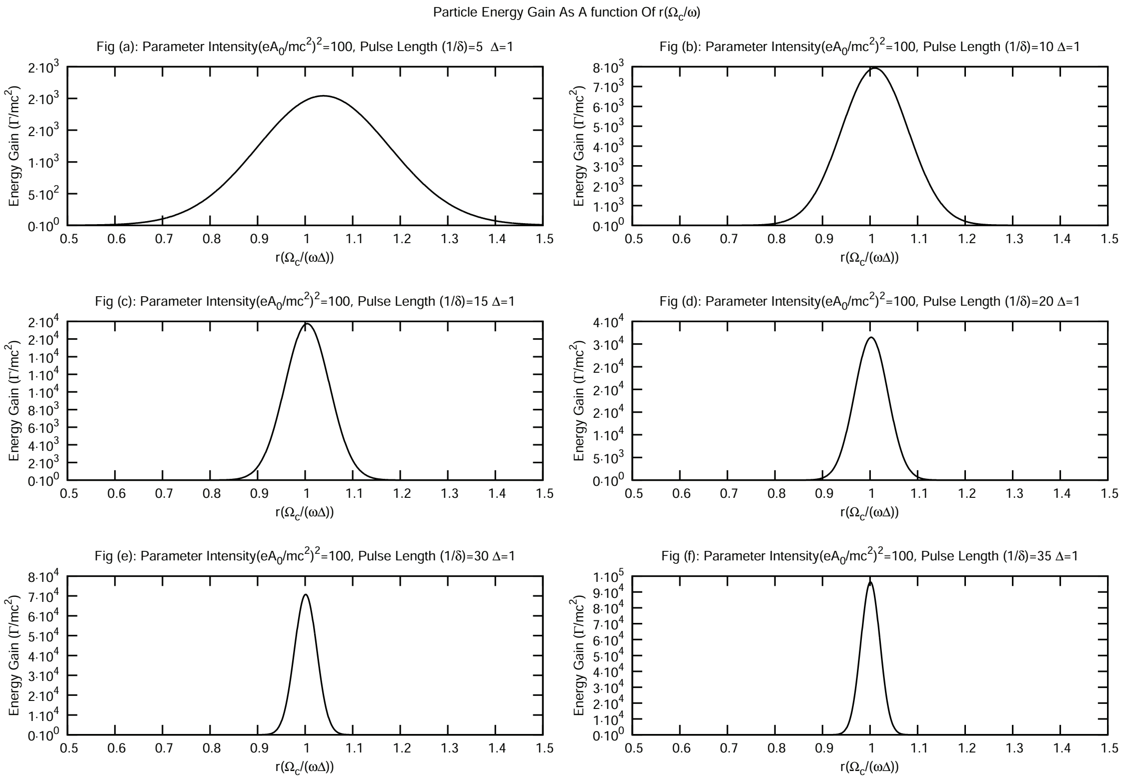

Figure 3.5: Resonant energy gained by a particle at the end of interaction with the finite duration laser pulse as a function of the applied static axial magnetic field keeping the laser amplitude constant at $eA_0/mc^2 = 10$.

In Fig.3.5, the final energy gain of a particle is plotted as a function of variable $r(= \frac{\Omega_c}{(\omega\Delta)})$; In subplots (a-b-c-d-e-f), the final energy gain is plotted for laser pulses with different pulse lengths and with the same peak amplitude. It can be seen from the plots that final energy gain by the particle is continuous and is in accordance with Fig.3.1, for the power spectrum of the laser pulse. The spectrum width of a final energy gain by the particle decreases with increase in the laser pulse length, which corresponds to the fact that the maximum resonant energy gain takes place when cyclotron frequency of the particle approaches the central laser frequency.

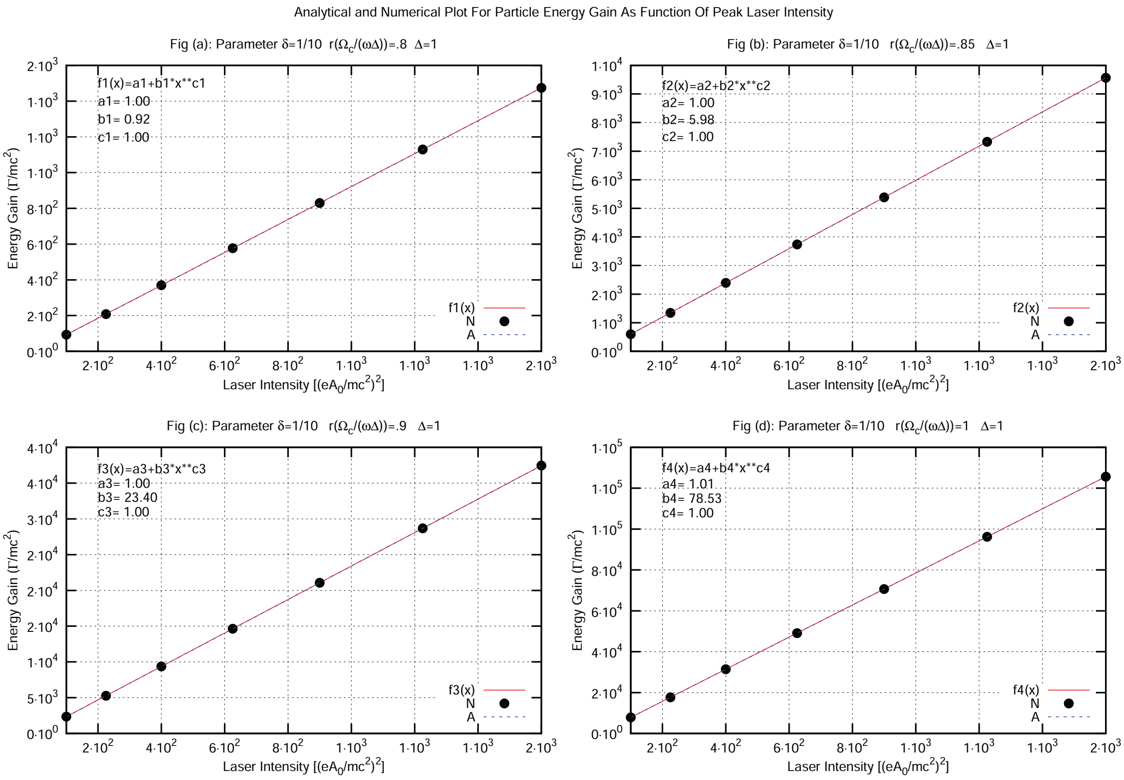

Figure 3.6: Analytical (A) and Numerical (N) plot for final energy gain of the particle as function of the peak laser intensity for the finite duration laser pulse of length of ten cycles($\frac{1}{\delta}$=10) corresponding to matching of different resonance frequencies with the laser spectrum.

In Fig.3.6, the functional dependence of the resonant final energy gain of the particle is parametrically studied using a fitting function as a function of the peak laser intensity at different values of $r(=\frac{\Omega_c}{\omega\Delta})$. From the values of the parameters (c1-c2-c3-c4) obtained by curve fitting, it can be inferred that the resonant energy gain of the particle increases linearly with the increase in the peak laser intensity. Further on comparing the subplots (a-b-c-d), it can be seen that the slope (b1-b2-b3-b4) describing the ratio of final energy gain to the input laser energy as a function of parameter $r(=\frac{\Omega_c}{\omega\Delta})$. Hence for a given laser intensity the final energy gain of the particle can be controlled by suitably adjusting this slope.

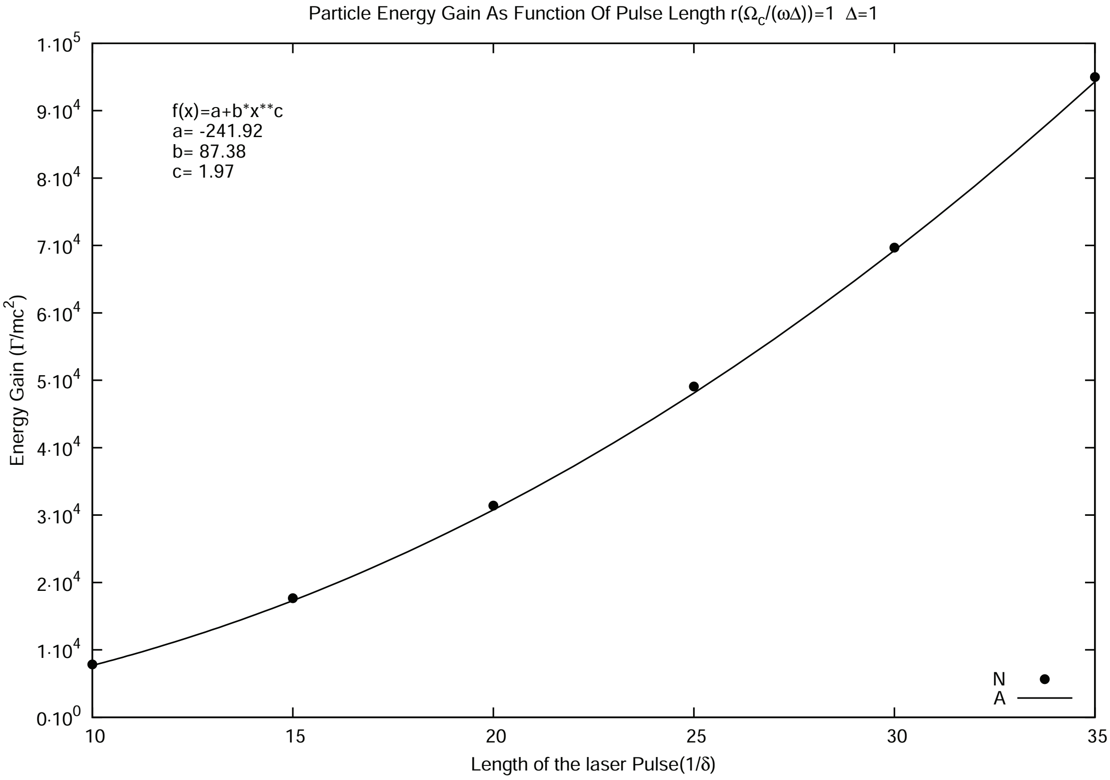

Figure 3.7: Final energy gain of the particle corresponding to the condition $r = 1$ and $eA_0/mc^2 = 10$ as a function of length of the pulse.

In Fig.3.7, corresponding to the condition $r(= \frac{\Omega_c}{\omega\Delta}) = 1$, the final resonant energy gain of the particle is studied as function of the laser pulse length $(\frac{1}{\delta})$, keeping the laser intensity constant. The parametric dependence is studied using fitting function from which it can be inferred that the final energy of the particle increases quadratically with the laser pulse length. This is in accordance with the above derived results for the particle energy gain.

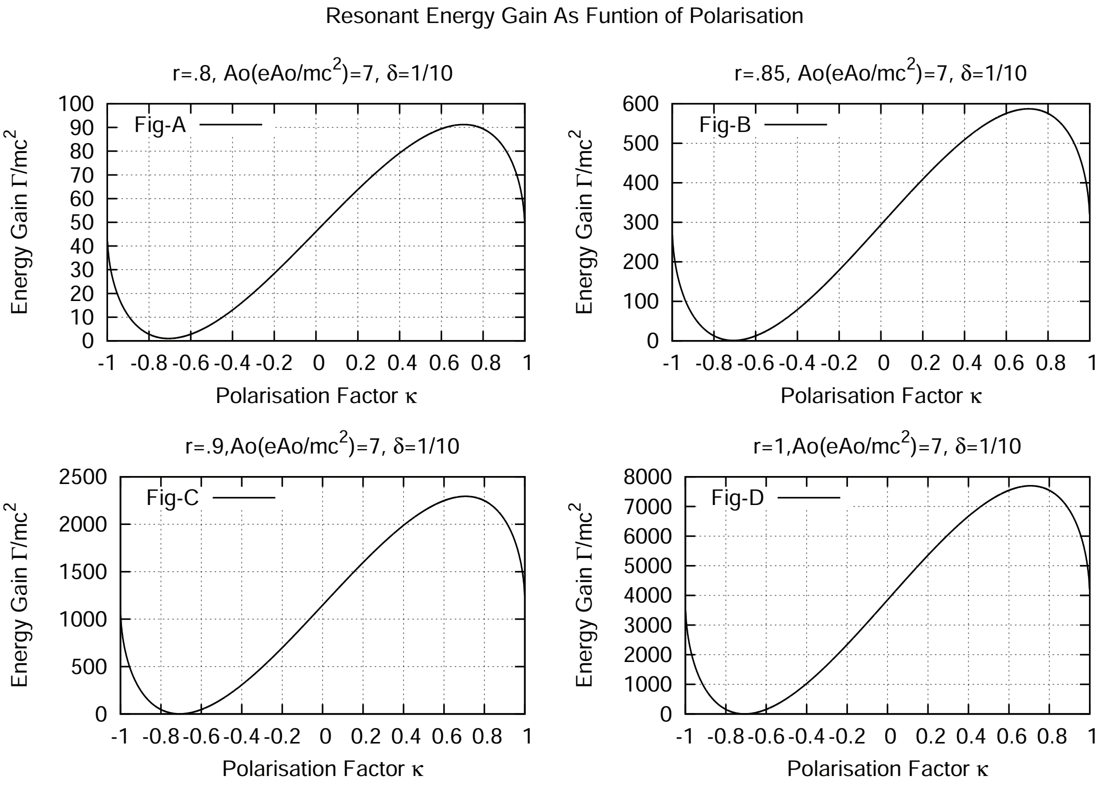

Figure 3.8: Energy gain of the particle as function of polarization parameter κ.

In Fig.3.8, the resonant energy gained by the particle at the end of pulse particle interaction is shown as a function of the polarization parameter κ. From the figure it can be inferred that the final energy gain by the particle depends upon the polarization parameter. The energy gain is maximum for the right circularly polarized pulse and minimum for left circularly polarization corresponding which corresponds to $\kappa = \pm 1/\sqrt{2}$ respectively. The final resonant energy gain is obtained for the same initial laser intensity and pulse duration, but correspond to different values of cyclotron frequency. From subplots-(A-B-C-D), it is evident that for a constant laser intensity and pulse length, the energy gain for each of the pulse polarization increases with increase in the cyclotron frequency and is maximum corresponding to the central frequency of pulse spectra. This gain is due to efficient acceleration by circularly polarized laser, which is made up of two linearly polarized laser pulses.

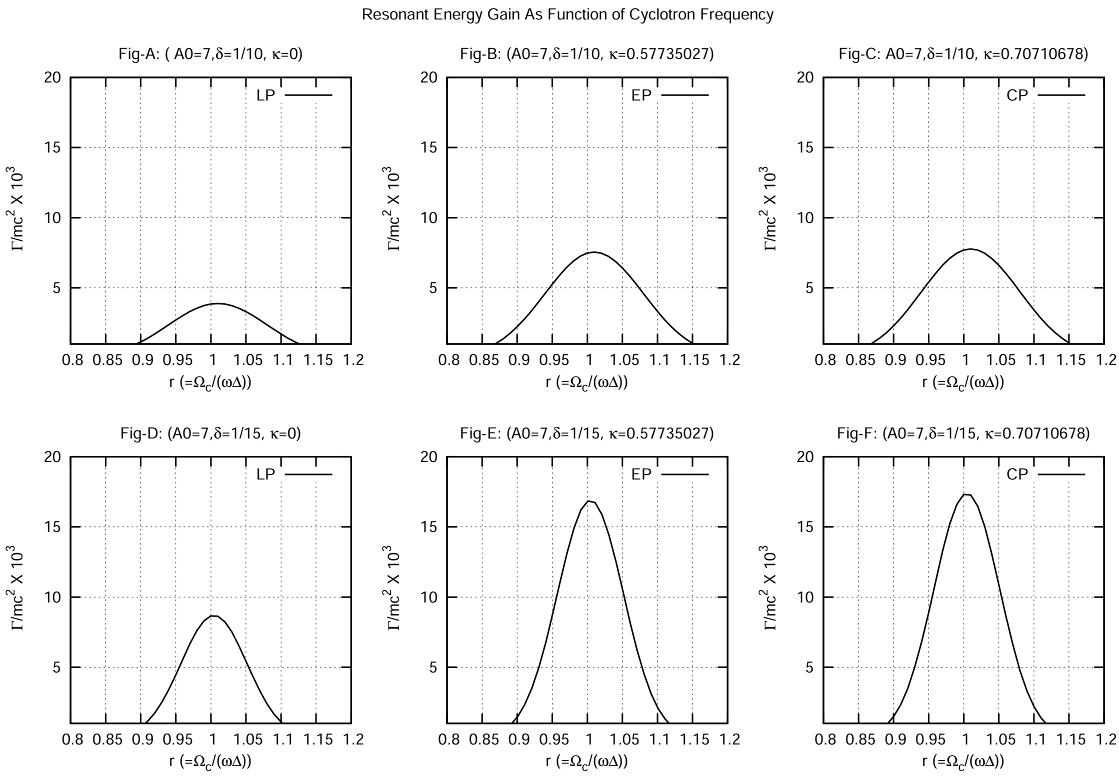

Figure 3.9: Energy gain of the particle as a function of parameter $r(= \Omega_c/(\omega\Delta))$ for different polarization states.

In Fig.3.9, the energy gain of the particle is plotted as function of the parameter $r(= \Omega_c/(\omega\Delta))$, the energy spectra of the particle is continuous, which is in accordance with the continuum in the frequency spectrum of a laser pulse. In this plot the laser intensity as well its pulse duration are kept constant and the resonant energy gain is studied for the different laser polarizations. It is evident from subplot(A-B-C), that for the same laser intensity the width as well as the height of the energy curve increases as the polarization of pulse is changed from linear to right circular. This implies that the cyclotron resonance can be achieved at lower axial magnetic fields and resultant energy gain improves for cyclotron frequency matching with the central frequency. On comparing the subplots (D-E-F) with (A-B-C) respectively of Fig.3.9, it can be seen that the for same laser intensity and polarization state, the resonant energy gain by the particle depends upon the length of the laser pulse. The increase in pulse length results in the decrease of the width of the energy spectra and increase in its height, in other words the higher values of axial magnetic field are required for the achieving cyclotron resonance. For a same laser intensity, the resonant energy gain corresponding to the matching of cyclotron frequency with the central frequency is found to be more for a longer pulse.

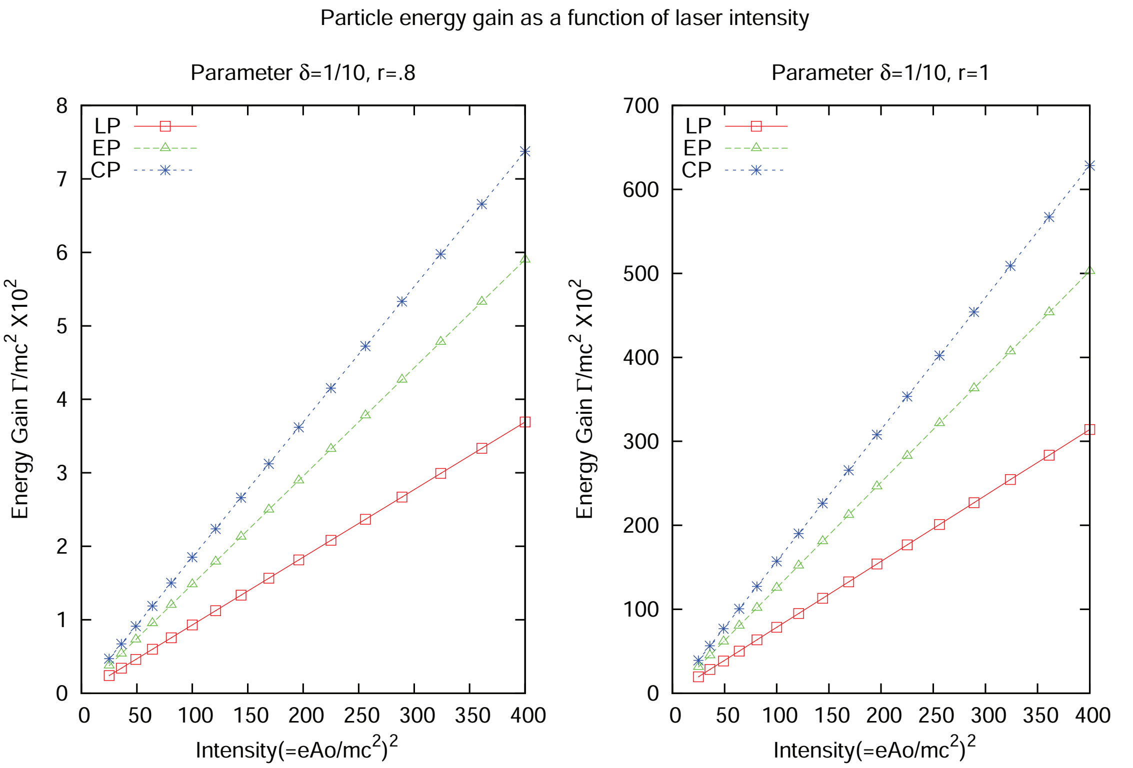

Figure 3.10: Energy gain of the particle as a function of peak laser intensity for different polarization states.

The scaling of resonant energy gain as function of laser intensity is described in Fig.3.10, corresponding to different laser polarizations and cyclotron frequencies. From the value of the fitting parameter **c=1** of the fitting function, it is clear that the resonant energy gain by the particle scales linearly with the peak laser intensity for different the polarization corresponding to values of $\kappa \rightarrow [0, 1]$. It can be further inferred for the same laser intensity the energy gain improves by varying the polarization from linear to right circular and also with the cyclotron matching frequency, which is maximum for when cyclotron frequency matches with laser central frequency.

3.4 Summary And Discussion

In this chapter, the non-resonant and resonant interaction of a particle with a laser pulse propagating along a static magnetic field has been studied analytically as well as numerically. The non-resonant interaction results in no net transfer of energy to the particle as a laser pulse slips past the particle. The particle is displaced along the direction of the laser propagation with no sideways displacement. For resonant interaction the cyclotron frequency of the particle should match with the characteristic frequency of the laser pulse spectrum.

It is evident from the results that the resonant interaction between the particle and a finite duration laser pulse differs significantly from the results of a continuous wave train previously discussed in the literature [38, 39, 32, 43]. The marked difference between the two phenomenon can be understood in terms of the frequency spectrum, which for a finite duration laser pulse has a finite resonance width about the central maximum as compared to that of a continuous wave for which the frequency spectrum is in the form of a delta function. In comparison to the particle interacting with the monochromatic continuous laser, the resonant phase locking time is found to be limited for the finite duration laser pulse. This is so because for a finite duration laser pulse, the particle interacts with spectrum of frequencies which lies in the resonance width, as a result the particle can remain phase locked with the laser only for a limited period of time. It is to be noted here that the present calculation is fundamentally different from the earlier solutions derived with temporally shaped $sin^2(\delta\xi)$ profile in Refs.[41, 42, 33]. The analytical results derived by the authors in Refs.[41, 42, 33] are actually valid for an infinite homogeneous plane wave with $sin^2(\delta\xi)$ modulation; and hence the analytical method adopted by the authors in Refs.[41, 42, 33] is not suitable for describing some characteristics of particle motion in the combined field of a finite duration laser pulse and static axial magnetic field, such as the continuous dependence of energy gain on "$r = \Omega_c/(\omega\Delta)$ ". In this work a temporally shaped Gaussian profile has been used for calculations, which suitably takes into account the effect of continuous spectrum of frequencies present in a finite duration laser pulse.

It has been shown that the finite resonance width of the frequency spectrum allows the generation of accelerated particles by suitable resonance matching of the particle cyclotron frequency with the laser spectrum. For a given finite duration laser pulse, the resonant energy gain of the particle scales linearly with the peak laser intensity. It is found that the slope of final energy gain with input laser intensity increases with increase in the parameter "r"; finally reaching a maximum for "r = 1 ". From the Fig.3.6 subplot (d), it can be shown that for a relativistically intense laser with a wavelength $\sim 1\mu m$, the particle energy can be simply calculated as $\Gamma = 78.53 \times (A_0)^2 \times .511Mev$; thus for $A_0 = 100, 105$ the final energy gain lies in TeV range. From the scaling of the particle energy as function of the laser pulse length obtained from Fig.3.7, for $r(\frac{\Omega_c}{\omega\Delta} = 1)$, it can be seen that the energy scales quadratically with the pulse length for the same A_0. For a laser wavelength of the order of $\sim 1\mu m$ one would require a magnetic field of the order of $\sim$ 100 MG for resonating with the central frequency $r(= \Omega_c/(\omega\Delta) = 1)$. Magnetic fields of the order of $\sim$ 100 MG and higher surviving for several pico-seconds have already been reported in simulations [116, 117] and experiments [118, 119, 120, 121] pertaining to intense laser solid interaction. The experimental idea of using high quasi-static magnetic field produced in the laser solid interaction for Auto-Resonant laser acceleration has been discussed in Ref.[122]. Further it has been shown that the resonant energy gain by the particle for the same laser parameters viz. pulse length and amplitude along with the same strength of static axial magnetic field depends upon the polarization of the laser pulse. For a positively charged particle, the energy gain is shown to be maximum for the right circularly polarized light.

Thus in conclusion interaction of the particle with the finite duration pulse in the presence of static axial magnetic field acts as a very efficient way of particle acceleration in the vacuum in MeV-TeV range. To accelerate the particle to the very high energies for short duration laser pulse one needs to have very high intensity in the range $10^{22} W cm^{-2}$ or long duration pulses can be used to accelerate the particles at lower laser intensity of the order of $10^{20} W cm^{-2}$.

3.5 Appendix

Values for different variables for y coordinate

$\mathbf{Cos}[\xi\Xi] = \mathbf{CS}; \mathbf{Sin}[\xi\Xi] = \mathbf{Sn}; \mathbf{Erfi} = \mathbf{Ei}; \mathbf{Erf} = E;$

$\mathbf{a1} = 1.0000004641733926; \mathbf{a2} = 1.0000006188980002;$

$\mathbf{a3} = \text{“1.”}; \mathbf{a4} = 0.5000009283470006;$

$\mathbf{a5} = 1.000001856694001; \mathbf{a6} = \mathbf{6.188980001819999{*}\hat{}\text{-}7};$

$\mathbf{a7} = \text{“0.707107”}; \mathbf{a8} = \text{“0.313329”}; \mathbf{a9} = \text{“2.”};$

$\mathbf{a10} = \text{“3.”}; \mathbf{a11} = \text{“1.”};$

$\mathbf{a12} = \text{“1.”}; \mathbf{a13} = \text{“1.”};$

$\mathbf{a14} = \text{“2.”}; \mathbf{a15} = \text{“1.”};$

$\mathbf{a16} = \text{“0.5”}; \mathbf{a17} = \text{“0.707107”};$

$\mathbf{a18} = \text{“0.500001”}; \mathbf{a19} = \text{“3.”};$

$\mathbf{c1} = \sqrt{\text{“1.”}@ - \text{“1.”}\kappa^2}; \mathbf{c2} = \left(1-\kappa^2\right)^{0.5};$

$\mathbf{d1} = \frac{1}{\delta^2}\left(\mathbf{a4} + 0.5\delta^4\xi^2 + \Xi(\mathbf{a5} + \mathbf{a4}\Xi) + i\mathbf{a6}\delta(1+\Xi)\phi + \mathbf{a3}\delta^2\phi^2\right);$

$\mathbf{d2} = 0.5\delta^2\xi^2 + \frac{(\mathbf{a1}+\mathbf{a1}\Xi)^2}{\delta^2} + \frac{i\mathbf{a2}(1+\Xi)\phi}{\delta} + \mathbf{a3}\phi^2;$

$\mathbf{d3} = \frac{1}{\delta^2}\left(\mathbf{a4} + 0.5\delta^4\xi^2 + \Xi(\mathbf{a10} + \mathbf{a4}\Xi) + i\delta(\mathbf{a9} + \mathbf{a6}\Xi)\phi + \mathbf{a3}\delta^2\phi^2\right);$

$\mathbf{d4} = \frac{1}{\delta^2}\left(\mathbf{a4} + 0.5\delta^4\xi^2 + \Xi(\mathbf{a5} + \mathbf{a4}\Xi) + i\mathbf{a9}\delta(1+\Xi)\phi + \mathbf{a3}\delta^2\phi^2\right);$

$\mathbf{d5} = \frac{1}{\delta^2}\left(\mathbf{a4} + 0.5\delta^4\xi^2 + \Xi(\mathbf{a10} + \mathbf{a4}\Xi) + i\delta(\mathbf{a6} + \mathbf{a9}\Xi)\phi + \mathbf{a3}\delta^2\phi^2\right);$

$\mathbf{d6} = 0.5\delta^2\xi^2 + \frac{(\mathbf{a11}+\mathbf{a11}\Xi)^2}{\delta^2} + \frac{i(1+\Xi)\phi}{\delta} + 0.5\phi^2;$

$\mathbf{d7} = 0.5\delta^2\xi^2 + \frac{(\mathbf{a11}+\mathbf{a11}\Xi)^2}{\delta^2} + \frac{i\mathbf{a12}(1+\Xi)\phi}{\delta} + 0.5\phi^2;$

$\mathbf{d8} = 0.5\delta^2\xi^2 + \frac{(\mathbf{a15}+\mathbf{a15}\Xi)^2}{\delta^2} + \frac{i\mathbf{a2}(1+\Xi)\phi}{\delta} + \mathbf{a16}\phi^2;$

$\mathbf{d9} = 0.5\delta^2\xi^2 + \frac{(\mathbf{a1}+\mathbf{a1}\Xi)^2}{\delta^2} + \frac{i\mathbf{a2}(1+\Xi)\phi}{\delta} + \mathbf{a16}\phi^2;$

$\mathbf{d10} = \mathbf{a13} + 0.5\delta^4\xi^2 + \Xi(\mathbf{a14} + \mathbf{a13}\Xi) + i\delta(\mathbf{a12} + \Xi)\phi + 0.5\delta^2\phi^2;$

$\mathbf{d10a} = \frac{\mathbf{d10}}{\delta^2}; \mathbf{d11} = \frac{1}{\delta^2}\left(\mathbf{a13} + 0.5\delta^4\xi^2 + \Xi(\mathbf{a14} + \mathbf{a13}\Xi) + i\delta(1 + \mathbf{a12}\Xi)\phi + 0.5\delta^2\phi^2\right);$

$\mathbf{d12} = 0.5\delta^2\xi^2 + \frac{(\mathbf{a17}+\mathbf{a17}\Xi)^2}{\delta^2} + \frac{i\mathbf{a6}(1+\Xi)\phi}{\delta} + \mathbf{a3}\phi^2;$

$\mathbf{d13} = 0.5\delta^2\xi^2 + \frac{(\mathbf{a17}+\mathbf{a17}\Xi)^2}{\delta^2} + \frac{i\mathbf{a9}(1+\Xi)\phi}{\delta} + \mathbf{a3}\phi^2;$

$\mathbf{d14} = \frac{1}{\delta^2}\left(\mathbf{a18} + 0.5\delta^4\xi^2 + \Xi(\mathbf{a19} + \mathbf{a18}\Xi) + i\delta(\mathbf{a9} + \mathbf{a6}\Xi)\phi + \mathbf{a3}\delta^2\phi^2\right);$

$\mathbf{d15} = \frac{1}{\delta^2}\left(\mathbf{a18} + 0.5\delta^4\xi^2 + \Xi(\mathbf{a19} + \mathbf{a18}\Xi) + i\delta(\mathbf{a6} + \mathbf{a9}\Xi)\phi + \mathbf{a3}\delta^2\phi^2\right);$

$\mathbf{d16} = \xi(@ - i + \delta\phi) + \frac{\phi(i\mathbf{a2}(1+\Xi)+\mathbf{a16}\delta\phi)}{\delta};$

$\mathbf{d17} = \frac{(\mathbf{a1}+\mathbf{a1}\Xi)^2}{\delta^2}; \mathbf{d18} = \frac{(\mathbf{a15}+\mathbf{a15}\Xi)^2}{\delta^2}; \mathbf{d19} = \xi\left(i + 0.5\delta^2\xi\right) + \frac{\phi(i\mathbf{a6}(1+\Xi)+\mathbf{a3}\delta\phi)}{\delta};$

$\mathbf{d20} = \frac{\mathbf{a4}+\mathbf{a5}\Xi+\mathbf{a4}\Xi^2}{\delta^2}; \mathbf{d21} = \frac{1}{\delta^2}\left(\mathbf{a4} + \Xi(\mathbf{a5} + \mathbf{a4}\Xi) + \delta\left(0.5\delta^3\xi^2 + i\mathbf{a9}(1+\Xi)\phi + \delta\left(i\xi + \mathbf{a3}\phi^2\right)\right)\right);$

$\mathbf{d22} = \xi\left(i + 0.5\delta^2\xi\right) + \frac{(\mathbf{a17}+\mathbf{a17}\Xi)^2}{\delta^2} + \frac{\phi(i\mathbf{a9}(1+\Xi)+\mathbf{a3}\delta\phi)}{\delta};$

$\mathbf{d23} = \xi\left(i + 0.5\delta^2\xi\right) + \mathbf{a3}\phi^2; \mathbf{d24} = \frac{i(\mathbf{a6}+\mathbf{a9}\Xi)\phi}{\delta};$

$\mathbf{d25} = \frac{\mathbf{a17}^2(1+\Xi)^2}{\delta^2}; \mathbf{d26} = \frac{\mathbf{a4}+\Xi(\mathbf{a10}+\mathbf{a4}\Xi)}{\delta^2}; \mathbf{d27} = \frac{\mathbf{a18}+\Xi(\mathbf{a19}+\mathbf{a18}\Xi)}{\delta^2};$

$\mathbf{d28} = \frac{\mathbf{a5}\Xi+\mathbf{a4}\left(1+\Xi^2\right)+i\mathbf{a9}\delta(1+\Xi)\phi}{\delta^2}; \mathbf{d29} = \frac{(1+\Xi)\left(\mathbf{a17}^2(1+\Xi)+i\mathbf{a9}\delta\phi\right)}{\delta^2};$

$\mathbf{d30} = \frac{i(\mathbf{a9}+\mathbf{a6}\Xi)\phi}{\delta}; \mathbf{d31} = -\mathbf{d17} - 0.5\delta^2\xi^2 - \frac{i\mathbf{a2}(1+\Xi)\phi}{\delta} - \mathbf{a3}\phi^2;$

$\mathbf{e1} = \frac{\mathbf{a7}i+\mathbf{a7}i\Xi-\mathbf{a7}\delta\phi}{\delta}; \mathbf{e2} = \frac{\mathbf{a7}i+\mathbf{a7}i\Xi+\mathbf{a7}\delta\phi}{\delta}; \mathbf{e3} = \frac{\mathbf{a7}@-\mathbf{a7}\Xi-\mathbf{a7}i\delta\phi}{\delta};$

$\mathbf{e4} = \frac{\mathbf{a7}@+\mathbf{a7}i\delta^2\xi-\mathbf{a7}\Xi-\mathbf{a7}i\delta\phi}{\delta}; \mathbf{e5} = \frac{\mathbf{a7}@+\mathbf{a7}\Xi-\mathbf{a7}i\delta\phi}{\delta};$

$\mathbf{e6} = \frac{\mathbf{a7}@+\mathbf{a7}i\delta^2\xi+\mathbf{a7}\Xi-\mathbf{a7}i\delta\phi}{\delta}; \mathbf{e7} = \frac{\mathbf{a7}@-\mathbf{a7}\Xi+\mathbf{a7}i\delta\phi}{\delta};$

$\mathbf{e8} = \frac{\mathbf{a7}@-\mathbf{a7}i\delta^2\xi-\mathbf{a7}\Xi+\mathbf{a7}i\delta\phi}{\delta}; \mathbf{e9} = \frac{\mathbf{a7}@+\mathbf{a7}\Xi+\mathbf{a7}i\delta\phi}{\delta};$

$\mathbf{e10} = \frac{\mathbf{a7}@-\mathbf{a7}i\delta^2\xi+\mathbf{a7}\Xi+\mathbf{a7}i\delta\phi}{\delta}; \mathbf{e11} = \frac{\mathbf{a7}i+\mathbf{a7}\delta^2\xi+\mathbf{a7}i\Xi-\mathbf{a7}\delta\phi}{\delta};$

$\mathbf{e12} = \frac{\mathbf{a7}\left(-\delta^2\xi+i(1+\Xi)+\delta\phi\right)}{\delta}$

Values for different variables for z coordinate

$\mathbf{Cos}[\xi\Xi] = \mathbf{CS}; \mathbf{Sin}[\xi\Xi] = \mathbf{Sn};$

$\mathbf{A1} = \text{“1.”}; \mathbf{A2} =$

$2.220446049250313\hat{} - 16; \mathbf{A3} = 4.440892098500626\hat{} - 16;$

$\mathbf{A4} = 1.9999999999999996; \mathbf{A5} = 0.9999999999999996;$

$\mathbf{A6} = 0.7071067811865475; \mathbf{A7} = 0.9999999999999998;$

$\mathbf{A8} = \text{“0.5”}; \mathbf{A9} = \text{“0.313329”};$

$\mathbf{A10} = \text{“0.5”}; \mathbf{A11} = \text{“0.5”};$

$\mathbf{A12} = 0.7071067811865474;$

$\mathbf{A13} = \text{“0.25”};$

$\mathbf{D1} = \sqrt{\text{“1.”}@ - \text{“1.”}\kappa^2}; \mathbf{D2} = \left(1@ - 1\kappa^2\right)^{0.5};$

$\mathbf{j1} = \frac{1}{\delta}\left(\mathbf{A6}i - \mathbf{A6}\delta^2\xi + \mathbf{A6}i\Xi + \mathbf{A6}\delta\phi\right); \mathbf{j2} = \frac{1}{\delta}\left(\mathbf{A6}i + \mathbf{A6}\delta^2\xi + \mathbf{A6}i\Xi - \mathbf{A6}\delta\phi\right);$

$\mathbf{j3} = \frac{1}{\delta}(\mathbf{A12}@ - \mathbf{A12}\Xi - \mathbf{A12}i\delta\phi); \mathbf{j4} = \frac{1}{\delta}(\mathbf{A12}@ + \mathbf{A12}\Xi - \mathbf{A12}i\delta\phi);$

$\mathbf{j5} = \frac{1}{\delta}(\mathbf{A12}@ - \mathbf{A12}\Xi + \mathbf{A12}i\delta\phi); \mathbf{j6} = \frac{1}{\delta}(\mathbf{A12}@ + \mathbf{A12}\Xi + \mathbf{A12}i\delta\phi);$

$\mathbf{j7} = \frac{1}{\delta}\left(\mathbf{A6}@ + \mathbf{A6}i\delta^2\xi - \mathbf{A6}\Xi - \mathbf{A6}i\delta\phi\right); \mathbf{j8} = \frac{1}{\delta}\left(\mathbf{A6}@ + \mathbf{A6}i\delta^2\xi + \mathbf{A6}\Xi - \mathbf{A6}i\delta\phi\right);$

$\mathbf{j9} = \frac{1}{\delta}\left(\mathbf{A6}@ - \mathbf{A6}i\delta^2\xi - \mathbf{A6}\Xi + \mathbf{A6}i\delta\phi\right); \mathbf{j10} = \frac{1}{\delta}\left(\mathbf{A6}@ - \mathbf{A6}i\delta^2\xi + \mathbf{A6}\Xi + \mathbf{A6}i\delta\phi\right);$

$\mathbf{j11} = \frac{1}{\delta}(\mathbf{A12}i + \mathbf{A12}i\Xi + \mathbf{A12}\delta\phi); \mathbf{j12} = \frac{1}{\delta}(\mathbf{A12}i + \mathbf{A12}i\Xi - \mathbf{A12}\delta\phi);$

$\mathbf{k1} = -\mathbf{A1} - 0.5\delta^4\xi^2 - \mathbf{A2}\Xi^2 + \delta((\text{“0.”}@ - 1i) - (\text{“0.”}@ + \mathbf{A3}i)\Xi)\phi - 0.5\delta^2\phi^2;$

$\mathbf{k2} = 0.5\delta^2\xi^2 + \frac{(-\mathbf{A4}-\mathbf{A7}\Xi)\Xi}{\delta^2} - \frac{\mathbf{A5}i\Xi\phi}{\delta} + 0.5\phi^2;$

$\mathbf{k3} = \frac{\mathbf{A8}@+(1@+0.5\Xi)\Xi}{\delta^2}; \mathbf{k4} = \frac{\mathbf{A10}@+(\mathbf{A5}@+\mathbf{A11}\Xi)\Xi}{\delta^2};$

$\mathbf{k5} = -\frac{\mathbf{A5}i\Xi\phi}{\delta}; \mathbf{k6} = \frac{\mathbf{A1}@+0.5\delta^4\xi^2+\mathbf{A2}\Xi^2+\delta(i+i\Xi)\phi+0.5\delta^2\phi^2}{\delta^2};$

$\mathbf{k7} = \mathbf{A8}@ + 0.5\delta^4\xi^2 + (-\mathbf{A5} - \mathbf{A11}\Xi)\Xi + \delta(2i + 2i\Xi)\phi + 0.5\delta^2\phi^2;$

$\mathbf{k8} = \mathbf{A8}@ + 0.5\delta^4\xi^2 + (\mathbf{A5}@ - \mathbf{A11}\Xi)\Xi + 2i\delta\phi + 0.5\delta^2\phi^2;$

$\mathbf{k9} = \mathbf{A8}@ + 0.5\delta^4\xi^2 + (\mathbf{A5}@ - \mathbf{A11}\Xi)\Xi + 2i\delta\Xi\phi + 0.5\delta^2\phi^2;$

$\mathbf{k10} = \mathbf{A8}@ + 0.5\delta^4\xi^2 + (-\mathbf{A5} - \mathbf{A11}\Xi)\Xi + 0.5\delta^2\phi^2;$

$\mathbf{k11} = \mathbf{A1}@ + \mathbf{A2}\Xi^2 + \delta\left(i + 1\delta^2\xi + i\Xi\right)\phi; \mathbf{k12} = \mathbf{A1}@ + 0.5\delta^4\xi^2 + \delta(i + i\Xi)\phi;$

$\mathbf{k13} = \mathbf{A1}@ + 0.5\delta^4\xi^2 + \mathbf{A2}\Xi^2 + \delta(i + i\Xi)\phi; \mathbf{k14} = \frac{\mathbf{A1}}{\delta^2} + 0.5\delta^2\xi^2 + \frac{(\mathbf{A5}i + \mathbf{A5}i\Xi)\phi}{\delta} + \mathbf{A2}\phi^2;$

$\mathbf{k15} = \frac{\mathbf{A1}}{\delta^2} + 0.5\delta^2\xi^2 + \frac{(\mathbf{A1}i + \mathbf{A5}i\Xi)\phi}{\delta} + \mathbf{A2}\phi^2;$

$\mathbf{k16} = \frac{\mathbf{A1}}{\delta^2} + 0.5\delta^2\xi^2 + \frac{(\mathbf{A5}i + \mathbf{A1}i\Xi)\phi}{\delta} + \mathbf{A2}\phi^2;$

$\mathbf{k17} = \frac{\mathbf{A1}}{\delta^2} + 0.5\delta^2\xi^2 + \frac{(\mathbf{A1}i + \mathbf{A1}i\Xi)\phi}{\delta} + \mathbf{A2}\phi^2;$

$\mathbf{k18} = \xi((\text{“}\mathbf{0.}\text{”}@ - 1i) - i\Xi) + \frac{\mathbf{A1}@ + \delta\left(i + 1\delta^2\xi + i\Xi\right)\phi}{\delta^2};$

$\mathbf{k19} = \xi((\text{“}\mathbf{0.}\text{”}@ - 1i) + i\Xi) + \frac{\mathbf{A1}@ + \delta\left(i + 1\delta^2\xi + i\Xi\right)\phi}{\delta^2};$

$\mathbf{k20} = \mathbf{A10}@ + 0.5\delta^4\xi^2 + (-1 - 0.5\Xi)\Xi + \delta(2i + 2i\Xi)\phi + 0.5\delta^2\phi^2;$

$\mathbf{k21} = \xi(i + i\Xi) + \frac{\mathbf{A1}@ + \delta\left(i + 1\delta^2\xi + i\Xi\right)\phi}{\delta^2};$

$\mathbf{k22} = \mathbf{A10}@ + 0.5\delta^4\xi^2 + (\mathbf{A5}@ - 0.5\Xi)\Xi + 2i\delta\phi + 0.5\delta^2\phi^2;$

$\mathbf{k23} = \mathbf{A10}@ + 0.5\delta^4\xi^2 + (\mathbf{A5}@ - 0.5\Xi)\Xi + 2i\delta\Xi\phi + 0.5\delta^2\phi^2;$

$\mathbf{k24} = \mathbf{A10}@ + 0.5\delta^4\xi^2 + (-1 - 0.5\Xi)\Xi + 0.5\delta^2\phi^2;$

$\mathbf{k25} = 0.5\delta^2\xi^2 + \frac{(2i + 2i\Xi)\phi}{\delta} + 0.5\phi^2; \mathbf{k26} = \frac{\mathbf{A8}@ + (-\mathbf{A5} - \mathbf{A11}\Xi)\Xi}{\delta^2};$

$\mathbf{k27} = \frac{\mathbf{A10}@ + (-1 - 0.5\Xi)\Xi}{\delta^2}; \mathbf{k28} = 0.5\delta^2\xi^2 + \frac{(-\mathbf{A4} - \mathbf{A7}\Xi)\Xi}{\delta^2} + 0.5\phi^2;$

$\mathbf{k29} = 0.5\delta^2\xi^2 + 0.5\phi^2; \mathbf{k30} = \frac{\mathbf{A8}@ + 2i\delta\phi + \Xi(-\mathbf{A5} - \mathbf{A11}\Xi + 2i\delta\phi)}{\delta^2};$

$\mathbf{k31} = \frac{\mathbf{A8}@ + \Xi(\mathbf{A5}@ - \mathbf{A11}\Xi + 2i\delta\phi)}{\delta^2}; \mathbf{k32} = \frac{\mathbf{A10}@ + 2i\delta\phi + \Xi(-1 - 0.5\Xi + 2i\delta\phi)}{\delta^2};$

$\mathbf{k33} = \frac{\mathbf{A10}@ + \Xi(\mathbf{A5}@ - 0.5\Xi + 2i\delta\phi)}{\delta^2}; \mathbf{k34} = \frac{\mathbf{A8}@ + (\mathbf{A5}@ - \mathbf{A11}\Xi)\Xi}{\delta^2};$

$\mathbf{k35} = \frac{\mathbf{A10}@ + (\mathbf{A5}@ - 0.5\Xi)\Xi}{\delta^2};$

4

Particle dynamics in a focused laser field

The particle dynamics is numerically studied in the field of a focused continuous and finite duration laser. The slow spatial modulation in the laser intensity has been used to model the focused laser field. The aim of the study is to determine the optimum initial position for maximum energy gain by the particle in a focused laser field as well as to determine the quantitative limit for earlier reported analytical work by **Kaw *et.al*[46]**. *A significant part of this work has been published ref.* **Sagar *et.al***[105].

4.1 Introduction

In chapter-2 and chapter-3, the particle dynamics has been studied in the homogeneous relativistically intense laser field. It has been shown in chapter-2, that a particle interacting with homogeneous laser field is symmetrically accelerated and decelerated by the laser field, resulting in no net transfer of energy. A scheme of laser driven auto-resonant particle acceleration has been described in chapter-3 for accelerating the particle from rest to relativistic energies. In this scheme the particle acceleration is achieved by subjecting it to the combined field of a laser and static axial magnetic field. The appropriate tuning of cyclotron frequency with the characteristic frequency results in the resonant acceleration of particle.

In this chapter, an alternate scheme of direct laser acceleration of particle in vacuum is described, in which the particle is accelerated by subjecting it to the focused field of a laser. The focusing causes an asymmetry in the acceleration and deceleration phase of the particle by a laser, which results in net transfer of energy to the particle. This asymmetry is a resultant of the configuration of the electric and magnetic field describing the focused laser field. The main difficulty in the theoretical study of this scheme is the correct mathematical description of the complex configuration of the fields arising due to the focusing of laser, which in turn hinder's the analytical study of the particle orbits. Thus considerable work has been done in this area[47], for the description of the fields, which has been subsequently used in the theoretical studies of the schemes of particle acceleration.

In general, the focusing of a laser results in the focused and de-focused regions, which are separated at a focal point. In the focused region, the strength of the fields increases reaching maximum at the focal point, beyond which the region is termed as de-focused region and the field strength decreases in moving away from the focal point. The mechanism of particle acceleration by this scheme can physically be described in a following way: at the beginning of the interaction the particle is assumed be at rest in the focused region and gets accelerated along the transverse direction by the electric field component of the laser. The transverse velocity gain results in simultaneous action by the magnetic field component of the laser and the $\vec{v} \times \vec{B}$ force pushes the particle along the propagation direction of laser. This cycle is repeated and the particle propagates into the focused region along the direction of the propagation of the laser. The particle moving in the focused region is subjected to ascending gradient in electric field, which in turn retards its forward motion and depending upon the initial conditions the particle might get reflected back in focused region or can enter the de-focused region. This makes the choice of initial position very important for the forward acceleration of the particle. The particle entering into the de-focused region is subjected to the descending gradient in the electric field, as a result the laser field is not able to extract the energy back from the particle. This results in the net transfer of energy to the particle along the direction of propagation of the field.

As mentioned above that the complex configuration of fields in the focused laser field limits the analytical study of the particle dynamics. Earlier Kaw*et.al*[46], have analytically studied the particle dynamics in the focused laser field using one dimensional focusing model. The slow spatial modulation of the laser intensity along the direction of propagation of the laser was chosen to the describe the focused laser field and hence one dimensional model. The analytical work was carried out in the limit that the adiabaticity parameter $\epsilon(= l_g/l_n << 1)$ is very small, here l_g, is the particle gyration length and $l_n(=\mid \frac{1}{a^2}\frac{da^2}{d(\epsilon x)} \mid^{-1})$, is the scale length of variation in intensity. In their study, optimum initial conditions have been derived in terms of initial position, peak intensity and laser pulse length for maximum energy gain by the particle. In this chapter the exact relativistic equation of motion is numerically solved to understand the dynamics of a particle in the field of focused continuous as well as finite duration laser field. At first the dynamics of the particle is studied in the field of a focused continuous laser, the study is further sub-divided into a focused and de-focused regions. As described earlier in the focused region, the laser intensity increases along the direction of propagation and becomes maximum at the focal point, the region beyond the focal point is termed as de-focused region in which the laser intensity decreases along the direction of propagation.

In the focused region, the particle moves along the increasing intensity gradient which retards the forward motion of the particle and as a result its gyration length is reduced. Earlier Kaw *et.al*[46] had derived an analytical expression, which describes the variation of adiabatic invariant as function of laser intensity, which implicitly depends upon the initial position. Using the analytical expression it was discussed that the particle dynamics depends upon the choice of initial position of the particle in the focused laser field. Depending upon the choice of initial conditions the particle can be reflected back into the focused region or it can stop at the focal point with no net longitudinal energy and lastly, it might get pushed into the de-focused region. It was further stated that the adiabaticity conditions are very well satisfied in this region. The present numerical work is used to verify the above specified predictions of the analytical work and hence to determine the optimum initial position of the particle for maximum energy gain.

Next, the particle motion is examined in the de-focused region, in this region the particle is subjected to the decreasing intensity gradient as a result the laser field is not able to extract energy out of the particle and it gets accelerated along the direction of laser propagation. The energy gain of the particle is expressed in terms of the adiabatic invariant, which is studied for different values of initial slowness parameters. The aim of the study is to determine the quantitative limit in terms of adiabaticity parameter 'ϵ' for the analytical energy estimate of the particle.

Further, the particle energy gain is studied in the field of a focused finite duration laser field. The numerical results are compared with the earlier derived analytical results by Kaw*et.al*[46]. In this study the particle energy gain is studied as a function of the parameter "f " and optimum initial conditions are determined in terms of laser intensity, pulse length and focal length for maximum energy gain by the particle.

The chapter has a following organization: In section (4.2), the exact relativistic equation of motion describing the particle dynamics in the field of continuous focused laser is numerically solved. The study is divided further into following two subsections. In subsection (4.2.1), the dynamics of the particle is examined in the focused region and results are compared with the earlier reported analytical work, which is aimed to determine the optimum initial position of the particle for maximum energy gain. In subsection (4.2.2), the particle dynamics is considered in the de-focused region and the energy gain of the particle is studied for different initial values of adiabaticity parameter ('ϵ'). This study determines the quantitative limit for the analytical adiabatic energy gain by the particle and corresponding changes in the adiabatic invariant. In section(4.3), the particle dynamics is numerically studied in the field of a focused finite duration laser field. The results of this parametric study provides the quantitative limit of the earlier analytical work carried out using adiabatic approximation and to optimize the particle energy gain in terms of peak laser intensity, pulse length and focal length. In section (4.4), the summary of the work and conclusions of the work are presented.

4.2 Charged particle dynamics in the field of relativistically intense inhomogeneous linearly polarized plane wave

In this section, the equations of motion describing the particle dynamics in the field of an adiabatically focused laser field which were earlier derived by Kaw*et.al*[46] have been re-derived. The vector potential describing the linearly polarized laser travelling along the $\hat{x}$ is given by:

$$\vec{A} = a\Theta(\delta\xi)P_1(\xi)\hat{y} \tag{4.1}$$

where the symbols represent the following: $\xi = (\omega t - kx)$ is the phase of the laser, $\Theta(\delta\xi)$ is pulse envelope, $P_1(\xi)$ is the oscillatory part, factor $\delta(= \frac{\lambda}{L})$ is ratio of the laser wavelength to the pulse length, $a(\epsilon x)$ is slowly modulated amplitude of the pulse. From here on the following normalization have been used in this chapter: $\vec{r} \to k\vec{r}, t \to \omega t, \vec{P} \to \frac{\vec{P}}{mc}, \Gamma \to \frac{\Gamma}{mc^2}, B \to \frac{qB}{m\omega c}, E \to \frac{qE}{mc\omega}, \hat{A} \to \frac{eA}{mc^2}$. For the focused field electric and magnetic fields are given by:

$$\vec{E} = -\frac{\partial A}{\partial t}\hat{y} = -\frac{\partial A}{\partial \xi}\hat{y} \qquad \vec{B} = \nabla \times \vec{A} = \frac{\partial A}{\partial x}\hat{z} = (-\frac{\partial A}{\partial \xi} + \epsilon\frac{\partial A}{\partial(\epsilon x)})\hat{z}$$

.

The normalized relativistic momentum and energy equation are given by,

$$\frac{d\vec{P}}{dt} = [\vec{E} + \frac{\vec{P}}{\Gamma} \times \vec{B}] \tag{4.2}$$

$$\frac{d\Gamma}{dt} = \frac{\vec{P}.\vec{E}}{\Gamma} \tag{4.3}$$

Here Γ is the relativistic factor defined as,

$$\Gamma = (1 + P_x^2 + P_y^2 + P_z^2)^{1/2}$$

and P_x, P_y, P_z are the four momentum components.
In the component form the equation of motion is given by,

$$\frac{dP_x}{dt} = \frac{P_y}{\Gamma}(-\frac{\partial A}{\partial \xi} + \epsilon\frac{\partial A}{\partial(\epsilon x)}) \tag{4.4}$$

$$\frac{dP_y}{dt} = -\frac{(\Gamma - P_x)}{\Gamma}\frac{\partial A}{\partial \xi} \tag{4.5}$$

$$\frac{dP_z}{dt} = 0 \tag{4.6}$$

$$\frac{d\Gamma}{dt} = -\frac{P_y}{\Gamma}\frac{\partial A}{\partial \xi} \tag{4.7}$$

Subtracting Eq.(4.4) from Eq.(4.7) and changing the variables using $\dot{\xi} = \frac{\Delta}{\Gamma}$,(where $\Delta = \Gamma - P_x$) results in the evolution equation for adiabatic invariant and transverse particle momentum,

$$\frac{d\Delta}{d\xi} = -\frac{\epsilon}{\Delta} P_y \frac{da(\epsilon x)}{d(\epsilon x)} \Theta(\delta\xi) P_1(\xi) \tag{4.8}$$

$$P_y = \alpha - A \tag{4.9}$$

$$P_z = C1 \tag{4.10}$$

where α and $C1$ are exact constant of motion, corresponds to canonical momentum. In this study the constant of motion $C1 = 0$, which represents that there is no motion along this direction and hence it is dropped from further calculations.

Thus the longitudinal momentum and energy of the particle can be represented as,

$$P_x = \frac{1-\Delta^2}{2\Delta} + \frac{(\alpha - A)^2}{2\Delta} \tag{4.11}$$

$$\Gamma = \frac{1+\Delta^2}{2\Delta} + \frac{(\alpha - A)^2}{2\Delta} \tag{4.12}$$

The particle position can be obtained by solving Eq.(4.5) and Eq.(4.6),

$$\frac{dx}{d\xi} = \frac{1-\Delta^2}{2\Delta^2} + \frac{(\alpha - A)^2}{2\Delta^2} \tag{4.13}$$

$$\frac{dy}{d\xi} = \frac{(\alpha - A)}{\Delta} \tag{4.14}$$

The phase averaged slow set of equations describing the particle position as well as the evolution of adiabatic invariant are required to study particle dynamics. They can be derived by substituting for P_y from Eq.(4.9) in Eq.(4.8) and averaging the resultant equation along with Eq.(4.13) over the fast motion. The temporal envelope of the pulse $\Theta(\delta\xi)$ is assumed to be constant over one gyration.

$$\frac{d\Delta^2}{d\xi_c} = -\frac{\epsilon}{2} \frac{da^2}{d(\epsilon x)} \Theta^2(\delta\xi) \tag{4.15}$$

$$\frac{d<x>}{d\xi_c} = \frac{1-\Delta^2}{2\Delta^2} + \frac{\alpha^2 + \frac{a^2\Theta^2(\delta\xi)^2}{2}}{2\Delta^2} \tag{4.16}$$

where $\xi_c = \hat{t} - <\hat{x}>$.

The Eq.(4.15) and Eq.(4.16) represent a general set of equations which are valid for different pulse profile as well various intensity profiles representing the focused field of a laser. The particle dynamics is first analyzed in the field of a continuous linearly polarized focused laser.

For the continuous laser $\Theta(\delta\xi) = 1$ and dividing Eq.(4.15) by Eq.(4.16) results in an equation describing the variation in adiabatic constant in terms of laser intensity,

$$\frac{d\Delta^2}{da^2} = -\frac{\Delta^2}{[\Delta^2 - 1 - \alpha^2 - a^2/2]} \tag{4.17}$$

The general solution of the above equation for an arbitrary initial conditions is given by:

$$\Delta = 1 + \frac{\alpha^2}{2} + \frac{a^2}{4} - [\frac{\alpha^2}{4}(\alpha^2 + a^2) + \frac{a^4}{16} + \frac{1}{2}(a^2 - A_0^2)]^{1/2} \tag{4.18}$$

In the following subsection (4.2.1) and (4.2.2), the focused laser field is represented the following intensity modulation given by

$$a^2 = A_0^2(1 \pm \epsilon x), \qquad x \lessgtr 0 \quad \text{and} \quad \frac{1}{\epsilon} = F = N \times A_0^2. \tag{4.19}$$

to study the particle motion in focused and de-focused region of the focused laser field respectively. In the above expression, F is the focal length of the focused region, it is normalized to the wavelength of the laser and defines a distance in which the intensity drops from maximum to zero on either side of the focal point; A_0 is the peak laser amplitude at the focal point of the laser. The proportionality between the laser intensity and focal length for the adiabatic description of the focusing model is a resultant of the fact that the particle displacement for a homogeneous case is proportional to intensity. Thus choosing large value of proportionality factor 'N ' could represent the adiabatic focusing of laser.

4.2.1 Particle dynamics in a focused laser field

In this subsection, the particle dynamics is studied in the focused region of a continuous laser, in which the laser intensity (or the electric field) increases along the direction of propagation and reaching maximum at the focal point. The gradient in the laser intensity in this region retards the forward propagation of the particle and as a result the dynamics depends upon the choice of initial position. The Eq.(4.18) describes the variation of adiabatic invariant with the laser intensity which in turn depends upon the initial particle position and in this equation 'a' is the initial laser amplitude seen by the particle. Earlier interesting observation were made by Kaw *et.al*[46] using the expression $(\frac{\alpha^2}{4}(\alpha^2+a^2)+\frac{a^4}{16}+\frac{1}{2}(a^2-A_0^2))$ in the bracket of the Eq.(4.18). For the case when the value of terms in the bracket is greater than zero, the particle propagates along the direction of the laser into the de-focused region. The details of particle dynamics in the de-focused region are described in the following subsection. For the second case, when the value of the terms in the expression is equal to zero, all the energy of the particle gets converted into the transverse motion. As a result, the particle stops at the focal point and keeps gyrating there, leading to no net energy transfer to the particle. For the case when the value of the expression is less than zero, the value of adiabatic invariant becomes complex, which signifies that particle cannot go further in space and gets reflected back into the focused region.

In this work, the relativistic equation of motion Eq.(4.2), is numerically solved using the linear intensity modulation described by the Eq.(4.19) and the above conditions have been verified. In the following figures, the results corresponding to the third case are illustrated for different initial conditions.

The particle trajectory and the evolution of the adiabatic invariant are shown in Fig.(4.1), which corresponds to the initial condition that particle is initially at rest and injected into the laser at the zero of vector potential such that the constant of motion corresponding to the transverse motion takes the value $\alpha = 0$. It can be seen from the figure, that for a choice of particular parameters the particle gets reflected from the focal point and the numerical value of adiabatic invariant is as per the analytical relation.

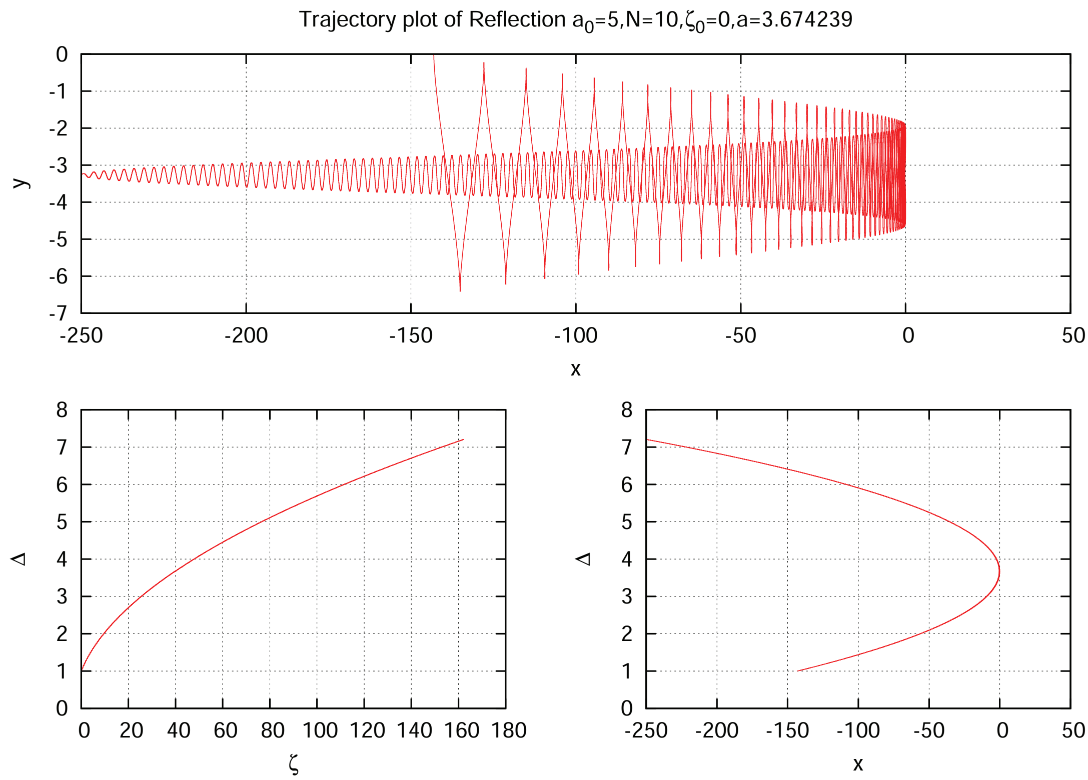

Figure 4.1: Particle is at initially at rest and starts interacting with the wave when its vector potential is zero.

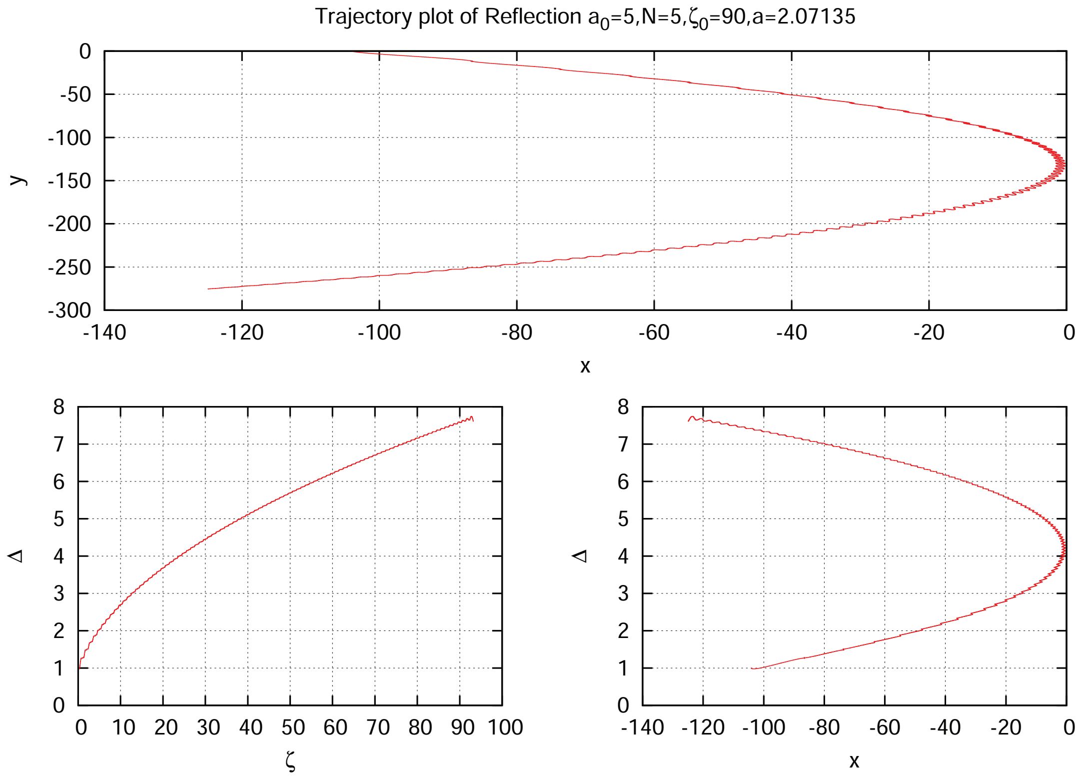

Figure 4.2: Particle is at initially at rest and starts interacting with the wave when its vector potential is maximum.

The Fig.(4.2), describes the particle trajectory and the evolution of the adiabatic invariant. The particle dynamics corresponds to the initial condition that the particle is at rest before the onset of the interaction and is injected into the laser at phase corresponding to the maximum of the vector potential. For this initial condition, the constant of motion associated with the transverse particle motion is given by $\alpha = a$. It can be seen from the figure that for a choice of the parameter, the particle gets reflected from the focal point of the laser. The numerically obtained value of the adiabatic invariant is in accordance with the analytical results.

The above numerical results verifies the earlier predictions reported in the analytical work by Kaw*et.al*[46] and gives a range of initial particle positions corresponding to different parameters for the forward acceleration of a particle. In this region, it can be seen the gyration length of the particle decreases as the particle moves into a region of higher intensity and the corresponding change in laser intensity over a gyration is very small as a result the adiabatic conditions are very well satisfied in this region. It has been further argued in ref.[46], that for a particle to have a maximum energy gain, it should be placed at a point which corresponds to maximum of the intensity and has minimum initial value of the adiabatic invariant. From the expression (4.18) it is evident that the focal point is the optimum initial position for a particle initially at rest and subjected to the zero of laser vector potential. The initial conditions $a = A_0$ and $\alpha = 0$, corresponds to the minimum initial value of the adiabatic invariant given by $\Delta = 1$.

4.2.2 Adiabatic acceleration of charged particle

In this subsection, the particle dynamics is studied in the de-focused region of the laser. This work is aimed to quantitatively study the effect of change in adiabaticity (or slowness) parameter on the particle dynamics in an adiabatically focused laser field, which in turn can be used to determine the limit of the analytical work. In this problem slowness parameter "$\epsilon(= l_g/l_n)$" is defined in terms of ratio of particle gyration length (l_g), to scale length of variation in the laser intensity ($l_n(=\mid \frac{1}{a^2}\frac{da(\epsilon x)^2}{d(\epsilon x)} \mid^{-1})$) over one gyration. In the following figures, the results obtained by numerically solving the exact relativistic equation of motion Eq.(4.2) are plotted, which describes the particle trajectory, momentum, final energy and the variation in the adiabatic invariant. The numerically obtained exact evolution of the adiabatic invariant is compared with the phase averaged adiabatic invariant obtained by solving average set of equations given by Eq.(4.15) and Eq.(4.16).

In figure(4.3), the particle dynamics is described in the de-focused region of the focused laser. From the subplots, it can be seen that the particle gains net forward energy along the direction of propagation of the laser in the de-focused region. This energy gain is result of the descending(or negative) gradient in the laser intensity (or electric field) seen by the particle, due to which the laser is not able to extract all the energy back from the particle. The energy gain along the direction of propagation leads to the increase in the gyration length of the particle, which in turn causes an increase in the value of adiabaticity parameter "ϵ". The increase in the value of "ϵ" causes the deviation between the exact and averaged values of the adiabatic invariant.

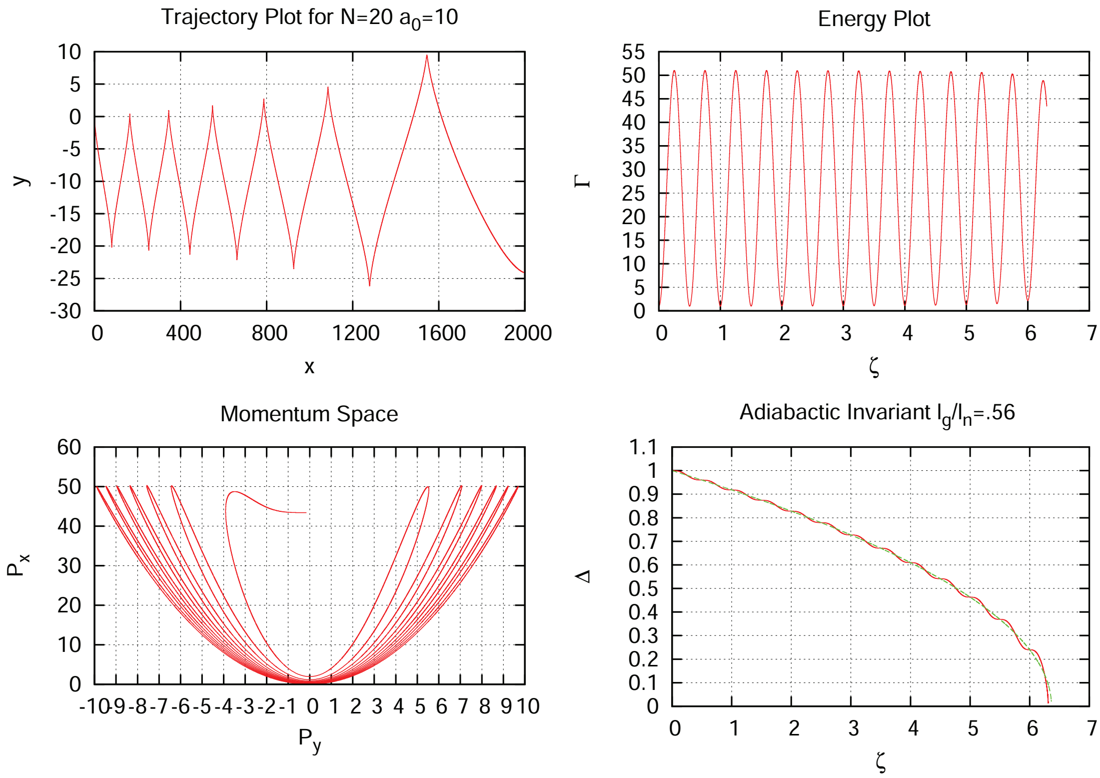

Figure 4.3: Plot for particle trajectory in configuration space, momentum space, total energy and adiabatic invariant for a focused laser pulse for N=20

It can be seen from the figure(4.4), that the rate of variation of the adiabaticity parameter "$\epsilon(= l_g/l_n)$" depends upon its initial value. The increase in initial value of the adiabaticity parameter enhances its rate of evolution by increasing the gyration length and decreasing the scale length of intensity variation. As result there is greater deviation between the exact numerical and phase averaged values of the adiabatic invariant. It is further to be noticed from the figure that the pulse particle interaction can terminate at any point between the gyration and hence would in principle would require the information of the fast phase for improving the adiabatic description of the particle dynamics.

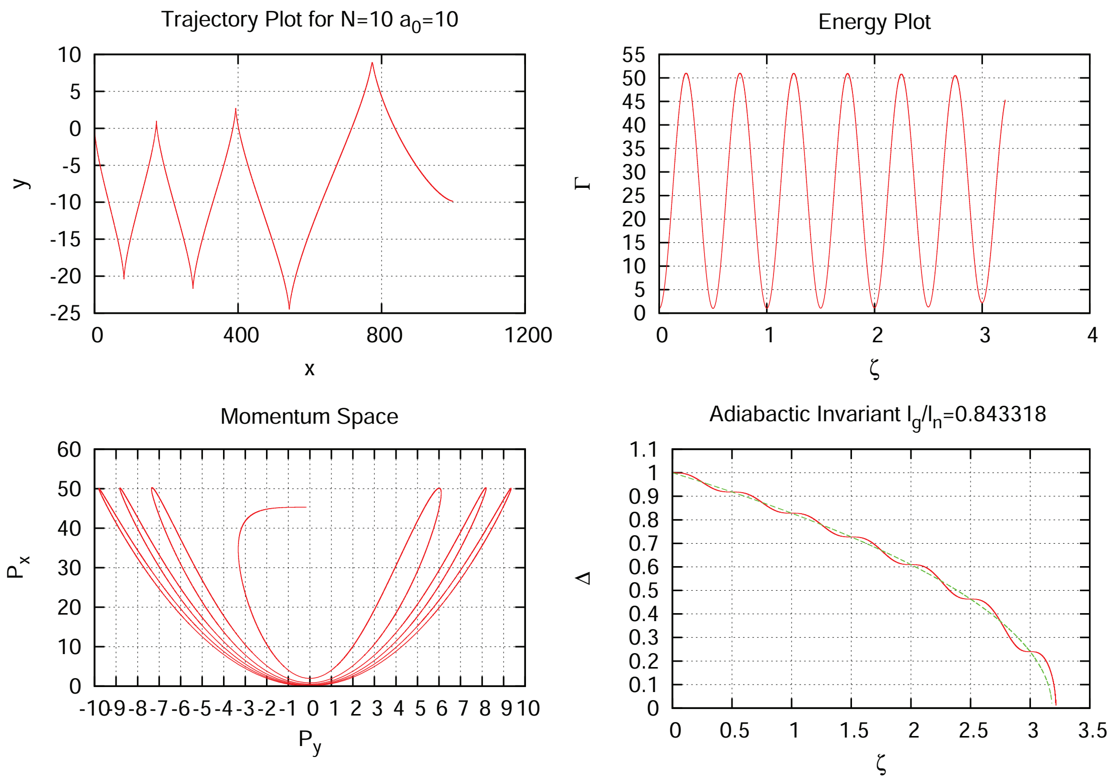

Figure 4.4: Plot for particle trajectory in configuration space, momentum space, total energy and adiabatic invariant for a focused laser pulse for N=10

From figure(4.5), it can been seen that the further increase in the initial value can make the adiabaticity parameter approach unity. At this stage the gyration length of the particle becomes greater than the scale length of the intensity variation, which in turn causes a vast difference in the numerical and phase averaged values of the adiabatic invariant. As the adiabaticity parameter attains a value of unity there is a complete breakdown of the adiabatic equations and the process can be termed as non-adiabatic.

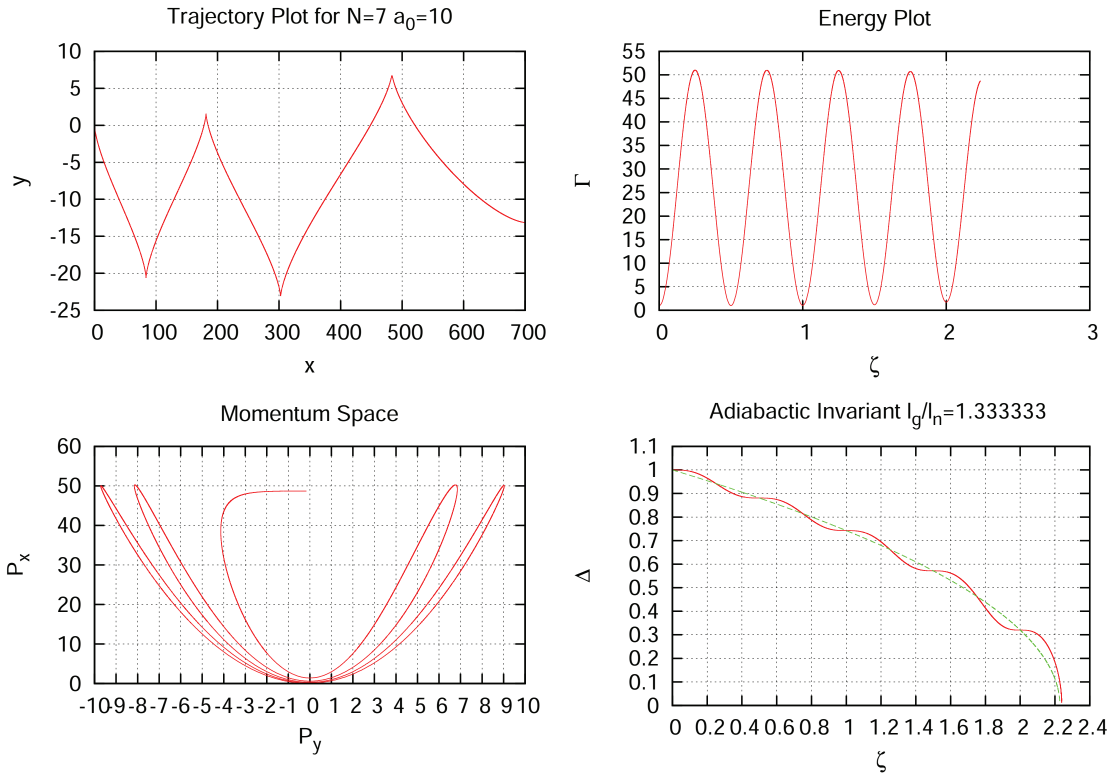

Figure 4.5: Plot for particle trajectory in configuration space, momentum space, total energy and adiabatic invariant for a focused laser pulse for N=7

In figure(4.6), the numerical and analytical energy gain by the particle is plotted along with corresponding adiabatic invariant as function of the focal length (or intensity $F = N \times a^2$) for the same initial slowness parameter. The value of final energy gain by the particle is given by Eq.(4.11), which depends upon the adiabatic invariant and laser vector potential only. The final numerical and phase averaged value of adiabatic invariant is determined at a point where the intensity drops to zero and marks the end of laser particle interaction. From the figure it can be seen that for an initially slow process, there is very good match between the numerical and phase averaged adiabatic energy gain by the particle. It is to be noted that even though the difference in the exact numerical and phase averaged value of adiabatic invariant is small, the corresponding variation in the energy gain is very large.

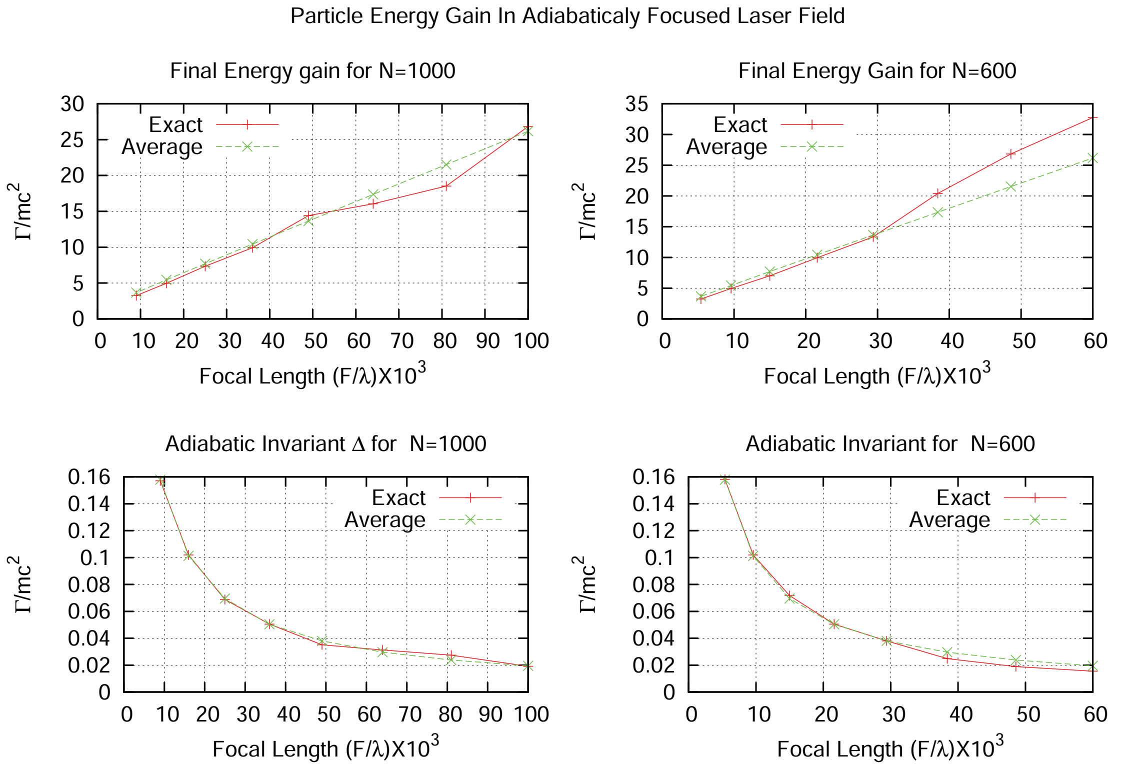

Figure 4.6: Particle energy gain Γ/mc^2 and adiabatic invariant in an adiabatically focused laser field as function of focal length F.

4.3 Particle acceleration in focused finite duration laser pulse

The study of particle dynamics in a focused field of a continuous laser in the last section gave a considerable physical insight into the mechanism of direct laser acceleration. However the study of particle motion in a continuous focused laser is an ideal case, a more realistic case is thus considered as per the previous analytical work by Kaw *et.al*[46] using a finite duration laser pulse. The linear spatial modulation in the laser intensity is used to describe the focused laser field, which is similar to the one used in the last section by Eq.(4.19). The variation in the laser intensity is defined by $a^2 = \delta f(F \pm x)$, for $x \lessgtr 0$, where $A_0^2 = \delta f F$ is the peak laser intensity, f is an external parameter and F is the focal length in which the intensity drops to zero in distance of F/λ wavelengths on either side of the focus.

In the earlier analytically work Kaw *et al.*[46] have studied the final energy gain by analytically solving the phase averaged equations Eq.(4.15) and Eq.(4.16). In their work, the authors have used $\Theta(\delta\xi) = sech(\delta\xi)$ to define the temporal envelope of the pulse, the particle was assumed to be at rest before the arrival of laser pulse and placed very close to focus. The final energy gain of the particle is measured at the point where the laser intensity drops to zero and is given by $\Gamma \simeq 1/(2\Delta_m)$ where Δ_m refers to the minimum value of Δ at that point. In the present work, the exact relativistic equation of motion given Eq.(4.2) is solved using the same set of assumptions and temporal profile for the pulse as described above.

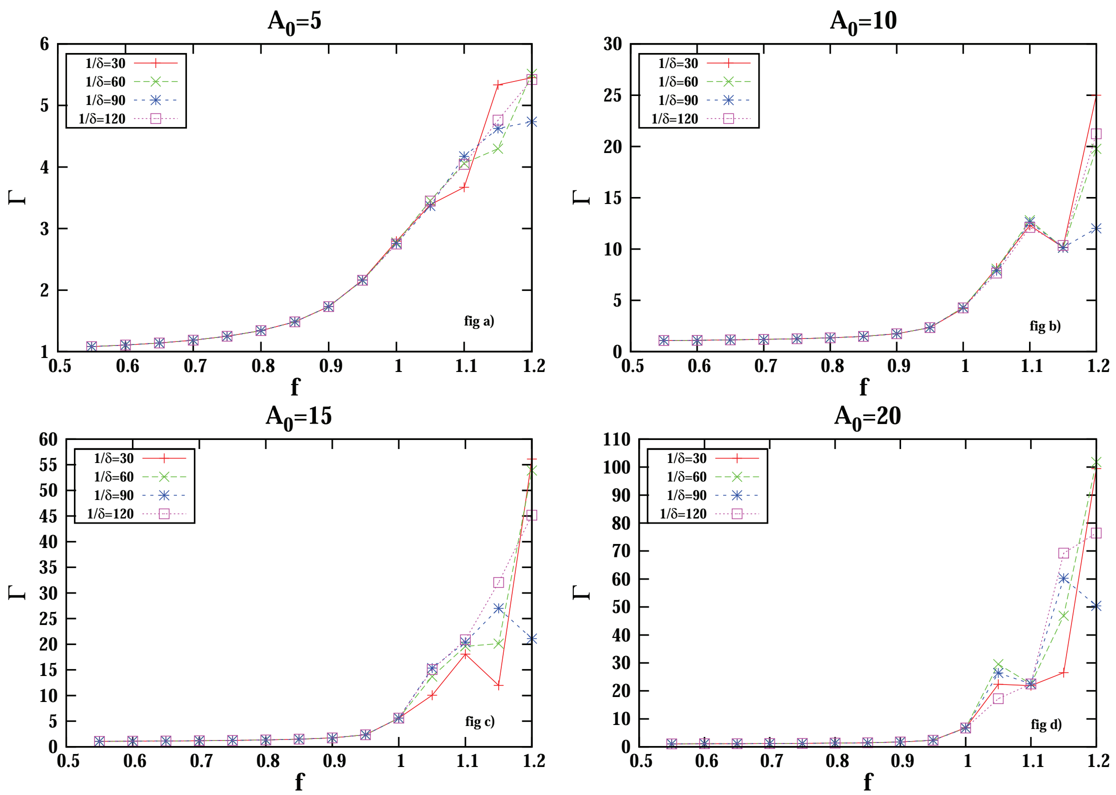

Figure 4.7: Plot for energy gain by the particle in the laser field as function of parameter f at different laser intensities A_0^2 and $1/\delta$.

In the Fig(4.7), the resultant final energy gain by the particle is plotted as a function of parameter "$f(=\frac{A_0^2}{\delta F})$". These results are obtained by solving the exact equation of motion numerically using Runge-Kutta method. In this study the length of the laser pulse ($1/\delta$) and peak laser intensity (A_0^2) are kept constant.

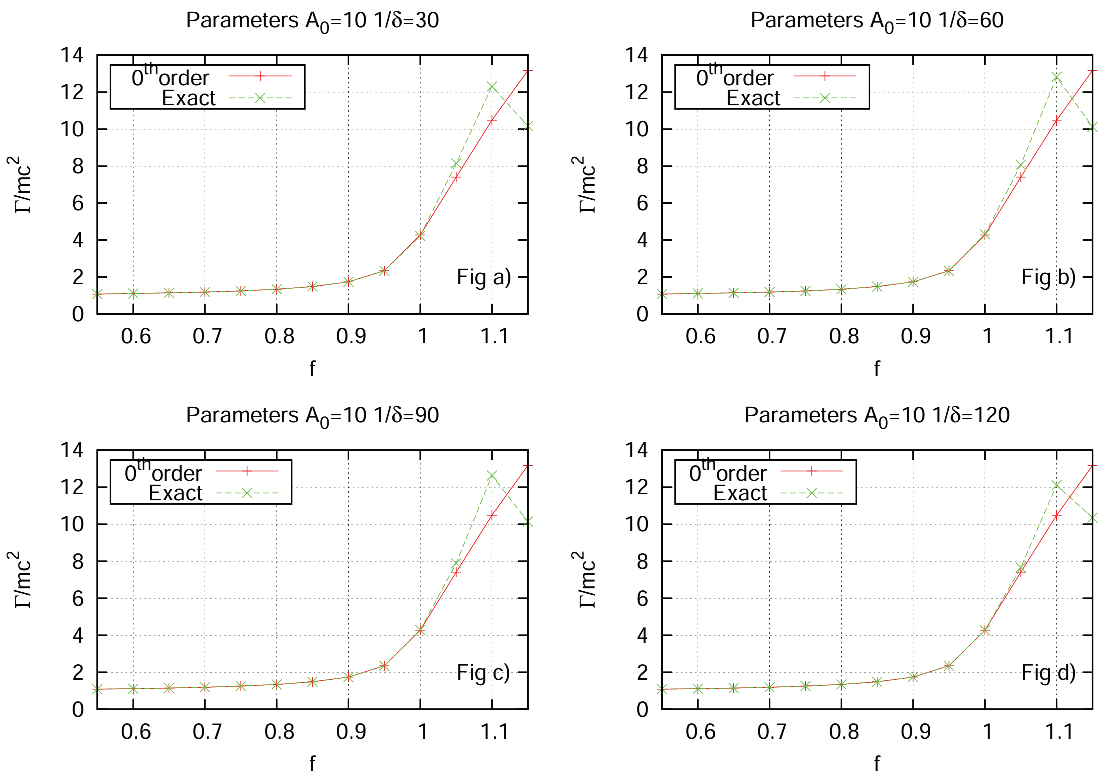

Figure 4.8: Plot for particle energy gain as function of $1/\delta$ at different laser intensities A_0^2 for fixed value of parameter f.

In Fig(4.8), the exact numerical results described in Fig(4.7), are compared with the resultant energy gain corresponding the phase average equations given by Eq.(4.15) and Eq.(4.16). These results corresponds to the same peak laser intensity (A_0^2) and different pulse lengths ($1/\delta$). On comparing the results in the different subplots it can be seen that, the numerical and analytical results have a very good matching the in the region $f < 1$ and $f \approx 1$, however the results diverge significantly in the region $f > 1$. It can further be seen from the figure, that the disagreement starts early with decrease in the length of the pulse. As per the earlier analytical work, the results of numerical study can be divided in the following three different parameter regimes, $f < 1$, $f \approx 1$ and $f > 1$, which gives further physical insight into the mechanism of particle acceleration described.

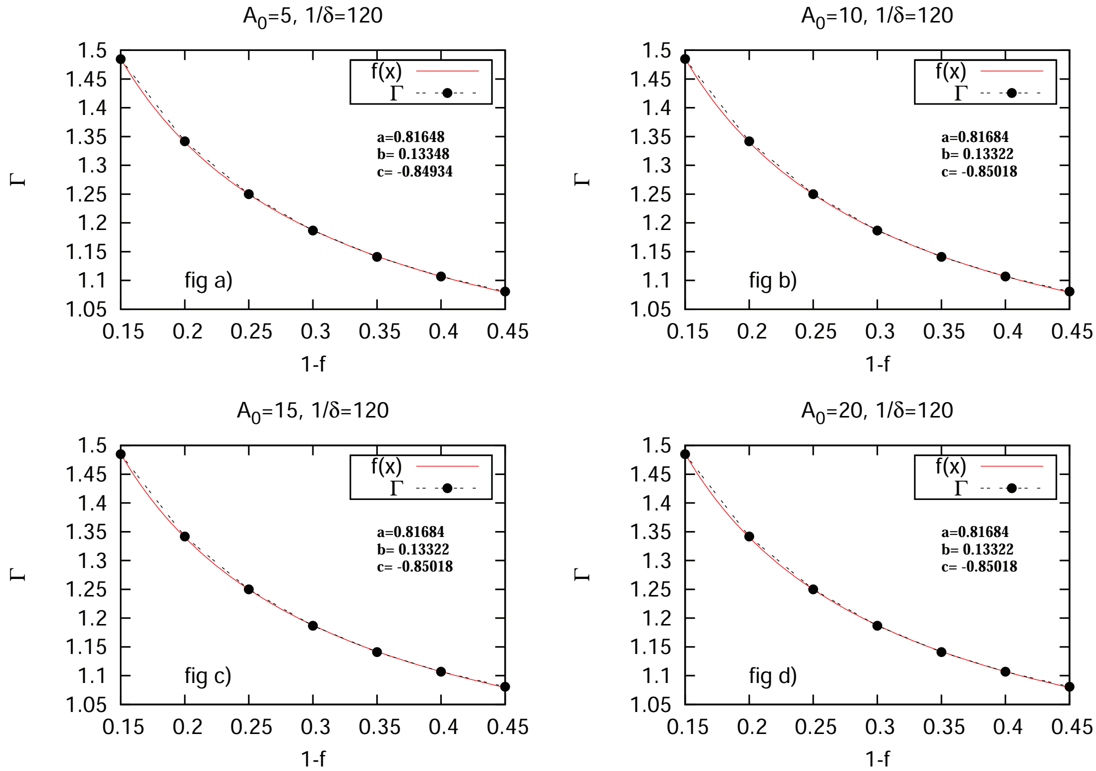

Figure 4.9: Plot for particle energy gain as function of f for the region $f < 1$.

In region 1, corresponding $f < 1$, the resultant final energy gain by the particle obtained on solving the exact equation of motion for different peak laser intensities is presented in Fig(4.9). It can be seen from the subplots, that the resultant final energy gain by a particle depends only upon parameter f and is independent of the laser intensity. The parametric dependence of the final energy gain by the particle on parameter f is established and is specified by the value of variable "c" shown in the figure. The results are in accordance with the analytical predictions given in the Kaw *et al.* ref.[46] and shown in Fig(4.8). In this regime, even though the adiabatic condition is very well satisfied and described by earlier analytical adiabatic approximations specified in ref.[46], yet it is not suitable for forward energy gain.

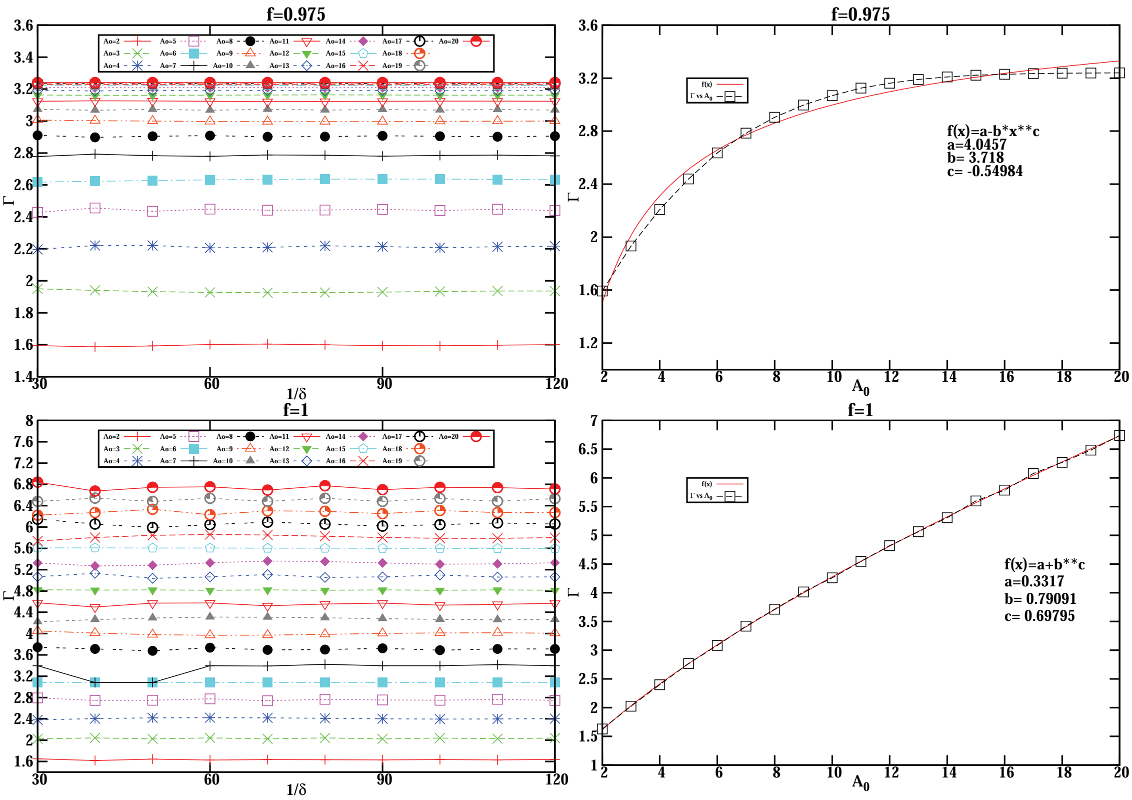

Figure 4.10: Plot of particle energy gain as a function of laser intensity A_0^2, in the region $f \approx 1$ for fixed value of $1/\delta$.

For region 2, corresponding to $f \approx 1$, the results of simulation are given in Fig(4.10). These results are aimed to study the dependence of resultant energy gain by a particle on peak laser intensity (A_0^2) and laser pulse length ($1/\delta$) keeping the value of parameter $f(= \frac{A_0^2}{\delta F})$ constant. From the figure, it can be seen that the resultant final energy gain by the particle depends upon the peak laser intensity (A_0^2) and is independent of pulse length ($1/\delta$). Using a fitting function the dependence of energy gain on laser amplitude is established and shown along with the values of the fitting parameters. From the value of parameter “c”, it can be seen that final energy of the particle in this regime increases approximately as $A_0^{2/3}$ of the laser amplitude. Thus it can be concluded that in the regime $f \approx 1$, the resultant particle energy gain improves with the laser intensity and is independent of pulse length. These results are in good qualitative as well as quantitative match with the previous predictions of the analytical work ref.[46].

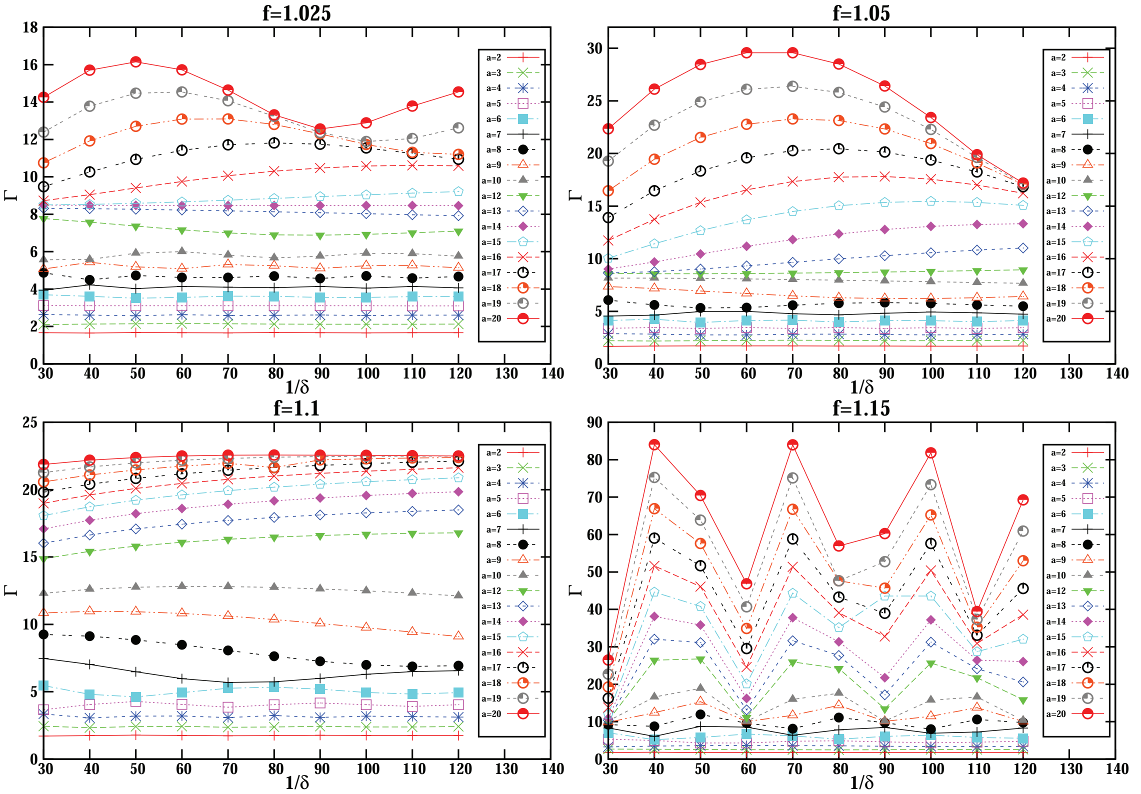

Figure 4.11: Plot for particle energy gain as function of $1/\delta$ at different laser intensities A_0 for fixed value of parameter f.

For region 3, corresponding to $f > 1$, a parametric study is carried out to establish the dependence of resultant final energy gain by the particle on the peak laser intensity (A_0^2), pulse length ($1/\delta$) and parameter $f(=\frac{A_0^2}{\delta F})$. In Fig.(4.11), the dependence of the particle energy gain on laser the pulse length ($1/\delta$) is described for different laser intensities (A_0^2), by keeping the value of parameter f constant. From the results it is evident that the regime can be further sub-divided into a region $A_0 \leq 8$ and $A_0 \geq 8$. In region $A_0 \leq 8$, the energy gain by particle is nearly independent of pulse length ($1/\delta$), but depends only upon the laser intensity. For $A_0 \geq 8$, the energy gain particle depends upon the pulse length ($1/\delta$) as well as on the peak laser intensity A_0^2.

4.4 Summary

The major findings of the study of particle dynamics in the focused laser field are summarized in this section. In this chapter, the particle dynamics is studied in the focused field of a continuous and finite duration laser to gain insight into the physical mechanism of direct laser acceleration. A slow linear spatial modulation in the laser intensity along the direction of propagation is used to describe the focused laser field. The exact relativistic equation of motion is numerically solved describing the particle dynamics in the focused continuous laser and results are used to study the particle motion in the focused and de-focused region. The numerical results are compared with the earlier analytical work by Kaw *et.al*[46] and it is shown that in the focused region, the particle dynamics depends upon the choice of the initial position which can subsequently result in reflection, stopping and acceleration of the particle. For a particle initially at rest and subjected to the zero of the laser vector potential, it shown that focal point is the optimum initial position for maximum energy gain. In this study, the parameter for the adiabatic (or slowness) process is given by "ϵ" and is defined as the ratio of the particle gyration length to the scale length of variation in the laser intensity over one gyration. It is further shown that in the focused region, the particle is subjected to the ascending acceleration gradient as a result its forward motion is retarded which in turn decreases its gyration length. Thus the adiabaticity parameter remains very small and the adiabatic conditions are very well satisfied in this region.

Next, the particle dynamics is studied in the de-focused region and the results the of the numerical study are used to determine the quantitative limit of the earlier analytical adiabatic work. In this region the particle gains energy along the direction of propagation of the particle and hence the gyration length of the particle increases in each subsequent gyration which leads to the evolution of the adiabaticity parameter. It is shown that the particle dynamics depends upon the initial choice of slowness parameter and increases rapidly when the initial value is large. The increase in the value of adiabaticity parameter causes the deviation between the exact numerical and phase averaged analytical estimates of the particle energy gain which is expressed in terms of adiabatic invariant. It is further shown that the for larger initial adiabaticity parameter the laser particle interaction can terminate at an arbitrary laser phase and thus making the information of the phase important for final energy estimation.

This study is extended to a more realistic case of finite duration laser pulse. A detailed numerical work is carried out to determine the optimum initial condition in terms of peak laser intensity (A_0^2), pulse length ($1/\delta$) and focal length (F) for maximum energy gain by the particle. The findings of the numerical work are compared with the earlier analytical work. In this work the resultant final energy gain of the particle is studied as a function of parameter "$f(=\frac{A_0^2}{\delta F})$", which is defined as the ratio of the product of peak laser intensity and the pulse length to the focal length of the focused laser field. It is shown that the numerical and analytical results agree in the parametric region $f \leq 1$. However there is significant difference in the numerical and analytical results in the parametric region $f > 1$. These results can not be described by the earlier analytical work and thus a higher order adiabatic theory is required for understanding the deviation in the resultant energy gain as well as for analytical estimation of the numerical results.

5

Adiabatic formulation for charged particle dynamics in an inhomogeneous electromagnetic field

In this chapter a higher ordered adiabatic theory is derived using the Lie-transform perturbation method for studying the particle dynamics in an inhomogeneous field of relativistically intense laser field. The newly derived theory is used for the analytical estimation of the numerically obtained particle energy gain. The contents of this chapter have been published in ref. **Sagar *et.al***[*105*].

5.1 Introduction

In chapter-2, the particle dynamics has been studied in the field of a homogeneous laser field. It has been shown that for a particle interacting with a homogeneous laser field, the dynamics is associated with the three constants of motion. These constants of motion correspond to symmetries associated with the independence of the Hamiltonian with respect to the two transverse coordinates and to the longitudinal coordinate 'x' and the time 't' except through the combination $t-x$. From Hamiltonian dynamics and Livouville's integrability theorem [43, 96, 97, 98, 104] it is known that a Hamiltonian describing a system with $'n'$ degrees of freedom is completely integrable if, $'n'$ invariants are present to characterize a solution of its $'2n'$ equations of motion. Thus it is an integrable problem with dynamical variables expressed in terms of constants of motion and laser vector potential only. However no net energy is transfered to the particle at the end of laser particle interaction.

In the previous chapter, a scheme of direct particle acceleration in vacuum has been studied in which the particle is subjected to the focused laser field. The slow spatial modulation in the laser intensity along the direction of propagation of the laser has been used to model the focused laser field. It has been shown that the focusing causes an inhomogeneity in the laser field, which results in the loss of one of the above specified three constants of motion. This makes the problem non-integrable and the dynamical variables cannot be described in terms of constants of motion and vector potential only as was possible previously.

In the earlier analytical work, Kaw *et.al*[46] have shown that for a slow spatial variation, the particle energy gain can be determined adiabatically. The slowness has been defined as, a ratio of the particle gyration length (l_g) to the scale length of inhomogeneity ($l_n(=|\frac{1}{a^2}\frac{da^2}{d(\epsilon x)}|^{-1})$) and is given by '$\epsilon(=l_g/l_n)$'. Thus for a particle dynamics to remain adiabatic, the value of adiabatic parameter should be much smaller than one ($\epsilon << 1$). However from the results of comprehensive numerical study carried out in the previous chapter, it has been found that the earlier theory is unable to account for energy gain by the particle in the parameter regime $f(=\frac{A_0^2}{\delta F}) > 1$, which corresponds to the tight focusing of laser and the symbols have following meaning, A_0^2 is the peak laser intensity, ($\delta = (\lambda/L)$) ratio of the fundamental laser wavelength to length of pulse, F is the focal length. Thus an improved adiabatic theory is required for physical understanding of the mechanism and to analytically account for the numerical results.

In this chapter, a higher order adiabatic theory is derived using the Lie transformation perturbation method which is based upon the Hamiltonian dynamics and canonical transformations. In this method a canonical transformation [94, 95, 97, 98, 104]from the lab variables to new phase averaged variables is carried out which simplifies the form of Hamiltonian. The new phase averaged variables are expressed in terms of lab variables as an asymptotic series in the powers of adiabaticity parameter. In this method carrying out a transformation from lab variables to phase averaged variables is equivalent to averaging over fast motion. The generators for such a transformation are derived and expressed in terms of Poisson brackets which are invariant under canonical transformation and this makes the whole formalism canonically invariant. The problem is simplified on transforming from lab variables to phase averaged variables. Finally the problem is solved by evolving the new phase averaged variables and subsequently carrying out an inverse transformation from the phase averaged variables to the lab variables. The variables as previously stated are expressed in the form of an asymptotic series in the powers of the adiabaticity parameter. In this work the adiabatic invariant has been derived up to second order of the adiabaticity parameter, which suitably takes into account the contribution of the fast dynamics to second order of adiabaticity parameter. It has been shown that the earlier work by Kaw*et.al*[46], corresponds to the first order of the present work. However it is to be pointed out that in the earlier work there was no inverse transformation from phase averaged variables to lab variables i.e, contribution from the fast dynamics was not taken into account.

The newly derived higher order adiabatic theory has been used for the analytical estimation of the numerically obtained energy gain by particle. The numerical results have been obtained using one-dimensional focusing model in which the laser intensity has a linear spatial modulation along the direction of propagation of the laser.

The chapter is organized in the following way: in section (5.2), particle dynamics is studied in the homogeneous field of finite duration laser using using Hamiltonian dynamics and canonical transformations. In section (5.3), particle dynamics is studied in the field of an inhomogeneous laser field using Hamiltonian dynamics and canonical transformations. In subsection (5.3.1), higher orders of adiabatic invariance are derived using method of Lie-transformation perturbation method. In section (5.4), the analytical estimates of the particle energy gain in the focused laser field are compared with the numerical results. In section (5.5), contains a brief summary of the topic.

5.2 Hamiltonian approach to charged particle dynamics

5.2.1 Homogeneous laser field:

The dimensionless Hamiltonian describing the motion of a charged particle placed in a linearly polarized finite duration laser pulse is given by,

$$H(\vec{r},\vec{P}) = \sqrt{1 + P_x^2 + (P_y - A(t-x))^2 + P_z^2} \tag{5.1}$$

with the following normalizations $H \to H/mc^2$, $P_{x,y,z} \to P_{x,y,z}/mc$, and $A_0 \to eA_0/mc^2, t \to \omega t, r \to kr$. The vector potential of the laser pulse is chosen to be $\vec{A}(\vec{r},t) = A_0\phi(\omega t - kx)\hat{y}$, where $\phi(\omega t - kx) = \Theta(\delta(\omega t - kx))P(\omega t - kx)$, P is the oscillatory part, Θ is the pulse shaping factor with $\delta = \frac{\lambda}{L} << 1$. As coordinates $'y'$ and $'z'$ are cyclic, therefore the corresponding conjugate canonical momentum components (α) and P_z are constants. This gives the $'y'$ component of particle momentum as

$$p_y = \alpha - A(t-x) \tag{5.2}$$

In the present geometry the particle dynamics is confined in $x-y$ plane only and there is no motion along z direction, hence it is removed from the calculations hereinafter. On canonically transforming the old Hamiltonian to the new Hamiltonian using a type II generating function [43, 98] defined as,

$$F_2 = (t-x)P_x^{'}. \tag{5.3}$$

The transformation equation for the Hamiltonian is,

$$H^{'} = H + \frac{\partial F_2}{\partial t} = H + P_x^{'} \tag{5.4}$$

with the transformed Hamiltonian $H^{'}$ given by,

$$H^{'} = \sqrt{1 + (P_x^{'})^2 + (P_y^{'} - A(\xi))^2} + P_x^{'} \tag{5.5}$$

and under canonical transformation the variables transform as,

$$P_x = \frac{\partial F_2}{\partial x} = -P_x^{'}; \qquad \xi = \frac{\partial F_2}{\partial P_x} = (t - x). \tag{5.6}$$

Since $H^{'}$ does not explicitly depend upon time, it is a third constant of motion and is denoted by Δ. In terms of old coordinates, it can be written

$$\Delta = \Gamma - P_x \qquad (\because P_x = p_x) \tag{5.7}$$

where P_x is the canonical momentum, p_x is the particle momentum and Γ (the total energy of the particle) is the value of the Hamiltonian given by Eq.(5.1). Using Eq.(5.1), Eq.(5.2) and Eq.(5.7), particle momentum and position can now be written in terms of constants of motion and vector potential as

$$P_x = \frac{1-\Delta^2}{2\Delta} + \frac{(\alpha - A(\xi))^2}{2\Delta} \qquad x = x_0 + \int_{\xi_0}^{\xi} \frac{P_x}{\Delta} d\xi \tag{5.8}$$

$$p_y = (\alpha - A(\xi)) \qquad y = y_0 + \int_{\xi_0}^{\xi} \frac{(\alpha - A(\xi))}{\Delta} d\xi \tag{5.9}$$

The above set of expressions, Eq.(5.8) and Eq.(5.9) describes the particle dynamics in the field of homogeneous laser. The position and momentum of the particle has been expressed in terms of constants of motion and vector potential only.

5.3 Inhomogeneous laser field:

In this section, the particle dynamics is studied in an inhomogeneous laser field which is due to slow spatial variation of laser intensity along the direction of propagation of laser pulse. In the presence of inhomogeneity, the vector potential of the laser pulse is given by $\vec{A}(\vec{r}, t, \epsilon x) = a(\epsilon x)P(\delta(t-x))\Theta(t-x)\hat{y}$, where as defined earlier, the slowness parameter ϵ is the ratio of particle gyration length to the scale length of intensity variation. For the sake of generality the functional form of laser amplitude $a(\epsilon x)$, has been kept arbitrary. The dimensionless Hamiltonian is given by,

$$H(\vec{r}, \vec{P}) = \sqrt{1 + P_x^2 + (P_y - A(\epsilon x, (t-x))^2}. \tag{5.10}$$

The Hamiltonian is cyclic in $'y'$ co-ordinate, hence the conjugate canonical momentum is conserved and is expressed as,

$$p_y + A(\epsilon x, (t-x)) = \alpha. \tag{5.11}$$

Using the type II generating function[104] for canonical transformation, which is defined by

$$F_2 = (t-x)J_\xi + xJ_\eta \tag{5.12}$$

the transformed Hamiltonian is given by

$$H^{'}(\xi, y, J_\xi, P_y; \epsilon\eta, J_\eta) = \sqrt{1 + (-J_\xi + J_\eta)^2 + (P_y - A(\epsilon\eta, \xi))^2} + J_\xi. \tag{5.13}$$

Hamiltonian $H^{'}$ is cyclic in $'t'$ and thus is a constant of motion given by $\Delta^{'}$. Under canonical transformation the variables transform as

$$P_x = \frac{\partial F_2}{\partial x} = -J_\xi + J_\eta; \qquad \xi = \frac{\partial F_2}{\partial J_\xi} = (t-x); \qquad \eta = \frac{\partial F_2}{\partial J_\eta} = x. \tag{5.14}$$

The corresponding Hamilton's equations may be expressed as

$$\frac{dJ_\xi}{dt} = -\frac{\partial H^{'}}{\partial \xi} = -\frac{1}{2\Gamma}\frac{\partial(\alpha - A(\epsilon\eta, \xi))^2}{\partial \xi} \tag{5.15}$$

$$\frac{dJ_\eta}{dt} = -\frac{\partial H^{'}}{\partial \eta} = -\frac{1}{2\Gamma}\frac{\partial(\alpha - A(\epsilon\eta, \xi))^2}{\partial \eta} \tag{5.16}$$

$$\frac{d\xi}{dt} = \frac{\partial H^{'}}{\partial J_\xi} = \frac{-(-J_\xi + J_\eta) + \Gamma}{\Gamma} = \frac{\Delta^{'} - J_\eta}{\Gamma} \tag{5.17}$$

$$\frac{d\eta}{dt} = \frac{\partial H^{'}}{\partial J_\eta} = \frac{-J_\xi + J_\eta}{\Gamma} \tag{5.18}$$

On expressing the new Hamiltonian in terms of old coordinates by substituting the value of J_ξ from Eq.(5.14), J_η is obtained from Eq.(5.16), Eq.(5.17) and Eq.(5.18) as,

$$J_\eta = -\int [\frac{\partial(\alpha - A(\epsilon\eta, \xi))^2}{2(\Delta^{'} - J_\eta)\partial\eta}] d\xi \tag{5.19}$$

In terms of the old coordinates, the Hamiltonian is expressed as,

$$H^{'} = \Delta - \epsilon \int [\frac{\partial(\alpha - A(\epsilon x, \xi))^2}{2\Delta\partial(\epsilon x)}] d\xi \tag{5.20}$$

Thus in the presence of an inhomogeneity the previously defined Δ is no longer an exact constant of motion. However in the adiabatic approximation i.e, $\epsilon << 1$, Δ is an adiabatic invariant and the particle dynamics can be studied adiabatically. The particle position and momentum can be described in terms of the laser vector potential, the constant of motion α and the adiabatic invariant as was done previously for the homogeneous case. In the present problem, the adiabatic invariant evolves and its evolution is obtained by solving the following Hamilton's equations,

$$\dot{\Delta} = -\frac{\partial H'}{\partial \xi} = \epsilon \frac{1}{2\Delta} \frac{\partial(\alpha - A)^2}{\partial(\epsilon x)} \tag{5.21}$$

$$\dot{\xi} = \frac{\partial H'}{\partial \Delta} = 1 + \epsilon \int \frac{1}{2\Delta^2} \frac{\partial(\alpha - A)^2}{\partial(\epsilon x)} d\xi \tag{5.22}$$

corresponding to the Hamiltonian given by Eq.(5.20) and along with the particle position. In the present form, the above equation cannot be solved due to the presence of both slow and fast variables. The solution can be obtained by transforming the Hamiltonian given by Eq.(5.20) into a simpler form and solving the problem in terms of the new coordinates and carrying out an inverse transformations.

5.3.1 Lie transformation perturbation method

In this subsection, the use of Lie transformation perturbation method is described which utilizes the Deprit perturbation series [99, 100, 101, 102, 103, 104] for solving the Eq.(5.21) and Eq.(5.22) describing the evolution of the adiabatic invariant. To begin with the Hamiltonian given by Eq.(5.20) is transformed from the present set of lab variables into phase averaged slow variables, in terms of which the new Hamiltonian is simplified. The derivation of such a generators of the transformation from lab variables to phase averaged variables and vice-versa is described below. These phase averaged variables are evolved using the phase averaged Hamiltonian and the solutions in terms of lab variables are obtained by carrying out an inverse transformation. The transformations derived are in the orders of adiabaticity parameter ϵ and in the present work are derived till second order of adiabaticity parameter. The method described here is general and can be extended to higher orders. The summary of basic aspects of Lie-transforms essential for the present work along with Deprit perturbation series is given in Appendix.

As per the theory of Lie transform, the evolution operator T can be represented by $T = exp(-L)$, where $Lf = [w, f]$ represents its operation upon any function $f(X,t)$ with $[,]$ denoting the Poisson brackets and function $w(X)$ is the Lie generator. The inverse evolution operator T^{-1} is given by $T^{-1} = exp(L)$. For the second order adiabatic theory the Lie generators to second order are expressed as,

$$w = w_{10} + \epsilon w_{11} + \epsilon w_2 \tag{5.23}$$

where w_1 and w_2 are first and second order Lie generators.

The explicit calculations are presented for deriving the generator of canonical transformation to second order. As a starting point for the calculations we consider the Hamiltonian derived in section II (5.20) for driving these generators,

$$H^{'} = \Delta - \epsilon \int [\frac{\partial(\alpha - A(\epsilon x, \xi)^2}{2\Delta\partial(\epsilon x)}] d\xi \tag{5.24}$$

In the present case $\Theta(\delta\xi) = sech(\delta\xi)$, $P(\xi) = sin(\xi)$ and for simplicity set $\alpha = 0$.

$\mathbf{Zeroth-order}$: In zeroth order the perturbation equation is given by

$$\bar{H}_0 = H_0 = \bar{\Delta} \tag{5.25}$$

$\mathbf{FirstOrder}$: First order correction to second order in adiabaticity parameter (ϵ^2): The Hamiltonian corresponding to fast motion is given by,

$$w_1 = w_{10} + \epsilon w_{11} \tag{5.26}$$

Using the first order perturbation equation,

$$\frac{\partial w_1}{\partial t} + L_1 H_o = (\bar{H}_1 - H_1) \tag{5.27}$$

As there is no explicit dependence on time the first term on the left hand side is zero. Hence re-writing the equation with $H_0 = \Delta = \Gamma - p_x$. Substituting the value of transformed unperturbed Hamiltonian H_0 from Eq.(5.7) in the following equation and solving with Δ and $(t-x)$ as independent variables,

$$(\frac{\partial w_{10}}{\partial \xi}\frac{\partial H_0}{\partial \Delta} - \frac{\partial w_{10}}{\partial \Delta}\frac{\partial H_0}{\partial \xi}) + \epsilon(\frac{\partial w_{11}}{\partial \xi}\frac{\partial H_0}{\partial \Delta} - \frac{\partial w_{11}}{\partial \Delta}\frac{\partial H_0}{\partial \xi}) + \epsilon(\frac{\partial w_{10}}{\partial (\epsilon x)}\frac{\partial H_0}{\partial p_x} - \frac{\partial w_{10}}{\partial p_x}\frac{\partial H_0}{\partial (\epsilon x)}) = (\bar{H}_{10} + \epsilon \bar{H}_{11} - H_1) \tag{5.28}$$

Separating in the powers of ϵ as

$$\frac{\partial w_{10}}{\partial \xi} = \bar{H}_{10} + \int \frac{a^{'} a \Theta(\delta\xi)^2}{2\Delta} d\xi - \int \frac{a^{'} a \Theta(\delta\xi)^2 cos(2\xi) d\xi}{2\Delta}$$
$$\frac{\partial w_{11}}{\partial \xi} = \bar{H}_{11} + \frac{\partial w_{10}}{\partial (\epsilon x)}$$

These equations can be solved by removing the secular part by equating it to arbitrary constant $\bar{H}_{10}$ and setting it to zero. In the absence of second order secular term in the Hamiltonian the arbitrary constant $\bar{H}_{11} = 0$ is set equal to zero. While considering fast motion for $\delta << 1$ one can write

$$\int \frac{a^{'} a \Theta(\delta\xi)^2 cos(2\xi) d\xi}{2\Delta} \approx \frac{a^{'} a \Theta(\delta\xi)^2}{2\Delta} \frac{sin(2\xi)}{2}$$

, this results in,

$$w_1 = \frac{a^{'} a \Theta(\delta\xi)^2}{2\Delta} \frac{cos(2\xi)}{4} + \epsilon \frac{(a^{'2} + a^{''} a)\Theta(\delta\xi)^2}{2\Delta} \frac{sin(2\xi)}{8} \tag{5.29}$$
$$\bar{H} = \bar{H}_0 + \epsilon \bar{H}_1 \tag{5.30}$$
$$\bar{H} = \bar{\Delta} - \int \frac{a^{'} a \Theta(\delta\xi)^2 d\xi}{2\bar{\Delta}} \tag{5.31}$$

Second – Order: For second order in the ϵ for the fast Hamiltonian w_2 the perturbation equation is given by,

$$\frac{\partial w_2}{\partial t} + L_2 H_o = 2(\bar{H}_2 - H_2) - L_1[\bar{H}_1 + H_1] \tag{5.32}$$

second order require only $w_2 = w_{20}$, for the present case $H_2 = 0$. Re-writing the above equation,

$$[w_{20}, H_0] = 2\bar{H}_2 - [w_{10}, (\bar{H}_1 + H_1)]$$

re-writing it we have,

$$\left(\frac{\partial w_{20}}{\partial \xi}\frac{\partial H_0}{\partial \Delta} - \frac{\partial w_{20}}{\partial \Delta}\frac{\partial H_0)}{\partial \xi}\right) = 2\bar{H}_{20} - \left(\frac{\partial w_{10}}{\partial \xi}\frac{\partial(\bar{H}_1+H_1)}{\partial \Delta} - \frac{\partial w_{10}}{\partial \Delta}\frac{\partial(\bar{H}_1+H_1)}{\partial \xi}\right)$$

on calculating various terms of the Poisson of the brackets gives,

$$\frac{\partial(2\bar{H}_1 + \{H_1\})}{\partial \xi} = \frac{a^{'}a\Theta^2(\delta\xi)}{2\Delta}cos(2\xi)$$
$$\frac{\partial(2\bar{H}_1 + \{H_1\})}{\partial \Delta} = \int \frac{a^{'}a\Theta(\delta\xi)^2 d\xi}{\Delta^2} - \frac{a^{'}a\Theta(\delta\xi)^2}{4\Delta^2}sin(2\xi)$$

Here the terms inside the curly bracket signify fast terms and on substituting the various terms,

$$\frac{\partial w_{20}}{\partial \xi} = 2\bar{H}_{20} - \frac{(a^{'}a)^2\Theta(\delta\xi)^4}{16\Delta^3} + \frac{a^{'}a\Theta^2(\delta\xi)}{4\Delta}sin(2\xi)\int \frac{a^{'}a\Theta^2(\delta\xi)d\xi}{\Delta^2}$$

The secular term can be removed by equating it to arbitrary constant

$$2\bar{H}_{20} - \frac{(a^{'}a)^2\Theta(\delta\xi)^4}{16\Delta^3} = 0$$

Thus second order generator is given as,

$$w_{20} = -\frac{a^{'}a\Theta^2(\delta\xi)}{8\Delta}cos(2\xi)\int \frac{a^{'}a\Theta(\delta\xi)^2 d\xi}{\Delta^2} + \frac{(a^{'}a)^2\Theta^4(\delta\xi)}{16\Delta^3}sin(2\xi)$$

The generators of the canonical transformation to second order are given by,

$$w_{10} = \frac{a^{'}a\Theta^2(\delta\xi)}{8\Delta}cos(2\xi) \qquad w_{11} = \epsilon\frac{(a^{'2} + a^{''}a)\Theta^2(\delta\xi)}{16\Delta}sin(2\xi)$$
$$w_2 = -\epsilon\frac{a^{'}a\Theta^2(\delta\xi)}{8\Delta}cos2\xi\int \frac{a^{'}a\Theta^2(\delta\xi)d\xi}{\Delta^2} + \frac{(a^{'}a)^2\Theta^4(\delta\xi)}{16\Delta^3}sin(2\xi) \tag{5.33}$$

On substituting the various terms, the Lie generator to second order in the adiabaticity parameter takes the following form

$$w = \frac{a^{'}a\Theta^2(\delta\xi)}{8\Delta}cos(2\xi) + \epsilon\frac{(a^{'2} + a^{''}a)\Theta^2(\delta\xi)}{16\Delta}sin(2\xi) - \epsilon\frac{a^{'}a\Theta^2(\delta\xi)}{8\Delta}cos2\xi \int\frac{a^{'}a\Theta^2(\delta\xi)d\xi}{\Delta^2} + \frac{(a^{'}a)^2\Theta^4(\delta\xi))}{16\Delta^3}sin(2\xi) \quad (5.34)$$

The transformation of the lab variables to the slow phase averaged variables is obtained by the operation of the evolution operator T, which to second order in ϵ is given by

$$\begin{aligned}
\bar{\Delta} &= T\Delta \\
\bar{\Delta} &= T_0\Delta + T_1\Delta + T_2\Delta \\
\bar{\Delta} &= \Delta - L_1\Delta + \frac{1}{2}L_1^2\Delta - \frac{1}{2}L_2\Delta \\
\bar{\Delta} &= \Delta - \epsilon[w_{10}, \Delta] - \epsilon^2[w_{11}, \Delta] + \frac{\epsilon^2}{2}[w_{10}, [w_{10}, \Delta]] - \frac{\epsilon^2}{2}[w_{20}, \Delta] \quad (5.35)
\end{aligned}$$

By computing and substituting the values of Poisson brackets, it is expressed as

$$\bar{\Delta} = \Delta + \epsilon\frac{a^{'}a\Theta^2(\delta\xi)}{4\Delta}sin(2\xi) - \epsilon^2\frac{(a^{'2} + a^{''}a)\Theta^2(\delta\xi)^2}{8\Delta}cos(2\xi) - \epsilon^2 \frac{(a^{'}a)^2\Theta^4(\delta\xi)}{32\Delta^3} - \epsilon^2\frac{a^{'}a\Theta^2(\delta\xi)}{8\Delta}sin(2\xi)\int\frac{a^{'}a\Theta^2(\delta\xi)d\xi}{\Delta^2} \quad (5.36)$$

Similarly the phase ξ is transformed as

$$\bar{\xi} = \xi - \epsilon[w_{10}, \xi] - \epsilon^2[w_{11}, \xi] + \frac{\epsilon^2}{2}[w_{10}, [w_{10}, \xi]] - \frac{\epsilon^2}{2}[w_{20}, \xi] \quad (5.37)$$

By computing the various Poisson brackets and substituting them gives the required series for averaged phase,

$$\bar{\xi} = \xi - \epsilon\frac{a^{'}a\Theta^2(\delta\xi)}{8\Delta^2}cos(2\xi) - \epsilon^2\frac{(a^{'2}+a^{''}a)\Theta^2(\delta\xi)}{16\Delta^2}sin(2\xi) + \epsilon^2\frac{(a^{'}a)^2\Theta^4(\delta\xi)}{128\Delta^4}sin(4\xi)$$
$$+ \epsilon^2(\frac{a^{'}a\Theta^2(\delta\xi)}{16\Delta^2}cos(2\xi)\int\frac{a^{'}a\Theta^2(\delta\xi)d\xi}{\Delta^2} + \frac{3(a^{'}a)^2\Theta^4(\delta\xi)}{32\Delta^3}sin(2\xi)) \tag{5.38}$$

Thus the lab variables are canonically transformed to new phase averaged variables which is equivalent to performing average over fast variables up to second order in ϵ. The above derived asymptotic series are not convergent and are valid in the limit $\epsilon << 1$. With the increase in the value of adiabaticity parameter ϵ, the adiabatic condition becomes harder to satisfy and hence requires higher order terms of the series to improve it. The series becomes fully divergent when the adiabaticity parameter approaches the limit $\epsilon \approx 1$. These calculations are accurate up to an order of (ϵ^n), where n is the order of invariance calculation and for the present study restricted up to $n = 2$.

The transformed phase averaged Hamiltonian to the second order in adiabaticity parameter in terms of phase averaged variables is given by,

$$\bar{H} = \bar{H}_0 + \epsilon\bar{H}_{10} + \epsilon^2\bar{H}_{11} + \epsilon^2\bar{H}_2 \tag{5.39}$$

where H_0, H_1 and H_2 are unperturbed Hamiltonians, all computed till second order in ϵ. The various terms have been derived above and are given by,

$$\bar{H}_0 = \bar{\Delta} \qquad \bar{H}_{10} = \epsilon\int\frac{a^{'}a\Theta^2(\delta\bar{\xi})}{2\bar{\Delta}}d\bar{\xi}$$
$$\bar{H}_{11} = 0 \qquad \bar{H}_2 = \frac{(a^{'}a)^2\Theta^4(\delta\bar{\xi})}{32\bar{\Delta}^3}.$$

On substituting various terms the new transformed phase averaged Hamiltonian is expressed as,

$$\bar{H} = \bar{\Delta} - \epsilon\int\frac{a^{'}a\Theta^2(\delta\bar{\xi})}{2\bar{\Delta}}d\bar{\xi} + \epsilon^2\frac{(a^{'}a)^2\Theta^4(\delta\bar{\xi})}{32\bar{\Delta}^3} \tag{5.40}$$

The variables $(\bar{\Delta}, \bar{\xi})$ are evolved using the Hamilton's equations corresponding to the averaged Hamiltonian given by Eq.(5.40). The particle position for the averaged case is obtained from $\bar{\Delta}$, as described earlier for the homogeneous case. The inverse transformation from the phase averaged variables to lab variables is carried out using inverse evolution operator T^{-1}. The inverse evolution operator T^{-1} is expressed in terms of the Lie operator as asymptotic series in ϵ. It is important to mention that, the Lie-transformation involves an operation on the functions, rather than the variables. The arguments of the functions are just dummy variables and hence variables in the Lie generator can be simply replaced by averaged variables. The operation of the inverse evolution operator T^{-1} is given by

$$\begin{aligned}
\Delta &= T^{-1}\bar{\Delta} \\
\Delta &= T_0^{-1}\bar{\Delta} + T_1^{-1}\bar{\Delta} + T_2^{-1}\bar{\Delta} \\
\Delta &= \bar{\Delta} + L_1\bar{\Delta} + \frac{1}{2}L_1^2\bar{\Delta} + \frac{1}{2}L_2\bar{\Delta} \\
\Delta &= \bar{\Delta} + \epsilon[w_{10}, \bar{\Delta}] + \epsilon^2[w_{11}, \bar{\Delta}] + \frac{\epsilon^2}{2}[w_{10}, [w_{10}, \bar{\Delta}]] + \frac{\epsilon^2}{2}[w_{20}, \bar{\Delta}]
\end{aligned} \tag{5.41}$$

This leads to

$$\Delta = \bar{\Delta} - \epsilon\frac{a^{'}a\Theta^2(\delta\bar{\xi})}{4\bar{\Delta}}sin(2\bar{\xi}) + \epsilon^2\frac{(a^{'2} + a^{''}a)\Theta^2(\delta\bar{\xi})}{8\bar{\Delta}}cos(2\bar{\xi}) - \epsilon^2\frac{(a^{'}a)^2\Theta^4(\delta\bar{\xi})}{32\bar{\Delta}^3} + \epsilon^2\frac{a^{'}a\Theta^2(\delta\bar{\xi})}{8\bar{\Delta}}sin(2\bar{\xi})\int\frac{a^{'}a\Theta^2(\delta\bar{\xi})d\bar{\xi}}{\bar{\Delta}^2} \tag{5.42}$$

Similarly the expression for inversion of variable $\bar{\xi}$ is given by

$$\xi = \bar{\xi} + \epsilon[w_{10}, \bar{\xi}] + \epsilon^2[w_{11}, \bar{\xi}] + \frac{\epsilon^2}{2}[w_{10}, [w_{10}, \bar{\xi}]] + \frac{\epsilon^2}{2}[w_{20}, \bar{\xi}] \tag{5.43}$$

By substituting the value of the Poisson brackets, one obtains

$$\xi = \bar{\xi} + \epsilon\frac{a^{'}a\Theta^2(\delta\bar{\xi})}{8\bar{\Delta}^2}cos(2\bar{\xi}) - \epsilon^2\frac{(a^{'2} + a^{''}a)\Theta^2(\delta\bar{\xi})}{16\bar{\Delta}^2}sin(2\bar{\xi}) + \epsilon^2\frac{(a^{'}a)^2\Theta^4(\delta\bar{\xi})}{128\bar{\Delta}^4}sin(4\bar{\xi}) - \epsilon^2(\frac{a^{'}a\Theta^2(\delta\bar{\xi})}{16\bar{\Delta}^2}cos(2\bar{\xi})\int\frac{a^{'}a\Theta^2(\delta\bar{\xi})d\bar{\xi}}{\bar{\Delta}^2} + \frac{3(a^{'}a)^2\Theta^4(\delta\bar{\xi})}{32\bar{\Delta}^3}sin(2\bar{\xi})) \tag{5.44}$$

The above derived expressions lab variables obtained carrying inverse transformation expressing lab variables in terms of the slow variables. This is equivalent to Hamilton's equations of motion corresponding to Hamiltonian given by Eq.(5.21) and Eq.(5.22) to an accuracy of ϵ^2. Thus the adiabatic theory takes into account the effect of fast variation on particle motion in the presence of an inhomogeneity in the laser field.

5.4 Acceleration of charged particle in vacuum by relativistically intense finite duration laser pulse

In this section, the above derived adiabatic theory is used to compare the analytical estimate of the particle energy gain with numerical results described in the previous chapter for a focused laser field. The numerical results have been obtained by solving the exact equation of motion for particle subjected to a focused laser field. A linear spatial intensity modulation along the direction of propagation of laser has been used to describe the focused laser. The energy gain has been studied as a function of parameter $f(=\frac{A_0^2}{\delta F})$, which as previously defined, is a ratio of product of peak laser intensity(A_0^2) and pulse length $(1/\delta)$ to the focal length (F). The final energy gain of the particle is measured at the point where the intensity of the laser drops to zero, which corresponds to the minimum value of variable Δ and thus the energy gain can be given by $\Gamma \approx (1+\Delta^2)/2\Delta$. It has been shown in the previous chapter that earlier analytical work by Kaw *et.al* is unable to account for numerically obtained particle energy gain in the parameter region $f > 1$ and $f - 1 > 0$.

In this work, the effect of fast variations has been taken into account in describing the lab variables (Δ, ξ) to first order, by retaining the corresponding terms in the expression Eq.(5.42) and Eq.(5.44). The evolution of the phase averaged variables $(\bar{\Delta}, \bar{\xi})$ in terms of which the lab variables have been described in Eq.(5.42) and Eq.(5.44) are governed by Hamilton$'$s equation corresponding to the phase averaged Hamiltonian given by Eq.(5.40). The earlier analytical work does not take into the account contribution from the fast dynamics and hence corresponds to the zeroth order of the present work. In the following figures Fig.(5.1) and Fig.(5.2) the final numerical energy gain by the particle has been compared with analytical results as a function of parameter "f" for fixed laser pulse lengths at different intensities and vice-versa. The final energy gain by the particle as function of the laser intensity in the region $f > 1$ and $f - 1 > 0$ has been described in the Fig.(5.3). The aim of this parametric study is to determine the optimum values of pulse length and laser intensity for adiabatic estimation of particle energy.

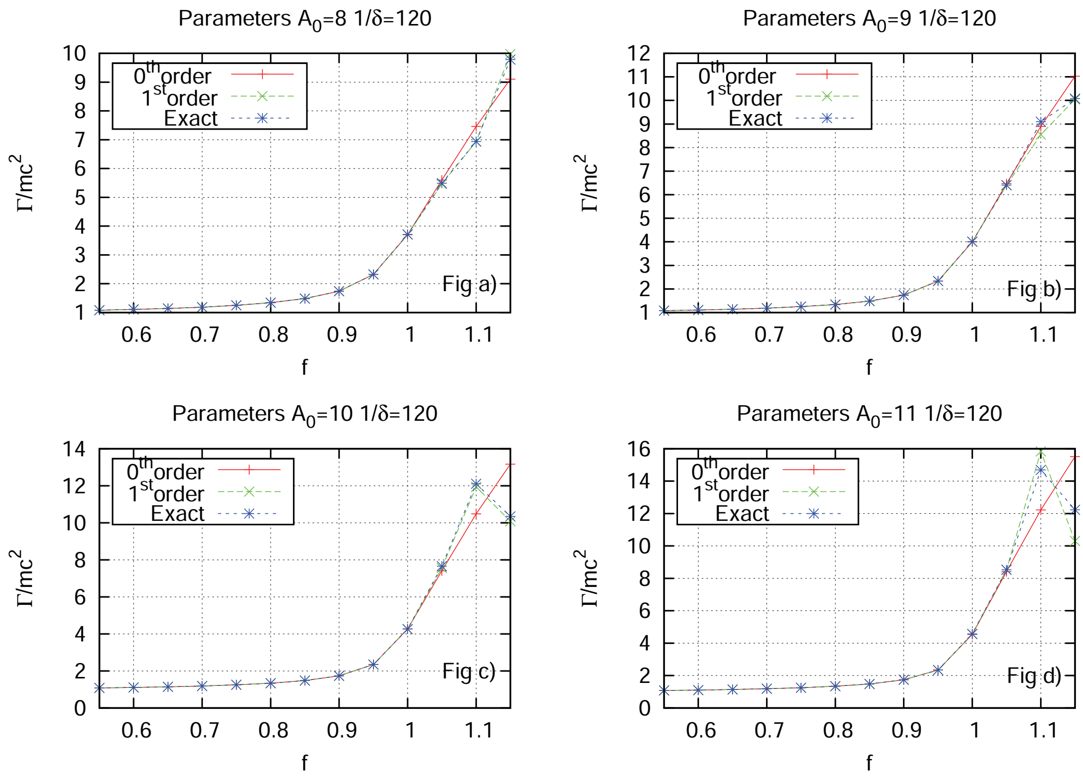

Figure 5.1: Numerically obtained final energy gain of the particle is compared with analytical results. The parametric study is for the final energy gain of the particle as function of variable "f", at different peak laser intensities A_0^2 for a fixed pulse length of laser$(1/\delta)$.

In Fig(5.1), the numerical results of the parametric study are plotted to depict the dependence of final energy gain by the particle on parameter "f" for different laser intensities and at same values of parameter delta $(\delta(= \lambda/L))$. On comparing the analytical and numerical results it can be seen that, their is smooth dependence of final particle energy gain on parameter "f" at lower intensities and for $f \leq 1$, which is as per the predictions of zeroth order theory. However comparing the analytical results with the numerical results in the subplots (a-b-c-d) of above figure, it can be seen that, their is difference in the zeroth order analytical and numerical results in the regime $f > 1$, which increases further with the laser intensity. The difference in the numerical and zeroth order adiabatic results can be attributed to the fast quiver motion, which becomes significant in the forward energy gain due to the increase in gyration length of the particle. The results of first order in terms of parameter "ϵ" are found to give better estimates to the numerical results. Thus it can be inferred that the inclusion of the fast dynamics which suitably takes into account the information of phase results in improved analytical energy estimates by providing information about the point of termination of pulse particle interaction.

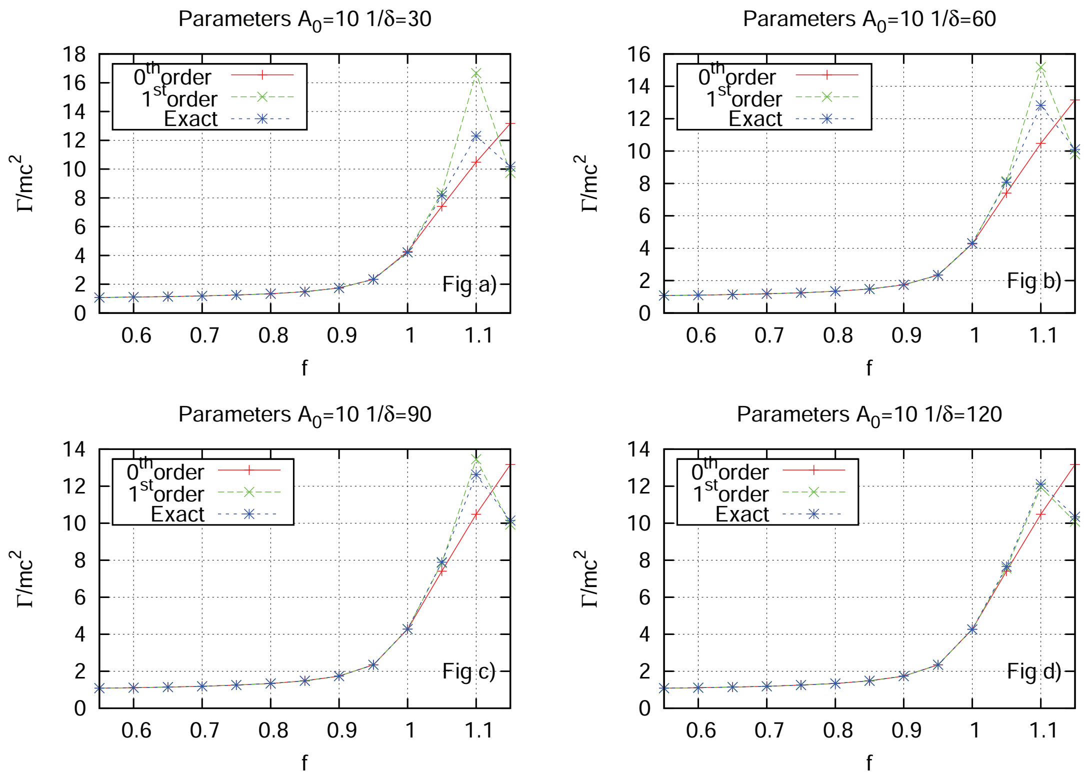

Figure 5.2: Numerically obtained final energy gain of the particle is compared with analytical results. The parametric study is for the final energy gain of the particle as function of variable f, for different pulse lengths $1/\delta$, keeping the peak laser intensity fixed.

In Fig(5.2), the dependence on energy gain on parameter "f" has been plotted for different delta $(1/\delta)$ values by keeping the laser intensity A_0^2 constant. The following observations can be made from the above figure; on comparing the numerical and analytical results, it is evident that for a given laser intensity, their is no significant improvement in the final energy gain of particle by changing the pulse length $(1/\delta)$. In $(f-1) > 0$ and $f > 1$ regime, the zeroth order analytical results are unable to give the numerical estimate of the particle energy gain for different pulse lengths. The matching between the analytical and numerical results improve on taking the first order corrections into account. The analytical estimation for first order adiabatic theory is better for the longer pulse($1/\delta$»1) as compared to shorter pulse. Thus it can be summarized that the results improve on taking the first order corrections into account and the analytical results have better agreement with the numerics for longer pulses, which have smaller initial value of adiabaticity parameter (ϵ).

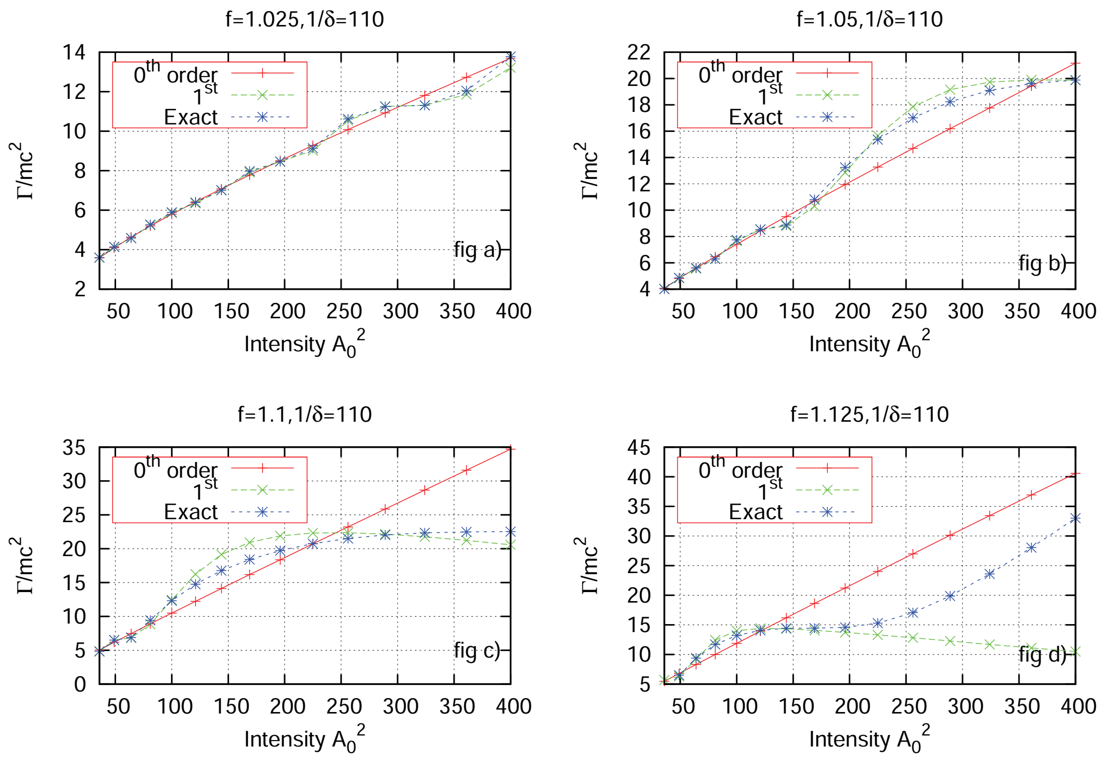

Figure 5.3: Parametric study for particle energy gain as a function of peak laser intensity A_0^2, at different values of f and fixed value pulse length$(1/\delta)$.

In Fig.(5.3), the final energy gain of the particle is studied as function of laser intensity A_0^2 for a given value of the parameters f and δ. It is evident from the results that the energy gain depends upon the laser intensity and there is a regime in which the energy gain increases linearly with laser intensity. For the linear regime the energy gain for a given laser intensity is higher for larger values of parameter f. In subplot (5.3b), the initial energy gain scales as $\sim (f-1)A_0^2/f^2$ which is in close agreement with the previous results Kaw *et al.* [46]. On further increasing the laser intensity the gain no longer remains linear. By comparing the subplots(a,b,c,d) in Fig.(5.3), it is evident that for higher values of f, the disagreement between the analytical prediction and exact numerical results begins at the lower values of intensity A_0^2. This is so because with increase in the value of f, the scale length of intensity variation reduces as result $\epsilon \sim 1$. Thus the adiabatic condition becomes harder to satisfy and the gain cannot be predicted using adiabatic theory.

5.5 Summary And Conclusions

Particle motion has been studied in the inhomogeneous laser field utilizing the canonical transformation and the method of Lie transform. An adiabatic formalism is developed for studying the effect of slow and gradual perturbation of the particle motion in the laser field. It is used to construct and calculate higher order approximations of adiabatic invariants for the near-integrable Hamiltonian system. For a slow variation in the laser intensity which corresponds to $\epsilon << 1$, the particle dynamics is associated with an adiabatic invariant. The dynamical variables i.e, particle position and momentum, are described by one of the constants of motion and the adiabatic invariant. It is found that for the present problem the adiabatic invariant evolves and the Hamilton's equation describing its evolution cannot be solved exactly in the given form. The evolution is obtained by transforming the old variables to the new variables in terms of which the Hamiltonian takes a simple form. By solving the corresponding Hamilton's equations and carrying out an inverse transformation, the evolution of the adiabatic invariant is found.

The transformations are carried out by using the Lie-generator which are derived and represented in the form of an asymptotic series of Poisson brackets in the powers of adiabaticity parameter ϵ. The representation in terms of the Poisson brackets makes the transformations generated by these operators canonical. The method described here is general and can be extended for the calculation of higher orders. The new set of phase averaged slow variables are derived by the operation of forward Lie-operator T and are in the form an asymptotic series in powers of the adiabatic parameter in terms of old co-ordinates. These series describing the transformed variables are non-convergent, requires higher orders of ϵ, which fully diverge in the limit $\epsilon \approx 1$. In terms of these phase averaged variables the form of the Hamiltonian is simplified and thus the Hamilton's equations are simpler to solve. The inverse transformation are derived using the inverse Lie-operator T^{-1} transforming the phase average variables to the lab variables. The evolution of the new phase averaged variable and the application of inverse transformation gives the desired solution.

Further, the adiabatic theory is used to estimate the energy gain of the particle in the field of focused finite duration pulse. It is shown that such an acceleration scheme can be used to generate electrons in the MeV range. The theoretical predictions on the basis of newly formulated adiabatic theory are in good agreement with the results obtained by solving the exact equation of motion. It is shown that in a process of continuous energy gain the gyration length can become of the order of scale length of intensity variation. This corresponds to a non-adiabatic limit (i.e $l_g \sim l_n$ is $\epsilon \approx 1$), beyond which the energy gain is non-adiabatic and can not be estimated by adiabatic theory.

6

Particle acceleration by cyclotron Auto-Resonance with a focused finite duration laser pulse

In this chapter a new scheme is described for accelerating the charged particle in vacuum. In this scheme the particle is subjected to the combined field of a focused finite duration laser pulse and static axial magnetic field.

6.1 Introduction

The previous chapters from (3-5) of the thesis have been devoted to the comprehensive theoretical study of different schemes of particle acceleration in vacuum. These studies provide deeper physical insight into the underlying mechanisms of the corresponding schemes, which in turn helps in further improving the existing schemes as well as in devising the newer schemes for particle acceleration.

In this context chapter-3, has been devoted to the theoretical study of auto-resonant scheme of particle acceleration in vacuum using a homogeneous finite duration laser pulse. In the auto-resonant acceleration scheme the particle is subjected simultaneously to the combined field of laser as well as static axial magnetic field and the particle acceleration is achieved as a result of self sustained resonance between laser frequency and cyclotron frequency. The condition for the self sustained resonance is given by $\omega - \vec{k}.\vec{v} = \frac{\Omega_c}{\Gamma}$, where Ω_c is the cyclotron frequency, Γ is the relativistic factor and "ω" is the laser frequency. For a finite duration laser pulse, it is well known that the frequency spectrum has a continuum in the Fourier space and the width of the spectra is inversely proportional to the length of the laser pulse. Thus for a given finite duration laser pulse with a fixed amplitude, particle with variable energies can be generated by tuning the cyclotron frequency of the particle with a characteristic frequency in the spectrum of the pulse. The energy spectra of the particle has a finite width and is shown to be continuous in parameter "$r(=\frac{\Omega_c}{\omega\Delta})$", where $\Delta(=\Gamma-P_x)$ is one of the constant of motion associated with particle dynamics in homogeneous laser field. The resonant time of interaction between the particle and laser is found to be finite. It has been shown from the study[45], that the resonant energy gain by the particle can be optimized in terms of laser intensity (A_0^2), length of the laser pulse ($1/\delta$) and cyclotron frequency (Ω_c) of the particle. The optimization can be done in a following way: In order for a particle to gain desired amount of energy it has to be accelerated which can be done by using an ultra intense very short duration laser pulse of large spectral width; this reduces the requirement of the static axial magnetic field. Alternatively, same energy gain can be achieved using a less intense but a long duration laser pulse which has the cyclotron resonant frequency of the order of central frequency. This increases the requirement of the static axial magnetic field which needs to be of the order of laser field.

An alternate scheme of direct particle acceleration has been described in chapter-4[46] and chapter-5[105], in this scheme the particle is subjected directly to the focused field of a laser. A slow spatial modulation in the laser intensity along the direction of its propagation is used to model the focused laser field. The particle is accelerated as a result of asymmetry in the electro-magnetic fields of a laser caused due to its focusing. In the focused laser field the intensity (or the fields) is strongest near the focus and decreases in moving away from it on the either side. The particle acceleration takes place in the de-focused region, in which the particle is initially accelerated along the electric field component of the laser near the focus and as result of $\vec{v}\times\vec{B}$ force, it is pushed away from the focus; far from the focus, the electric field of laser is weak and thus is not able to extract the energy back from the particle. As result the net energy is transfered to the particle along the direction of propagation of the laser. In this study, the optimum conditions resulting in the maximum energy gain are obtained in terms of initial position and parameter "$f(=\frac{A_0^2}{\delta F})$", defined in terms of peak laser intensity(A_0^2), pulse length ($1/\delta$)and focal length of the particle(F). It has been shown that in order to maximize the energy gain the particle should initially be placed at the focus and the parameter "f" should be given by "$f \geq 1$".

In this chapter a new scheme is described for accelerating the charged particle in vacuum, this scheme is based upon the above described schemes of particle acceleration. In this scheme the particle is subjected to the combined field of a focused finite duration laser pulse and homogeneous static axial magnetic field. The focused field of a laser pulse is described by a slow spatial variation in laser intensity along the direction of pulse propagation. The study is intended to understand the dynamics of a particle in such an arrangement and to determine its effect on the resultant energy gain by the particle. It is further to be explored that whether the new schemes can be optimized in terms of various parameters such as pulse length($1/\delta$), peak laser intensity(A_0^2), parameter "f" and static axial magnetic field (or initial cyclotron frequency) to maximize the energy gain by the particle.

The organization of the chapter is the following: In section(6.2), the relativistic equation of motion is described which governs the motion of the particle in the combined field of a focused laser field and static axial magnetic field. The constants of motion associated with the particle dynamics are derived from the equation of motion. Section(6.3), contains the results obtained by numerically solving the equation of motion. Section(6.4) contains the summary of the work and conclusions of the work.

6.2 Particle Dynamics In Combined Field Of Focused Laser Pulse And Static Axial Magnetic Field

A linearly polarized focused finite duration laser pulse traveling along $\hat{x}$ direction in the presence of a constant homogeneous axial magnetic field can be described by following vector potential,

$$\vec{A} = \left(A(\epsilon x)\Theta(\delta(\xi))P_1(\xi) - \frac{B_0 z}{2} \right) \hat{y} + \frac{B_0 y}{2}\hat{z} \tag{6.1}$$

where the symbols represents the following: $\xi = (\omega t - kx)$ is the phase of the laser, $\Theta(\delta\xi) = exp(-\frac{(\delta\xi)^2}{2})$ is pulse envelope, $P_1(\xi)$ is the oscillatory part, factor $\delta(= \frac{\lambda}{L})$ is ratio of the laser wavelength to the pulse length, B_0 is the magnitude of the external magnetic field.The focused field of the laser can be described by slow spatial variation in the laser intensity which is given by,

$$A^2(\epsilon x) = Ff\delta(1 \pm \tfrac{x}{F}) \text{ for } x \lesseqgtr 0;$$

The peak laser intensity is given by $A_0^2 = Ff\delta$ at the focal point.

The electric and magnetic fields corresponding to the above described vector potential of the laser are defined as,

$$\vec{E} = -\frac{1}{c}\frac{\partial \vec{A}}{\partial t} \qquad\qquad \vec{B} = \nabla \times \vec{A}. \tag{6.2}$$

The variables can be expressed in the dimensionless form by using the following normalizations: $\vec{r} \to k\vec{r}, t \to \omega t, \vec{P} \to \frac{\vec{P}}{mc}, \Gamma \to \frac{\Gamma}{mc^2}, B \to \frac{qB}{m\omega c}, E \to \frac{qE}{mc\omega}, \hat{A} \to \frac{eA}{mc^2}, \Omega_c \to \frac{qB_0}{mc\omega}$.

The normalized relativistic momentum and energy equation are given by,

$$\frac{d\vec{P}}{dt} = [\vec{E} + \frac{\vec{P}}{\Gamma} \times (\vec{B} + \vec{\Omega}_c)] \tag{6.3}$$

$$\frac{d\Gamma}{dt} = \frac{\vec{P}.\vec{E}}{\Gamma} \tag{6.4}$$

Here Γ is the relativistic factor defined as,

$$\Gamma = (1 + P_x^2 + P_y^2 + P_z^2)^{1/2}$$

and P_x, P_y, P_z are the four momentum components. On re-writing the equations in component form,

$$\frac{dP_x}{dt} = -\frac{P_y}{\Gamma}\left(\frac{\partial A_y}{\partial \xi} + \epsilon\frac{\partial A(\epsilon x)}{\partial(\epsilon x)}\Theta(\delta(\xi)P_1(\xi))\right) \tag{6.5}$$

$$\frac{dP_y}{dt} = -\frac{(\Gamma - P_x)}{\Gamma}\frac{\partial A_y}{\partial \xi} + \frac{P_z\Omega_c}{\Gamma} \tag{6.6}$$

$$\frac{dP_z}{dt} = -\frac{P_y\Omega_c}{\Gamma} \tag{6.7}$$

$$\frac{d\Gamma}{dt} = -\frac{P_y}{\Gamma}\frac{\partial A_y}{\partial \xi} \tag{6.8}$$

On expressing the above equations Eq.(6.5) to Eq.(6.8) in terms of laser phase ξ and using $\dot{\xi} = \Delta(= \Gamma - P_x)$, components of particle momentum takes the following form,

$$P_y = \alpha_1 - A_y + z\Omega_c \tag{6.9}$$

$$P_z = \alpha_2 - y\Omega_c \tag{6.10}$$

where α_1 and α_2 are constants of motion which correspond to the conservation of transverse canonical momenta. It is shown above, that in the presence of a slow spatial variation in laser intensity along the direction of propagation, the particle dynamics is associated with two constants of motion.

The longitudinal component of the particle′s momentum and its energy are given by,

$$P_x = \frac{1-\Delta^2}{2\Delta} + \frac{P_y^2 + P_z^2}{2\Delta} \tag{6.11}$$

$$\Gamma = \frac{1+\Delta^2}{2\Delta} + \frac{P_y^2 + P_z^2}{2\Delta} \tag{6.12}$$

The position of the particle can be obtained solving the following equations,

$$\frac{dx}{d\xi} = \frac{P_x}{\Delta} \tag{6.13}$$

$$\frac{dy}{d\xi} = \frac{P_y}{\Delta} \tag{6.14}$$

$$\frac{dz}{d\xi} = \frac{P_z}{\Delta} \tag{6.15}$$

On subtracting the Eq-(6.5) and Eq-(6.8), it can be seen that in the presence of an inhomogeneity in a laser field, the variable "Δ" is no longer an exact constant of motion. However, it has been shown earlier in chapters '4' and '5' of the thesis, that for a slow spatial variation the variable "Δ" acts as an adiabatic invariant and its evolution is described by the following equation,

$$\frac{d\Delta}{dt} = -\epsilon \frac{P_y}{\Gamma} \frac{\partial A(\epsilon x)}{\partial(\epsilon x)} \Theta(\delta(\xi)) P_1(\xi). \tag{6.16}$$

The above derived equation (6.16) for an adiabatic invariant depends upon the longitudinal position of a particle. The expression for the longitudinal particle position can be derived using Eq-(6.11) and Eq-(6.13). The coupled set of differential equations describing the evolution of an adiabatic invariant and corresponding the longitudinal particle position expressed in terms of variable 'ξ' are given by,

$$\frac{d\Delta^2}{d\xi} = -2\epsilon P_y \frac{\partial A(\epsilon x)}{\partial(\epsilon x)} \Theta(\delta(\xi)) P_1(\xi) \tag{6.17}$$

$$\frac{dx}{d\xi} = \frac{1-\Delta^2}{2\Delta^2} + \frac{y^{'} + z^{'}}{2\Delta^2} \tag{6.18}$$

In the above expression $y^{'}$ and $z^{'}$, are the derivatives of the particle position w.r.t to variable 'ξ' and it is evident from these expressions, that the longitudinal particle position depends upon the transverse co-ordinates. The evolution of the particle along the transverse co-ordinates can be derived by using Eq-(6.9) and Eq-(6.10) representing the transverse particle position. As result of the axial magnetic field, the particle carries out a cyclotron motion in the transverse plane and is described by a set following coupled differential equations,

$$\frac{d^2y}{d\xi^2} + r^2 y = r\frac{\alpha_2}{\Delta} - \frac{1}{\Delta}\frac{dA_y}{d\xi} \tag{6.19}$$

$$\frac{d^2z}{d\xi^2} + r^2 z = -r\left(\frac{\alpha_1}{\Delta} - \frac{A_y}{\Delta}\right) \tag{6.20}$$

where $r(\epsilon x) = \frac{\Omega_c}{\omega\Delta}$.

The above described equations Eq-(6.19) and Eq-(6.20) for the cyclotron motion of a particle in turn depends upon the adiabatic invariant. Therefore solution of Eq-(6.17 to 6.20) is required to determine the complete particle dynamics in the combined field of a focused finite duration laser pulse and static axial magnetic field. The unmagnetized motion of the particle described earlier in chapter four of thesis, corresponds to setting variable "$r = 0$", which reduces the set of four differential equations to a set of two differential equations for particle position and adiabatic invariant.

It is evident from the above equations, that the analytical work described in chapter '4' for the evolution of an adiabatic invariant using a slow set of equations can not be carried out for the present set of equations. This difficulty arises because of the complicated expressions resulting from the solutions of equations Eq-(6.19) and Eq-(6.20) which cannot be simply segregated into the slow and fast motion. However, it is worthwhile to examine these equations closely, as the equations Eq-(6.17 to 6.20) provides a physical insight into the mechanism of particle acceleration. It can be seen that in the typical case of forward acceleration i.e particle moving the de-focused laser field, the value of adiabatic invariant "Δ" decreases. The decrease in the value of variable "Δ" results in the initial energy gain by the particle from the focused laser field which in turn changes the ratio "r ". This increase in the value of variable "r " leads to the matching of the particle cyclotron frequency with a characteristic frequency in the laser spectra. Thus the initial energy gain by the particle drives the non-resonant particle to resonance with the laser field and the combined action of laser focusing and axial magnetic field increases the efficiency of this scheme for accelerating the particles.

As pointed out above the complicated structure of the transverse co-ordinates limits the adiabatic analytical analysis of the problem. Thus in the present work the exact relativistic equation of motion given by Eq-(6.3) is numerically solved and results of the parametric study has been presented in the next section.

6.3 Numerical Results

This section contains the results of the parametric study obtained by numerically solving the exact equation of motion using R-K(Runge-Kutta) method for a particle subjected to the combined field of a focused finite duration laser pulse and static axial magnetic field.The study is intended to determine the simultaneous effect of focusing and axial magnetic field on the particle dynamics, which can be used for optimizing the parameters to maximize the energy gain. In this work a slow linear spatial modulation in the laser intensity along the direction of propagation is used to describe the focused laser field. In this numerical study the particle is initially placed at the focal point which corresponds to the optimized position for maximum energy gain by the particle. The particle is assumed to be at rest before the onset of the interaction and it interacts with rising edge of the laser pulse. In this study the laser intensity as well as pulse length are kept constant.

In order to understand the simultaneous effect of the laser focusing and axial magnetic field, the study has been carried out in two parts. In the first part the particle energy gain is studied as a function of the focusing parameter "$f(=\frac{A_0^2}{\delta F})$" for different cyclotron frequencies of the particle. The aim of study is to determine the effect of the axial magnetic field on the energy gain by the particle in a focused laser field. The results of this study provides a detailed information of the focusing parameters for maximum energy gain by the particle.

In the second part the optimum values of the focusing parameter 'f' obtained in the first part are used for studying the particle energy gain as function of the cyclotron frequency of the particle. This study is aimed to determine the effect of laser focusing on the energy gain by the particle in the lower cyclotron frequency (or low axial magnetic field) range, which lies outside the characteristic frequency spectrum of the laser pulse. In this study the final energy gain by the particle is studied as the function of cyclotron frequency for different values of focusing parameter. The results of above two studies are combined to determine the optimum parameters in terms of focused laser field ("f") and static axial magnetic field (Ω_c). These results have been used further to optimize the conditions for maximum energy gain by the particle.

The results of numerical study, describing the resonant energy gained by the particle as function of parameter "f" are described in Fig(6.1). These results are obtained by keeping laser parameters (viz. peak laser intensity and pulse length) constant and varying the strength of static axial magnetic field. The resultant energy gain by the particle in the field of a focused laser pulse are compared with an un-magnetized case described in subplot-a of the figure, in which the energy gain begins at the values of parameter $f \geq 1$. The results of energy gain by the particle by focused laser field in the presence of an axial magnetic field are subplots-(b-c-d-e-f) and in these subplots the strength of axial magnetic field increases in going from subplot(b-f). From the results, it is evident that the particle energy gain improves on increasing the strength of axial magnetic field(or initial cyclotron frequency). The other important observation can be made from these results are that the energy gain of the particle can be significantly increased for a given value of parameter "f" by increasing the applied axial magnetic field and the energy gain starts at lower values of parameter "f".

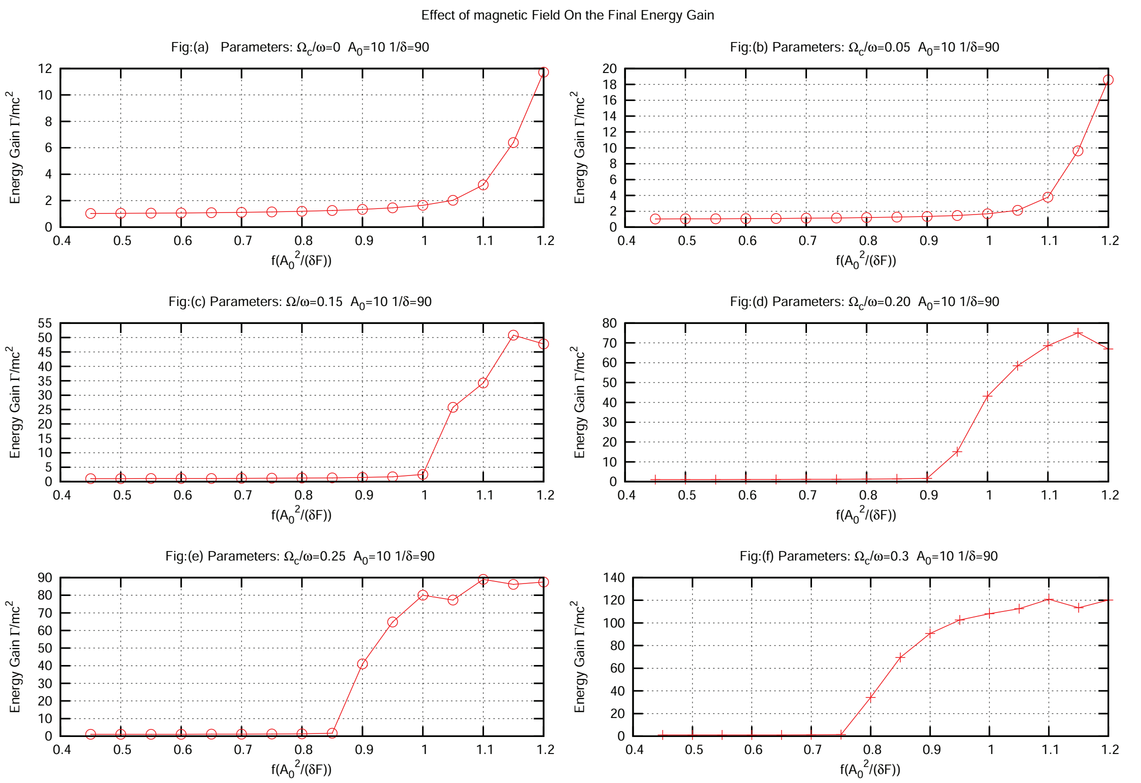

Figure 6.1: Resonant energy gain by the particle as a function of focusing parameter "f"

The next part of the study given in Fig(6.2), it is aimed at exploring the dependence of particle energy gain as function of the cyclotron frequency for fixed focusing parameters. In this study the laser parameters i.e, the intensity as well as pulse length are again kept constant. The energy gain by the particle is obtained as function of cyclotron frequency at different values of parameter 'f'. It is evident from the plot, that as a result of focusing the energy gain by the particle starts at the lower cyclotron frequencies. On comparing the results, it is further shown that the resonant energy gain by the particle depends upon the parameter 'f ' and for higher values of variable 'f ', the energy gain extends for very low cyclotron frequencies. Thus it can be inferred that initial energy gained by the particle as a result of tight focusing improves the energy gain as well as leads to the significant lowering the value of applied axial magnetic field.

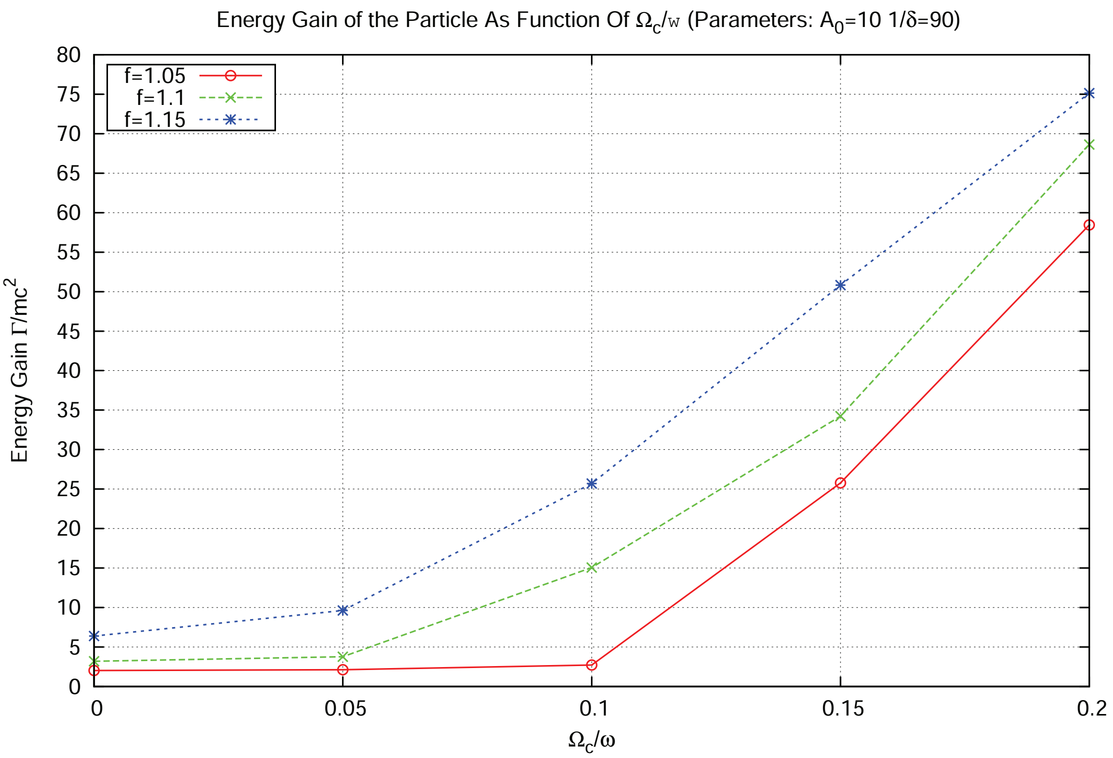

Figure 6.2: Resonant energy gain by the particle as a function of the initial cyclotron frequency of the particle Ω_c for fixed value of focusing parameter

From the above results, it can be concluded that the particle gains energy in the parameter limit $f \geq 1$ of the focused laser pulse which can be further improved to one order higher and using static axial magnetic field one order lower than the magnetic field of the laser. In the last part of the simulation, the scaling of particle energy gain with the laser intensity is shown in the Fig(6.3). The energy gain is obtained for the cyclotron frequency much smaller than the central frequency and by varying the values of parameter "f". The fitting function along with the parameters is shown in the figure. It is evident from the values of fitting parameter (c1-c2-c3-c4) in the figure, that the energy gain by the particle scales linearly with the peak laser intensity of the laser pulse.

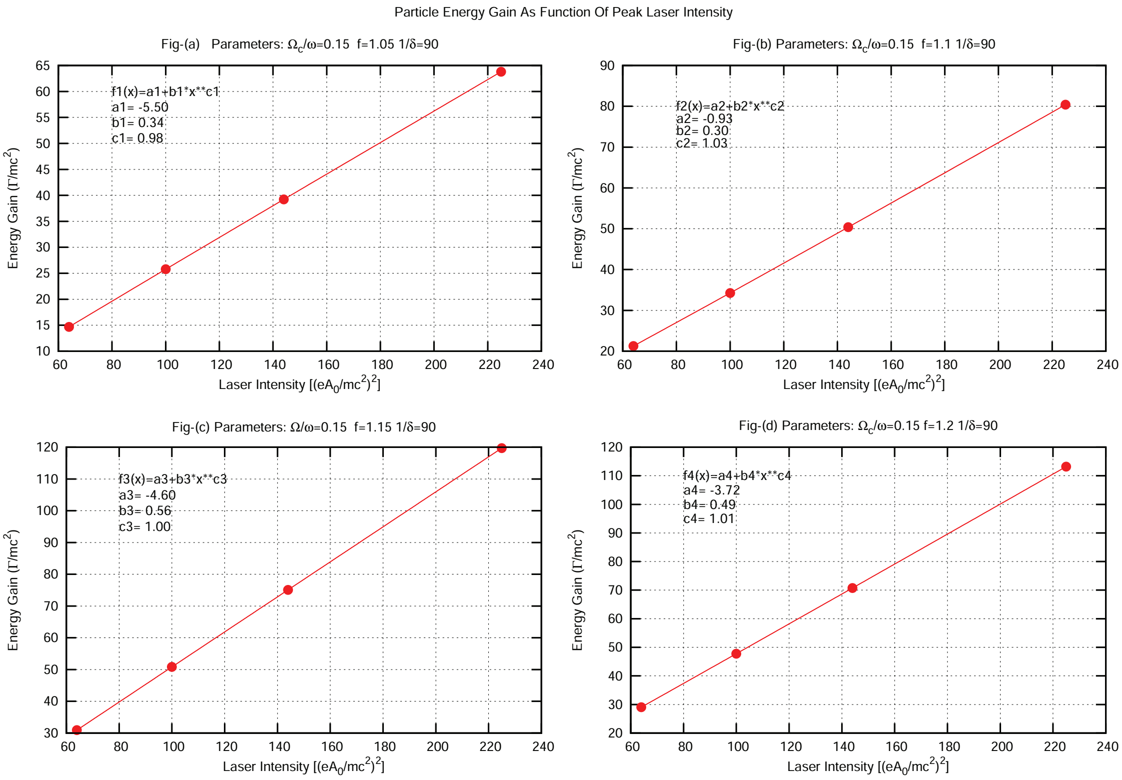

Figure 6.3: The resonant energy gain by the particle as function of laser intensity at different values of the focusing parameter "f"

6.4 Summary and Discussion

A new scheme based upon the auto-resonant acceleration scheme and direct laser scheme is presented in this chapter. In this scheme the particle is subjected to the combined field of a focused finite duration laser pulse. The dynamics of the particle in this configuration is studied by solving the relativistic equation of motion numerically. The parametric study is aimed to determine the optimum conditions for maximum energy gain by the particle. The study is carried in two steps at first the effect of magnetic field is studied on the particle dynamics in the focused laser pulse. It has been shown that the energy gain by the particle improves significantly with the increase in the value of axial magnetic field. On increasing the value of the axial magnetic field the energy gain begins at lower values of the parameter "f". These results provide the optimum focusing conditions in the presence of the magnetic field for the maximum energy gain of the particle. This study is used to determine the dependence of the resonant energy gain by the particle as function of cyclotron frequency. It has been shown that the for the value of parameter $f \geq 1$, the energy spectra of the particle as function of the initial cyclotron frequency is significantly broadened and as a result the energy gain is significantly improved at the lower values of the initial cyclotron frequency. These results are used to further optimize the energy gain by the particle.

The above numerical results can be understood by analyzing the equations describing the cyclotron motion of the particle together with equation of the evolution of the adiabatic invariant. It can be seen from these equations that this mechanism acts as a two step process in which the initially non-resonant particles i.e whose cyclotron frequency lies outside the characteristic frequency spectrum of the laser pulse, are accelerated by the focused laser field. The initial energy gain by the particle in the focused laser field drives the particle to the cyclotron resonance with the laser pulse. The combined effect of the two step results in large acceleration of particles.

In this process, as stated above the initial energy gained by the particle reduces the magnitude of laser intensity and axial magnetic field value required for particle acceleration as compared to un-focused case. This overall reduction in required laser intensity and axial magnetic field makes this scheme an efficient mechanism for accelerating the charged particle to large energies.

7 Conclusions and Future Work

This chapter contains the summary and major conclusions of the work reported in the various chapters. The outline of the future works has also been described at the end of the chapter.

7.1 Summary and Conclusions

The laser driven acceleration of a charged particle in vacuum has been a topic of great interest, which provides a compact as well as cheaper alternative to conventional accelerators. A number of theoretical studies on the topic have been reported spanning over several decades and the recent impetus to the topic is due to the advent of CPA technique, which has led to the availability of high powered table top lasers for the experimental realization of these schemes. The motion of a particle in these lasers become relativistic within one laser period and thus requires a deeper insight into the mechanism of fundamental interaction between the laser and particle in vacuum. This understanding of the interaction forms the basis for devising various schemes of particle acceleration in vacuum. This thesis is devoted to the theoretical study of laser driven acceleration of charged particle in vacuum. In this thesis, following two schemes of particle acceleration namely: "Laser Driven Auto Resonant Acceleration" and "Direct acceleration of particle by focused laser fields" have been studied both analytically as well as numerically. From different studies, it is found that these schemes have relatively higher rates of acceleration compared to other the schemes. It has been further shown that, these two schemes can be easily combined to enhance the efficiency of acceleration process. The chapter wise summary of the work and main conclusions are given below.

In chapter two, the physical aspects of particle dynamics in the field of a relativistically intense homogeneous, continuous as well as pulsed laser are studied by solving the exact relativistic equation of motion and also the corresponding Hamilton-Jacobi equation, which encompasses the review of several previous works on the topic. The motion of charged particle in a relativistically intense laser field is a fully integrable problem due to the presence of three exact constants of motion corresponding to its three degrees of freedom. The exact analytical expressions for the dynamical variables viz. position, momentum as well as energy are expressed in terms of constants of motion and vector potential only. Further, a set of exact expressions for the dynamical variables in the field of a finite duration laser pulse has been reported for the first time corresponding to the $Gaussian$ and $Sech$ shaped temporal envelopes, which gives unambiguous comparison between numerical and analytical results.The exact analytical expressions derived for a continuous laser have been used to study the particle dynamics in the 'average rest' and 'Lorentz boosted' frame of reference, which further improves the understanding of the particle dynamics. From the analytical and numerical study it has been shown that, in the continuous laser, the interaction of charged particle with a relativistically intense laser does not result in the net transfer of energy from the laser to the particle. The particle gets displaced along the direction of propagation of laser and the displacement of a particle found to be proportional to the laser intensity. The results are even valid for a finite duration laser pulse which includes the light pressure effects, due to which the particle is symmetrically accelerated in the rising front of the pulse and symmetrically decelerated in the trailing edge in a process getting displaced along the direction of propagation.

In chapter three, the particle dynamics has been analytically and numerically studied for the first time using a Gaussian shaped temporal envelope in the combined field of a finite duration laser and static axial magnetic field. This interaction forms the basis for laser driven auto-resonant scheme of charged particle acceleration in vacuum. The renewed interest in this scheme is due to the availability of high powered lasers as well as experimental generation of ultra high quasi-static magnetic fields of the order of hundreds of mega-gauss, some of which survives for duration much longer than the laser pulse particle interaction time.

In this scheme, the initial laser particle resonance is itself sustained due to the precise cancellation of two relativistic effects associated with the particle dynamics namely:"relativistic mass effect " and "relativistic Doppler effect". The "relativistic mass effect" is caused due to the particle acceleration along the electric field component of the laser, which results in the lowering of its cyclotron frequency and the "relativistic Doppler effect" caused by the magnetic field of the laser along the direction of its propagation, as result of which the wave frequency as seen by the particle is lower than the actual frequency. Due to the cancellation of these two relativistic effects, the particle gets phase locked in the quasi-electrostatic field of a laser, which causes its continuous acceleration.

In contrast to the mechanism described above using a continuous monochromatic laser which has single frequency, the particle in the field of a finite duration laser pulse interacts with spectrum of frequencies and can be accelerated by the tuning its cyclotron frequency with the characteristic laser frequency in the spectra. It has been shown that the choice of Gaussian envelope gives unambiguous comparison between the analytical and numerical work in contrast to the earlier used Sin^2 envelope. From the study it has been shown that, the energy gain by the particle typically using a laser with wavelength $1 \sim \mu m$ is given by $\Gamma = 78.58 \times A_0^2 \times .511 Mev$ which can be optimized to lies in Mev-Tev range for an input peak laser amplitude in the range ($A_0 \sim 1, 10^2$), pulse duration($1/\delta \sim 5, 90$) and applied magnetic field in the range($\sim 100MG$). In the optimization process, the particles of given energy can either be generated using short duration($1/\delta \sim 5, 10$), higher powered lasers($10^{22} Wcm^{-2}$) with lesser axial magnetic fields($\sim 70, 80MG$) than that of laser or using lesser intense($10^{20} Wcm^{-2}$), longer laser pulses($1/\delta \sim 80, 90$) with higher axial magnetic field($\sim 100MG$) of the order of laser field. It has been further shown that for a given laser parameter viz, intensity, pulse length along with external axial magnetic field, the energy gain for a positively charged particle can be enhanced by changing the polarization of the laser. The energy gain is found to be maximum for the right circularly polarized laser field, which is approximately double than that for a plane polarized laser field and minimum for the left circularly polarized laser.

In chapter four, an another scheme has been described for accelerating the charged particle in vacuum by subjecting it directly to the focused laser field. The net transfer of energy from the laser to the particle in this scheme is due to an asymmetry in the acceleration and deceleration phase of the focused laser field. The electric as well as magnetic fields describing the focused laser grows stronger as one approaches the focus and grows weaker in moving away from the focal point. A considerable work has been done in this area, for the description of the fields, which has been subsequently used in the theoretical studies of the particle acceleration in the focused laser field. The main difficulty in the theoretical study of this scheme is the correct mathematical description of the complex configuration of the fields arising due to the focusing of laser, which in turn hinder's the analytical study of the particle orbits. Thus a simplified one dimensional model has been used to theoretically i.e. numerically as well as analytically study the particle dynamics in the focused laser field. In this study, optimum initial conditions for maximum energy gain by the particle are determined in terms of initial position, intensity and focal length using both continuous as well as finite duration laser field. From the results obtained by numerically solving the exact relativistic equation of motion and comparing them with the analytical results, it has been shown that the focal point is the optimum initial position for maximum energy gain. It has been further shown, that the energy gain by a particle increases linearly with the peak laser intensity, which can be analytically estimated in the adiabatic limit ($\epsilon(=\frac{l_g}{l_n}) << 1$), where l_g, is the particle gyration length and l_n, is the scale length of variation of inhomogeneity. For a finite duration laser, the particle energy gain has been studied as a function of parameter $f(=\frac{a_0^2}{\delta F})$ and it has been found that such an acceleration scheme using a laser with wavelength of the order of approx. ($\sim 1\mu m$) and having corresponding peak intensity in the range $10^{18}-10^{20}Wcm^{-2}$ of duration $1/\delta \sim [30, 120]$ cycles can be used to generate electrons in the MeV range. On comparing the numerical results with the analytical results, it has been found that in the region corresponding to ($f > 1$), the earlier derived adiabatic calculations does not provide the correct estimates of the energy gained by a particle. Hence an improved analytical theory is required to account for the energy gain by a particle.

In chapter five, a higher ordered adiabatic theory has been derived to study the motion of a charged particle in an inhomogeneous field of a relativistically intense laser field. The inhomogeneity in the laser field is due to slow spatial variation in laser intensity along the direction of propagation of the laser, which is a characteristic of focused and de-focused laser field. It has been shown that in the presence of such an inhomogeneity, the particle dynamics is devoid of one of the constants of motion associated with the symmetry of the particle dynamics in the one of the co-ordinates along the direction of propagation of laser($\hat{x}$) and time($\hat{t}$). As a result, the dynamical variables viz. position, momentum and energy cannot be expressed in terms of constants of motion as was possible for homogeneous case. In the thesis, it has been shown that for a slow perturbation which corresponds to ($\epsilon(=\frac{l_g}{l_n}) << 1$), the particle dynamics can be studied adiabatically by expressing the dynamical variables in terms of an adiabatic invariant and constants of motion. The higher orders of the invariance have been calculated using the method of Lie-transformation perturbation and canonical transformations in the powers of adiabaticity parameter(ϵ). Further, the adiabatic theory has been used to estimate the energy gain of the particle in the field of a focused finite duration pulse. The theoretical predictions on the basis of newly formulated adiabatic theory are shown to be in good agreement with the results obtained by solving the exact equation of motion numerically. It has been found that in a process of continuous energy gain the gyration length can become of the order of scale length of intensity variation. This corresponds to a non-adiabatic limit (i.e $\epsilon(=\frac{l_g}{l_n}) \sim 1$), beyond which the energy gain is non-adiabatic and can not be estimated by adiabatic theory.

In chapter six, a new scheme has been described for accelerating the charged particle in vacuum, this scheme is based upon the earlier described “laser driven auto resonant acceleration” and “acceleration by focused laser field” schemes of particle acceleration. From the study of above mentioned schemes it has been concluded that a particle with a desired final energy using a laser driven autoresonant acceleration scheme can be obtained in the following two ways: a) using lesser intense, long duration laser pulse with an axial magnetic field of the order of laser magnetic field or b)using short duration, ultra intense laser pulse with lower axial magnetic field. In the second acceleration scheme, in which the particle is subjected directly to a focused laser field, it has been shown that, the energy gain is maximum for a particle initially placed close to the focus and in the parameter regime ($f(=\frac{a_0^2}{\delta F})) > 1$) and ($f-1$) significantly greater than zero. These results have motivated for devising a scheme to further increase the efficiency of acceleration process and simultaneous reduction in the requirement of laser power as well as the axial magnetic field.

Thus in this scheme, the particle is subjected to a combined field of a focused finite duration laser pulse and homogeneous static axial magnetic field by assuming the particle to be initially at rest and placed closed to focal point. As earlier, a slow linear spatial modulation in the laser intensity along the direction of propagation has been chosen to describe the focused field. To understand as well as to optimize the acceleration scheme the study has been carried out in two steps at first, the effect of magnetic field has been studied on the particle dynamics in the focused field of laser pulse. It has been shown that the energy gain improves significantly with the increase in the value of axial magnetic field. Further, the energy gain begins at lower values of “f” with the increase in the value of the axial magnetic field. These results provide the optimum focusing conditions in the presence of the magnetic field for the maximum energy gain of the particle. In the second step, the energy gain of the particle is studied as a function of initial cyclotron frequency for values of “$f > 1$” and it has been shown that for fixed laser intensity, the energy gain for the magnetized case is greater than that of the un-magnetized case, which further improves with increase in the value of parameter “f”. Thus from these studies, it has been concluded that the combined effect focusing and magnetic field improves the efficiency of the scheme by increasing the energy gain as well as simultaneously reducing the requirement of peak laser intensity and axial magnetic field. The improved efficiency of the scheme is caused due to the initial energy gained by the particle from the focused field, which drives the initially non-resonant particle to the cyclotron resonance as a result, it gets further accelerated and thus improving the overall energy gain.

7.2 Future Directions

The results presented in this thesis illustrate several interesting physical phenomena and provide a basis for further investigations as direct extensions to this work. In this regard, some open problems are suggested below which can be addressed in the future.

1. From the study of particle acceleration schemes described in the thesis, it has been shown that in these schemes the resultant energy gain by the particle can be very large. The velocity of the particle corresponding to such

a large energy gain lies very close to the speed of light and at such a large velocities, the effect of self-force arising due to the radiation reaction can become important, which has been neglected in the present studies. However it is well known from the studies ref.[123, 124, 125] that, the correct mathematical description of the self-force at such a large velocities has been a topic of intense research in the classical electrodynamics. Thus it would be interesting to understand structure of the self-force arising due to radiation reaction and study its effect on the dynamics of a particle.

2. In the thesis, the study has been carried out using a single particle approach which represents an ideal situation corresponding to physical condition $\frac{\omega_p}{\omega} << 1$, where ω_p is the plasma frequency and ω is the laser frequency. It would be interesting to determine the limit of such an analysis for application to multi-particle systems in which the inter particle interactions can become significant and has its effect on the dynamics of the particle. Also one would like to study the particle dynamics taking into account the background effects arising due to the medium.

3. In this thesis, the particle acceleration in a focused laser field has been analytically studied using a simplified one dimensional focusing model. To this, an improvement can be carried out in the following two ways: Firstly, one would like to explore the feasibility of extending these analytical calculations to determine the energy gain of the particle with an improved model of focusing. Secondly, the another area of investigation as mentioned previously, in the thesis is the understanding and determining of the exact structure of electric and magnetic fields near the focus. This description is important for improving the understanding of the dynamics as well as in optimizing the conditions of maximum energy gain by the particle.

4. The other interesting area which can be looked upon, is analytical study of particle acceleration with chirped laser fields. In this scheme the frequency of the laser is varied in such a way that the particle remains in the accelerating phase of the laser and thus resulting in large energy gain.

A

Lie transform Perturbation Method

A.1 Lie Transformation Perturbation Method

The time evolution of any function $f(X,t)$ from $t_0 \to t$ is given by

$$f(X,t) = P_H(t_0 \to t) \circ f(X_0, t_0)$$

where $X_0 = X(t_0)$ are the initial conditions and $P_H(t_0 \to t)$ is the time evolution operator. The evaluation of $P_H(t_0 \to t)$, which is equivalent to solving the equations of motion, may not be possible for the original choice of variables. The Lie transforms theory is used to map the phase space in X onto the phase space spanned by the new set of variables Y. The canonical transformation $T(X,t)$ for this mapping is such that $Y = T(X,T).X$, where $T(X,t) = exp[-L(X,t)]$ with $L(X,t)$ being the lie operator. $L(X,t)$ is obtained from the generating rating function $w(X,t)$ such that $L.f = [w,f]_{PB}$ where $[,]$ denotes the Poisson brackets in X phase space. The transformation is chosen in such a way that the new Hamiltonian $\bar{H}(Y,t)$ with the corresponding time evolution operator $P_{\bar{H}}(t_0 \to t)$is easier to evaluate. An important and basic property of Lie transform operator is that it generates canonical transformations and that it commutes with any function of the space variables. The latter property implies that the evolution of $f(X_0,t_0)$ can be obtained by transforming to new variables set Y_0, applying the time evolution operator $P_{\bar{H}}(t_0 \to t)$ to the transformed function back to the original variables X,

$$f(X,t) = T(X_0,t_0) \circ P_{\bar{H}}(t_0 \to t) \circ T^{-1}(X_0,t_0) \circ f(X_0,t_0)$$

The above described procedure apart from being applicable to integrable systems, also serves as perturbation method for solving approximately near integrable systems in which the Hamiltonian has a small non-integrable part of the order of ϵ. In such cases the canonical transformation can be constructed as a power series of ϵ by utilizing the method of the Deprit [99, 100, 101, 102, 103, 104]. According to this method , the old Hamiltonian H, the new Hamiltonian $\bar{H}$ and the transformation generator T along with the Lie generator expanded in power series of ϵ and may be presented by

$$H = \sum_{n=0}^{\infty} \epsilon^n H_n \tag{A.1}$$

$$\bar{H} = \sum_{n=0}^{\infty} \epsilon^n \bar{H}_n \tag{A.2}$$

$$T = \sum_{n=0}^{\infty} \epsilon^n T_n \tag{A.3}$$

$$w = \sum_{n=0}^{\infty} \epsilon^n w_{n+1} \tag{A.4}$$

Where the expansion of w has been appropriately chosen in orders to generate the identity transformation $T_o = I$ to the lowest order.The n^{th} order forward and backward transformation generators are given by

$$T_n = -\frac{1}{n} \sum_{n=0}^{\infty} T_m L_{n-m} \tag{A.5}$$

$$T_n^{-1} = \frac{1}{n} \sum_{m=0}^{n-1} L_{n-m} T_m^{-1} \tag{A.6}$$

up to fourth order are given below

$$T_o = I \tag{A.7}$$

$$T_1 = -L_1 \tag{A.8}$$

$$T_2 = -\frac{1}{2}L_2 + \frac{1}{2}L_1^2 \tag{A.9}$$

$$T_3 = -\frac{1}{3}L_3 + \frac{1}{6}L_2L_1 + \frac{1}{3}L_1L_2 - \frac{1}{6}L_1^3 \tag{A.10}$$

The inverse operator is given by

$$T_o^{-1} = I \tag{A.11}$$

$$T_1^{-1} = L_1 \tag{A.12}$$

$$T_2^{-1} = \frac{1}{2}L_2 + \frac{1}{2}L_1^2 \tag{A.13}$$

$$T_3^{-1} = \frac{1}{3}L_3 + \frac{1}{6}L_1L_2 + \frac{1}{3}L_2L_1 + \frac{1}{6}L_1^3 \tag{A.14}$$

The equations providing the Lie generator w and the new Hamiltonian $\bar{H}$, to third order can derived from the general perturbation equation

$$\frac{\partial w_1}{\partial t} + L_1H_o = (\bar{H}_1 - H_1) \tag{A.15}$$

$$\frac{\partial w_2}{\partial t} + L_2H_o = 2(\bar{H}_2 - H_2) - L_1[\bar{H}_1 + H_1] \tag{A.16}$$

$$\frac{\partial w_3}{\partial t} + L_3H_o = 3(\bar{H}_3 - H_3) - L_1[\bar{H}_2 + 2H_2] - L_2[\bar{H}_1 + \frac{1}{2}H_1] - \frac{1}{2}L_1^2H_1\,\mathrm{e} \tag{A.17}$$

the general n^{th} order perturbation equation can be written as

$$\frac{\partial w_n}{\partial t} + L_nH_o = n(\bar{H}_n - H_n) - \sum_{m=1}^{n-1}[L_{n-m}\bar{H}_m + mT_{n-m}^{-1}H_m] \tag{A.18}$$

By selecting the arbitrary function $\bar{H}_m$ so that the angle independent part of the r.h.s is eliminated. Further for the case of adiabatic perturbation the Lie operator is separated in the form of fast and slow component. That is expressed in the following manner

$$L = L_f + \epsilon L_s \tag{A.19}$$

$$L_f = (\frac{\partial w_n}{\partial \xi}\frac{\partial}{\partial \Delta} - \frac{\partial w_n}{\partial \Delta}\frac{\partial}{\partial \xi}) \tag{A.20}$$

$$L_s = \sum_i [\frac{\partial w_n}{\partial(\epsilon q_i)}\frac{\partial}{\partial(\epsilon p_i)} - \frac{\partial w_n}{\partial(\epsilon p_i)}\frac{\partial}{\partial(\epsilon q_i)}] \tag{A.21}$$

here $w = w(\xi, \Delta, \epsilon p, \epsilon q, \epsilon t)$. As can be seen from the above expressions T_n^{-1} is given in terms of the coefficients of power series expansion of L_f and L_s as an n^{th} order polynomial in ϵ. The term $\frac{\partial w_n}{\partial t}$ in the nth-order perturbation equation is itself of the order ϵ : $\frac{\partial w_n}{\partial t} \rightarrow \epsilon \frac{\partial w_n}{\partial(\epsilon t)}$. One of the procedures for solving this equation is to expand w_n and $\bar{H}_n$ as power series in ϵ.

$$w_n = \sum_{k=0}^{\infty} \epsilon^k w_{nk} \tag{A.22}$$

and equate the like powers of ϵ. This gives a chain of equations which can be solved successively for $w_{n0}, w_{n1......}$. At each step in the chain, a corresponding $\bar{H}_{nk}$ is chosen to eliminate the secular term in the fast variable ξ. The method is equivalent to other methods of carrying out the averaging. It is systematic in that it automatically separates the fast and slow variables by order ϵ, thus allowing an average over the fast variable in any order to eliminate the secular terms.

Bibliography

[1] Strickland, and Mourou,G., Opt. Commun. **56**, 219 (1985).

[2] M. D. Perry and G. Mourou, Science **264**, 917 (1994).

[3] G. A. Mourou, C. P. J. Barty and M. D. Perry, Phys.Today **51**, 22 (1998).

[4] K.Shimoda, Appl. Opt. 1, **33** (1962).

[5] T.Tajima and J.M.Dawson, Phys. Rev. Lett. **43**, 267 (1979).

[6] M. O.Scully and M.S.ZUBAIRY, Phys. Rev. A **44**, 2656 (1991).

[7] T.Hauser, W.Scheid and H.Hora, Phys. Lett. A **186**,189 (1994).

[8] P.Sprangle, E.Esarey and J.Krall, Phys. Plasmas **3**,2183 (1996).

[9] G.Malka, E.Lefebvre and J.L.Miquel, Phys. Rev. Lett. **78**,3314 (1997).

[10] P.Mora and B.Quesnel, Phys. Rev. Lett. **80**, 1351 (1998).

[11] B.Quensal and P.Mora, Phys. Rev. E **58**, 3719 (1998).

[12] S.V.Bulanov and A.M.Prohorov, Plasma Physics and Controlled Fusion **48**,B29 (2006).

[13] Ujjwal Sinha, Phys. Plasmas 19, 043104 (2012).

[14] J. Krüger and M. Bovyn, J. Phys. A: Math. Gen. **9**, 1841, (1976).

[15] J.V. Shebalin, IEEE Trans. Plasma Sci., **16**, 390, June (1988).

[16] S. Acharya and A. C. Saxena, IEEE Trans. Plasma Sci. **21**, 257 (1993).

[17] L. D. Landau and E. M. Lifshitz, The Classical Theory of Fields, pp. 118, (Pergamon, Oxford, 1975).

[18] E. S. Sarachick and G. T. Schappert, Phys. Rev. D. **1**, 2738 (1970).

[19] J. N. Bardsley, B. M. Penetrante, and M. H. Mittleman, Phys. Rev. A, **40**, 3823, (1989).

[20] P. Gibbon, Short Pulse Interactions with Matter: An Introduction, pp. 31,(Imperial College, London, 2005).

[21] A. L. Galkin, V. V. Korobkin, M. Yu. Romanovsk, and O. B. Shiryaev, Phys. Plasmas **15**, 023104 (2008).

[22] J. H. Yang, R. S. Craxton and M. G. Haines, Plasma Phys. Control. Fusion **53**, 125006 (2011).

[23] A. A. KolomenskiiÏ and A. N. Lebedev, Dokl. Akad.Nauk SSSR **145**, 1259 (1962) [Sov. Phys. Dokl. **7**, 745 (1963)].

[24] A. A. KolomenskiiÏ and A. N. Lebedev, Zh. 'Eksp. Teor. Fiz. **44**, 259 (1963) [Sov. Phys.JETP **17**, 177 (1963)].

[25] V. Ya. DavydovskiiÏ, Zh. Éksp. Teor. Fiz. **43**, 886 (1962) [Sov. Phys. JETP **16**, 629 (1963)].

[26] V. P. Milant'ev, Usp. Fiz. Nauk **167**, 3 (1997) [Phys. Usp.40 , 1 (1997)].

[27] C. S. Roberts and S. J. Buchsbaum, Phys. Rev. A **135**, 381 (1964).

[28] A. Bourdier and S. Gond, Phys. Rev. E **62**, 4189 (2000).

[29] A. Bourdier and S. Gond, Phys. Rev. E **63**, 036609 (2001).

[30] Bao-Liang Qian, IEEE Trans. Plasma Sci. **27**, 1578 (1999).

[31] B.L. Qian, Phys. Plasmas **7**, 537 (2000).

[32] R. Ondarza and F. Gomez, IEEE Trans. Plasma Sci. **29**, 903 (2001).

[33] R. Ondarza and F. Gomez, IEEE Trans. Plasma Sci. **32**, 808 (2004).

[34] A. Loeb and L. Friedland, Phys. Rev. A **33**, 1828 (1986).

[35] A. Loeb, L. Friedland, S. Eliezer, Phys. Rev. A **35**, 1692 (1987).

[36] V. P. Milant'ev, Zh. Tekh. Fiz. **64**, 166 (1994) [Tech.Phys. **39**, 608 (1994)].

[37] V. P. Milant'ev, Usp. Fiz. Nauk **167**, 3 (1997) [Phys. Usp. **40**, 1 (1997)].

[38] Y. I. Salamin and F. H. M. Faisal, Phys. Rev. A **58**, 3221 (1998).

[39] Y. I. Salamin, F. H. M. Faisal, C. H. Keitel, Phys. Rev. A **62**, 053809 (2000).

[40] K. P. Singh, Phys. Rev. E **69**, 056410 (2004).

[41] F. H. M. Faisal and Y. I. Salamin, Phys. Rev. A **60**, 2505 (1999).

[42] Y. A. Salamin and F. H. M. Faisal, Phys. Rev. A **61**, 043801 (2000).

[43] A. Bourdier and D. Patin, Eur. Phys. J. D **32**, 361 (2005).

[44] Angus, Justin and Kraheninnikov,Sergei, Phys. Plasmas **16**, 113103 (2009).

[45] Vikram Sagar,Sudip Sengupta and P Kaw, Phys.Plasmas **19**, 113117 (2012).

[46] P. K. Kaw and R. M. Kulsrud, Phys. Fluids **16**, 321 (1973).

[47] L. Cicchitelli, H. Hora, and R. Postle, Phys. Rev. A **41**, 3727 (1990).

[48] L.C.Steinhauer and W.D.Kimura, J. Appl. Phys. **72**, 3237 (1992).

[49] B. Quesnel and P. Mora, Phys. Rev. E **58**, 3719 (1998).

[50] J. Pang, Y. K. Ho, X. Q. Yuan, N. Cao, Q. Kong, P. X. Wang, L. Shao, E.H. Esarey, and A. M. Sessler, Phys. Rev. E **66**, 066501 (2002).

[51] P. X. Wang, Y. K. Ho, X. Q. Yuan, Q. Kong, N. Cao, L. Shao, A. M.Sessler, E. Esarey, E. Moshkovich, Y. Nishida, N. Yugami, H. Ito, J. X. Wang, and S. Scheid, J. Appl. Phys. 91, **856** (2002).

[52] S. X. Hu and A. F. Starace, Phys. Rev. Lett. **88**, 245003 (2002).

[53] A. Maltsev and T. Ditmire, Phys. Rev. Lett. **90**, 053002 (2003).

[54] G. V. Stupakov and M. S. Zolotorev, Phys. Rev. Lett. **86**, 5274 (2001).

[55] Y.I.Salamin, G. R. Mocken, and C. H. Keitel, Phys. Rev. ST Accel. Beams **5**,101301 (2002).

[56] Yousef. I. Salamin and Christoph H. Keitel, Phys. Rev. Lett. **88**, 095005 (2002).

[57] S. G. Bochkarev and V. Yu. Bychenkov. Quantum Electron. **37**, 273 (2007).

[58] F. V. Hartemann, S.N. Fochs, G.P. Le. Sage, N.C. Luhmann Jr., J. G. Woodworth, M. D. Perry, Y. J. Chen and A. K. Kerman, Phys. Rev. E **51**, 4833 (1995).

[59] Y. I. Salamin, Z. Harman, and C. H. Keitel, Phys. Rev. Lett. **100**, 155004 (2008).

[60] A. L. Galkin, V. V. Korobkin, M. Yu. Romanovsk, and O. B. Shiryaev, Phys. Plasmas **15**, 023104 (2008).

[61] K. I. Popov, V. Yu. Bychenkov, W. Rozmus, R. D. Sydora and S. S. Bulanov, Phys. Plasmas **16**, 053106 (2009).

[62] Lin Dai, Jian-Xing Li, Wei-Ping Zang and Jian-Guo Tian, Optics Express **19**, 9303 (2011).

[63] K.P.Singh, D.N.Gupta and V.Sajal, Laser Part. Beams **27**, 635 (2009).

[64] WANG, Xiaoshan, Du, Hongchuan, HU, Bitao., Laser Part. Beams **30**, 225 (2012).

[65] F.âĂĽV. Hartemann *et al.*, Phys. Rev. E **58**, 5001 (1998).

[66] HE. Feng Yu Wei, Lu Peixinang, XU Han XU, Qian Liejia, Shen Baifei, Yuan Xiao, Li Ruxin, and Xu Zhizhan, Phys. Rev. E **68**, 046407 (2003).

[67] E. Esarey, P. Sprangle and J. Krall, Phys. Rev. E **52**, 5443 (1995).

[68] B. Hafizi, A. Ting, E. Esarey, P. Sprangle, and J. Krall, Phys. Rev. E **55**, 5924 (1997).

[69] P. Sprangle, E. Esarey, J. Krall and A. Ting, Opt. Commun. **124**, 69 (1996).

[70] Y.I.Salamin and C.H.Keitel, J. Phys. B **33**, 5057 (2000).

[71] Y. I. Salamin, Physics Letters A **335**, 289 (2005).

[72] D. N. Gupta and Hyyong Suk, Journal of the Korean Physical Society **54**, 376 (2009).

[73] Yousef I Salamin and Christoph H Keitel, J. Phys. B: At. Mol. Opt. Phys. **33** 5057 (2000).

[74] Yousef I. Salamin, Physics Letters A **375**,795 (2011).

[75] R. B.Palmer, J. Appl. Phys.**43**, 3014 (1972).

[76] E. D. Courant, C. Pellegrini, and W. Zakowicz, Phys. Rev. A **32**, 2813 (1985).

[77] I. Wernick and T. C. Marshall, Phys. Rev. A **46**, 3566 (1992).

[78] P. Sprangle and C. M. Tang, Nucl. Sci. **28**, 3346 (1981).

[79] R. H. Pantell and T. I. Smith, Appl. Phys. Lett. **40**, 753 (1982).

[80] A. C. Ting and P. Sprangle, Part. Accel. **22**, 149 (1987).

[81] T. B. Zhang and T. C. Marshall, Phys. Rev. E **50**, 1491 (1994).

[82] A. Van Steenbergen, J. Gallard, J. Sandweiss, and J.-M. Fang, Phys. Rev. Lett. **77**, 2690 (1996).

[83] F. V. Hartemann *et.al*, Phys. Plasmas **6**, 4104 (1999).

[84] X. Y. Wu, P. X. Wang, and S. Kawata, Appl. Phys. Lett. **100**, 221109 (2012).

[85] C. J. Yuan, X. Y. Wu, J. X. Wang, and P. X. Wang,ÂăPhys. PlasmasÂă**18**, 104509 (2011).

[86] M.J. Malachowski, A. Dubik, Journal of Achievements in Materials and Manufacturing Engineering **48**, 87 (2011).

[87] F. Sohbatzadeh, S. Mirzanejhad, H. Aku, S. Shouri, Phys. Plasmas. **17**, 083108-1 (2010).

[88] K. P. Singh, Appl. Phys. Lett. **87**, 254102 (2005).

[89] D. N. Gupta and H. Suk, Phys. Plasma **13**, 013105 (2006).

[90] D. N. Gupta and H. Suk, Phys. Plasma **13**, 044507 (2006).

[91] D. N. Gupta and H. Suk, Laser Part. Beams **25**, 31 (2007).

[92] Q.Mao, Q.Kong,Y.K.Ho*et al.*, Lasers Part. Beams **28**, 83.(2010).

[93] S. P. Goreslavsky and N. B.Narozhny, J. Nonlinear Optic. Phys. Mat. **04**, 799 (1995).

[94] Goldstein,H. Classical Mechanics, 2nd ed. Addison-Wesley,Massachussetts (1980).

[95] Struckmeier Jurgen, J.Phys.A:Math.Gen.**38** 1257,(2005).

[96] V.I.Arnold, Dynamical Systems III Springer-Verlag, Berlin (1988).

[97] M.Tabor. ,Chaos and Integrability in nonlinear dynamics (John Wiley and Sons, New York) (1989).

[98] A.Bourdier and Drouin, Laser and Particle Beams, **27**, 545 (2009).

[99] A.Deprit, Celestial Mechanics **1**, 12 (1969).

[100] A.J.Dragt and J.M.Finn,J.Math. Phys. **17**,2215 (1976).

[101] John. R.Cary, Physics Reports **79**, 129 (1981).

[102] D.Boccaletti and G.Pucacco, Theory of orbits (Springer-Verlag, New York) (2002).

[103] Y.Kominis, Phys. Rev. E **77**, 016404 (2008).

[104] A.J.Licthenberg and M.A.Liebermann, Regular and Stochastic Motion, Springer-Verlag, New York (1983).

[105] Vikram Sagar, Sudip Sengupta, P Kaw, Journal Laser and Particle Beams, Vol. **31**, issue 03, pp. 439-455 (2013).

[106] E. N..Parker, J. Geophys. Res., **66**, 2673 (1961).

[107] J.M.Rax, Phys. Fluids B **4**, 3962 (1992).

[108] Norman M.Kroll,and Kenneth M.Watson, Phys.Rev.A, **8**, 804 (1973).

[109] Vashapati, Phys.Revs, **128**, 664 (1962).

[110] J.J.Sanderson, Phys.Lett. **8**, 114 (1965).

[111] W.H.Louisell, H.William, F.Lam.Juan, A.Copeland Drew, and B.Colson William, Phys. Rev. A **19**, 288 (1979).

[112] J.Meyer-ter-vehn and Z.M.Sheng, Phys. Plasmas **6**, 641 (1999).

[113] M.Tanimoto, M.Kato, S.Miura, E.Saito, N.Koyama and J.K.Koga, Phys. Rev.E **68**, 026401 (2003).

[114] A.Bourdier and M.Drouin, Laser Part. Beams **27**, 545 (2009).

[115] D.Patin, A.Bourdier and E.Lefebvre, Laser and Particle Beams **23**, 297 (2005).

[116] A. Pukhov and J. Meyer-ter-Vehn, Phys. Rev. Lett. **76**, 3975 (1996).

[117] B. Qiao, S. Zhu, C. Y. Zheng, and X. T. He, Phys. Plasmas **12**, 053104 (2005).

[118] M.Tatarakis, A.Gopal, I.Watts, F.N. Beg *et al.*, Phys. Plasmas **9**, 2224(2002).

[119] Tatarakis, M., I. Watts, F. N. Beg, *et al.*, Nature (London) **415**, 280 (2002).

[120] U. Wagner, M. Tatarakis, A. Gopal, F. N. Beg, E. L. Clark, A. E. Dangor, R. G. Evans, M. G. Haines, S. P. D. Mangles, P. A. Norreys, M. S. Wei, M. Zepf, and K. Krushelnick, Phys. Rev. E **70**, 026401 (2004).

[121] Sudipta Mondal, V. Narayanan, Wen Jun Ding, Amit D. Lad, Biao Hao, Saima Ahmad, Wei Min Wang, Zeng Ming Sheng, Sudip Sengupta, Predhiman Kaw, Amita Das and G.Ravindra Kumara, PNAS May 22, **Vol. 109** No. 21, 8011-8015 (2012).

[122] A. Loeb and S. Eliezer, Phys. Rev. Lett. **56**, 2252 (1986).

[123] F. V. Hartemann and N. C. Luhmann, Jr., Phys. Rev. Lett. **74**, 1107 (1995).

[124] Richard T. Hammond, Phys. Rev. A **81**, 062104 (2010).

[125] Richard T. Hammond, EJTP **7**, 221 (2010).